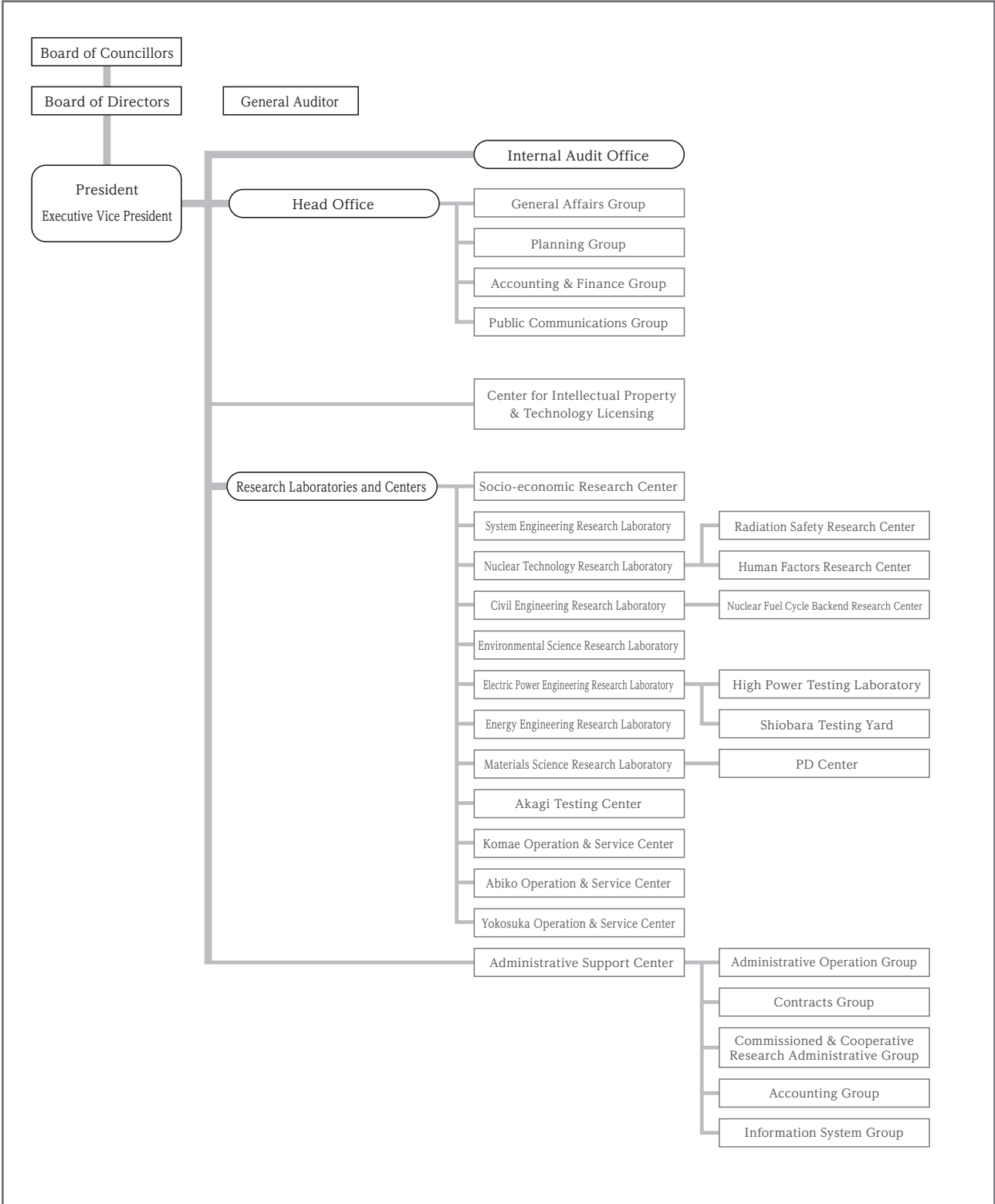


Central Research Institute of Electric Power Industry

Annual Research Report Fiscal Year 2013



Organization of the Central Research Institute of Electric Power Industry



Central Research Institute of Electric Power Industry

Annual Research Report Fiscal Year **2013**



Contents

1. Outline of Research Activities	1
CRIEPI's R&D Portfolio in FY2013 (Pillars of research and eight research laboratories)	

2. Major Research Results	5
--	---

Priority Subjects / Priority Subjects with Limited Terms

Establishment of Optimal Risk Management

Safety Assessment of LWR Systems	6
Assessment for the Effects of Natural Hazards on Nuclear Facilities	8
Improvement of the Safety Assessment on External Natural Hazards for Nuclear Facilities	10
Assessment of Radioactive Material Diffusion in the Environment and its Remediation Effectiveness	12
Establishment of Methodologies to Evaluate Fires in Nuclear Facilities	14
Quantitative Evaluation of Low-Dose Radiation Risk and its Reflection on Radiation Protection	16
Development and Systematization of Long-term Safety Assessment Technologies for Radioactive Waste Disposal	18
Development of Long-Term Storage Management Technologies for Spent Fuel	20
Development of Prediction Methods for Meteorological and Climatic Impact on Power Facilities	22
Establishment of Protective Measure Technologies against Wind and Snow Damage of Overhead Transmission and Distribution Facilities	24
Development of Lightning Risk Management Schemes	26
Well-functioning Electricity Market and Network Neutralization	28
Analyses of Energy Saving and Environment Institutions from an Economics and Energy Security Perspective	30
Scientifically and Economically Rational Scenarios for Reducing CO ₂ Emissions	32

Further Improvement of Facility Operations and Maintenance Technologies

Structural Integrity Evaluation of Reactor Pressure Vessels and Core Internals	34
Integrity of Components and Piping in Nuclear Power Plants	36
Assessment of Cable Insulating Performance Used in Nuclear Power Plants	38
Research of Advanced Nondestructive Evaluation	40
Development of Life Assessment Technology for High Temperature Structural Components of High Chromium Steels	42
Development of Comprehensive Assessment Techniques for the Impact of Thermal Power on Atmospheric Environment	44
Development of Technologies for Supporting Construction and Maintenance of Power Plants with Consideration to Biodiversity Conservation	46
Synthesis System of Numerical Analysis for Current and Sediments in Rivers and Reservoirs	48
Development of Maintenance Technologies for Aged Power Transmission and Distribution Facilities	50
Development of Soundness Assessment Techniques for Aged Overhead Transmission Steel Towers	52

Development of a Supply/Demand Infrastructure for Next-Generation Electric Power

Improvement of Operation and Control Technologies to Diversify Fuel Types for Pulverized Coal-fired Power Plants	54
Sophisticated Technology for Low-Grade Energy Resources	56

Assessment of System Security Assuming High Penetration of Photovoltaics	58
Development of a Next-Generation Coordination System for Power Demand and Supply	60
Next-generation Communications Network Systems	62
Feasibility of Demand Response Suitable for Japan	64
Development and Evaluation of Advanced Heat Pumps	66
Establishment of Evaluation Technologies for High Performance Secondary Batteries	68
Basic Technology Subjects	
Socio-Economic Research Center	70
System Engineering Research Laboratory	72
Nuclear Technology Research Laboratory	74
Civil Engineering Research Laboratory	76
Environmental Science Research Laboratory	78
Electric Power Engineering Research Laboratory	80
Energy Engineering Research Laboratory	82
Materials Science Research Laboratory	84
3. Major New Research Facilities	87
4. Activities	93

1. Outline of Research Activities

CRIEPI's R&D Portfolio in FY2013
(Pillars of research and eight research laboratories)

1. Outline of Research Activities

In FY2013, CRIEPI promoted research aimed at developing a robust and flexible energy supply/demand infrastructure in order to provide a stable supply of electric power, which is the foundation of Japan's economic activity. This research was promoted under the "Three Pillars of Research", which govern our mid-term directives; namely "Establishment of Optimal Risk Management", "Further Improvement of Facility Operations and Maintenance Technologies" and "Development of a Supply/Demand Infrastructure for Next-generation Electric Power". CRIEPI also leveraged collective strength and took priority action to address the pressing issues of nuclear power plant safety and natural disaster reduction on transmission and distribution facilities.

Of the technologies believed to be essential now or in the near future to the electric power industry, CRIEPI has selected 32 priority subjects to maintain, inherit, and develop the technologies which are considered to be essential to current and near future to the electric power industry. Of these priority subjects, CRIEPI's collective strength particularly focused on resolving 10 priority subjects with limited terms which were considered to be urgent and, consequently, produced solid results. Priority subjects and priority subjects with limited terms for which collaboration was deemed necessary were grouped into 11 categories and research in these areas was promoted effectively. Furthermore, 36 basic technology subjects were established and through leveraging the characteristics and expertise of 8 specialized research laboratories* we strengthened our research capability by basic technological strength and areas of specialty, which is the source of solving problems faced by the electric power industry. In concrete terms, we engaged in the following activities;

- 1) The accumulation of data and know-how through field investigations, experiments and measurements.
- 2) The development, maintenance and improvement of analytical techniques.
- 3) Basic research to conceive new ideas.

The major research results produced in FY2013 are described in Chapter 2 (Major Research Results). The chapter lists the respective goals and results of both the priority subjects addressed by each subject and the basic technology subjects addressed by each specialized research laboratory.

To support technology infrastructure of the electric power industry as well as maintain and strengthen CRIEPI's basic research capability, large-scale research facilities including the following were installed; large-scale tsunami physical simulators able to reproduce tsunami-inundation flow, full-scale test facilities for snow-storm damage to overhead transmission lines capable of monitoring and verifying countermeasures for strong winds, wet snow accretion and galloping phenomena on electrical wires and conductors, an advanced combustion test facility for diversification of available fuel types enabling mock combustion utilizing various fuels, a test facility for the carbonization of biomass able to evaluate the optimal condition settings in carbonization technology and a test facility for development and evaluation of heat pumps in industrial and commercial use which is utilized in the evaluation of various heat pump product performance.

*Socio-economic Research Center, System Engineering Research Laboratory, Nuclear Technology Research Laboratory, Civil Engineering Research Laboratory, Environmental Science Research Laboratory, Electric Power Engineering Research Laboratory, Energy Engineering Research Laboratory, and Materials Science Research Laboratory.



CRIEPI's R&D Portfolio in FY2013 (31st March, 2014)

Priority Subjects / Priority Subjects with Limited Terms

Priority Subjects: ● Priority Subjects with Limited Terms: ○ Basic Technology Subjects: ◆ Subject group: Frame enclosure
■: Atomic power ■: Power generation (except for atomic power) ■: Electric power circulation
■: Demand side ■: Society and economy

Establishment of Optimal Risk Management

Nuclear Power Plant Safety

- Safety Assessment of LWR Systems
- Assessment for the Effects of Natural Hazards on Nuclear Facilities
- Improvement of the Safety Assessment on External Natural Hazards for Nuclear Facilities
- Assessment of Radioactive Material Diffusion in the Environment and its Remediation Effectiveness
- Establishment of Methodologies to Evaluate Fires in Nuclear Facilities

Radiation Risks

- Quantitative Evaluation of Low-Dose Radiation Risk and its Reflection on Radiation Protection

Nuclear Fuel Cycle and Backend Technologies

- Development and Systematization of Long-term Safety Assessment Technologies for Radioactive Waste Disposal
- Development of Long-Term Storage Management Technologies for Spent Fuel

Natural Disaster Reduction on Transmission and Distribution Facilities

- Development of Prediction Methods for Meteorological and Climatic Impact on Power Facilities
- Establishment of Protective Measure Technologies against Wind and Snow Damage of Overhead Transmission and Distribution Facilities
- Development of Lightning Risk Management Schemes

Energy and Environment Institutions

- Well-functioning Electricity Market and Network Neutralization
- Analyses of Energy Saving and Environment Institutions from an Economics and Energy Security Perspective
- Scientifically and Economically Rational Scenarios for Reducing CO₂ Emissions

Further Improvement of Facility Operations and Maintenance Technologies

Nuclear Power Plant Maintenance

- Structural Integrity Evaluation of Reactor Pressure Vessels and Core Internals
- Integrity of Components and Piping in Nuclear Power Plants
- Assessment of Cable Insulating Performance Used in Nuclear Power Plants
- Research of Advanced Nondestructive Evaluation

Construction, Operation and Maintenance of Power Generation Facilities

- Development of Life Assessment Technology for High Temperature Structural Components of High Chromium Steels
- Development of Comprehensive Assessment Techniques for the Impact of Thermal Power on Atmospheric Environment
- Development of Technologies for Supporting Construction and Maintenance of Power Plants with Consideration to Biodiversity Conservation
- Synthesis System of Numerical Analysis for Current and Sediments in Rivers and Reservoirs

Operation and Maintenance of Transmission and Distribution Facilities

- Development of Maintenance Technologies for Aged Power Transmission and Distribution Facilities
- Development of Soundness Assessment Techniques for Aged Overhead Transmission Steel Towers

Development of a Supply/Demand Infrastructure for Next-Generation Electric Power

Next-generation Thermal Power Technologies

- Improvement of Operation and Control Technologies to Diversify Fuel Types for Pulverized Coal-fired Power Plants
- Sophisticated Technology for Low-Grade Energy Resources

Next-generation Power Grid Technologies

- Assessment of System Security Assuming High Penetration of Photovoltaics
- Development of a Next-Generation Coordination System for Power Demand and Supply
- Next-generation Communications Network Systems
- Feasibility of Demand Response Suitable for Japan

Energy Utilization Technologies

- Development and Evaluation of Advanced Heat Pumps
- Establishment of Evaluation Technologies for High Performance Secondary Batteries

Basic Technology Subjects

Socio-Economic Research Center

- ◆ Utility Management and Policy
- ◆ Economic and Social Systems
- ◆ Energy Technology Assessment

System Engineering Research Laboratory

- ◆ Electric Power Systems
- ◆ Customer Systems
- ◆ Communications System
- ◆ Mathematical Informatics

Nuclear Technology Research Laboratory

- ◆ Nuclear Reactor Systems Safety
- ◆ Nuclear Fuel and Reactor Core
- ◆ Nuclear Fuel Cycle
- ◆ Human Factors

Civil Engineering Research Laboratory

- ◆ Geosphere Science
- ◆ Earthquake Engineering
- ◆ Structural Engineering
- ◆ Fluid Dynamics
- ◆ Underground Energy Utilization Technologies

Environmental Science Research Laboratory

- ◆ Atmospheric and Marine Environment
- ◆ River and Coastal Environment
- ◆ Biological Environment
- ◆ Bioengineering
- ◆ Environmental Chemistry

Electric Power Engineering Research Laboratory

- ◆ High-voltage and Insulation
- ◆ Lightning and Electromagnetic Environment
- ◆ Applied High Energy Physics
- ◆ Electric Power Application
- ◆ High Current Technology

Energy Engineering Research Laboratory

- ◆ High Efficiency Power Generation
- ◆ Advanced Fuel Utilization
- ◆ Heat Pump and Thermal Storage
- ◆ Energy Conversion Engineering
- ◆ Innovative Numerical Simulation Technology

Materials Science Research Laboratory

- ◆ Structural Materials
- ◆ Materials for Energy Conversion and Storage
- ◆ Advanced Functional Materials for Power Electronics
- ◆ High Performance SiC Semiconductor for Power Electronics
- ◆ Materials Science Research Fundamentals

2. Major Research Results

Priority Subjects / — Establishment of Optimal Risk Management
Priority Subjects Further Improvement of Facility Operations
with Limited Terms and Maintenance Technologies
Development of a Supply/Demand Infrastructure
for Next-Generation Electric Power

Basic Technology Subjects

Priority Subjects / Priority Subjects with Limited Terms

Establishment of Optimal Risk Management

Further Improvement of Facility Operations and Maintenance Technologies

Development of a Supply/Demand Infrastructure for Next-Generation Electric Power

Basic Technology Subjects

Safety Assessment of LWR Systems

Background and Objective

In order to enhance the safety of nuclear power plants, it is necessary to reveal their vulnerabilities through quantitative risk assessment and simulations using an analysis model which reproduces phenomena in as much detail as possible. It is also necessary to add and modify

equipment which is effective in improving safety. To this end, we aim to sophisticate the evaluation system applied to improve safety measures, and develop a quantitative evaluation of the effectiveness of these measures.

Main results

1 Evaluation on characteristics of severe accident analysis codes

In order to investigate the differences in characteristics of MAAP5.01^{*1} and MELCOR2.1^{*2}, severe accident (SA) analyses for a TBU^{*3} sequence in a representative BWR plant were conducted for both these codes. The hydrodynamic responses inside a reactor pressure vessel (RPV) at an early phase (until the onset of fuel relocation) were relatively consistent. However, significant differences were observed

in the onset timing of the major physical phenomena after the core support plate failure (Fig. 1). When direct containment heating (DCH) is considered to occur, the primary containment vessel (PCV) fails just after the RPV failure (Fig. 1). In this case, concrete ablation in the pedestal cannot be observed and hydrogen generation due to molten core - concrete interaction (MCCI) significantly decreases (Fig. 2) (L13006).

2 Development of BWR building hydrogen / vapor behavior evaluation method

Behavior of hydrogen, which flows into a reactor building through a reactor containment in an SA, was analyzed using a three-dimensional computational fluid dynamics (CFD) code. The lumped parameter (LP) model, which was developed to predict CFD calculation results, was expanded so as to also cover counter current flow

through side openings such as blow-out panels (Fig. 3). The CFD calculations and LP evaluations were compared with various conditions and the results were in good agreement. This implies that the present LP model can save time and computational resources by predicting the results before CFD calculations.

3 Development of measurement technology for sophisticating the evaluation model used during reactivity initiated accidents (RIA)

A Reactivity Initiated Accident (RIA) is an event in which the reactor power increases rapidly and surface of a cladding tube dries up in less than 1 second. During an RIA, it is important to accurately evaluate the behavior of boiling bubble and fuel temperature from the perspective of considering reactivity feedback^{*4}. In this study, a technology was developed to enable measurement

of void fraction and transient temperature in a direct heating system which simulates RIA. A wire mesh sensor covered with insulating material and a thermocouple which a balance circuit were constructed, and it has become possible to measure two-phase flow with high temporal and spatial resolution (Fig. 4).

4 Development of level 1 PRA model for common cause failures due to external events

Based on the level 1 PRA model (probabilistic risk assessment model for the evaluation of core damage frequency) of the typical BWR plant for internal and seismic events developed in 2012, a prototype PRA model for additional effects of tsunami hazards was developed. Additionally, for

the development of fragility data to input in this model, tsunami fragilities^{*5} of watertight doors and sea water pumps were studied and issues for investigation were identified for the methodology to link tsunami fragilities to tsunami hazards.

*1 MAAP: Severe accident analysis code under development by EPRI (U.S.). Mainly used by the electric utility side.

*2 MELCOR: Severe accident analysis code under development by U.S.NRC. Mainly used by regulatory bodies in Japan.

*3 Station blackout with no emergency power supply and no recovery of short and long term A/C power

*4 The effect of suppressing reactor power corresponding to fuel temperature elevation at the occurrence of a reactivity initiated accident (RIA).

*5 Tsunami fragility: Conditional probability of loss of function of components in the event of a tsunami of a certain magnitude

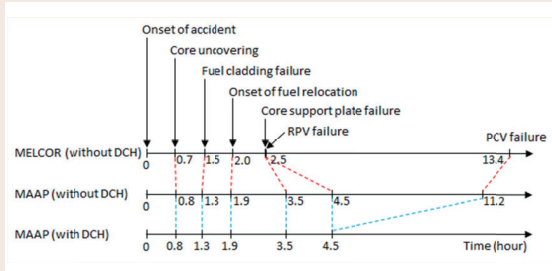


Fig. 1: Comparison of chronology in a TBU sequence
 Significant differences are observed in the onset timing of the major physical phenomena after the core support plate failure between analytical results of MAAP and MELCOR. When the DCH is considered to occur in the TBU sequence, the PCV fails just after the RPV failure.

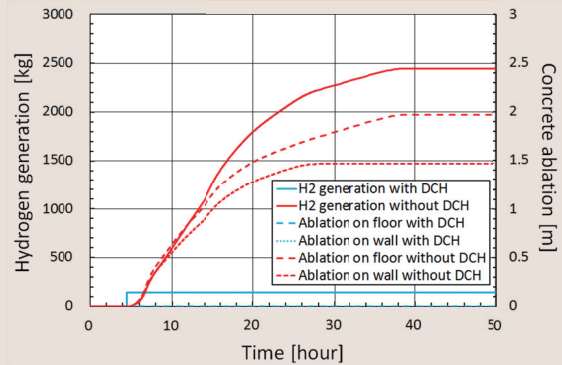


Fig. 2: Effect of DCH on hydrogen generation and concrete ablation in the pedestal in a TBU sequence

In the case of a TBU sequence, pressure in the RCS at the time of a RPV failure remains high. Hence, high temperature molten debris is discharged from the RPV to PCV with pressurized steam. This leads to the occurrence of DCH and results in the generation of thermal and mechanical loads to the PCV. When the DCH is considered to occur, most of the molten debris is discharged to the drywell from the pedestal. Consequently, concrete ablation in the pedestal cannot be observed and hydrogen generation due to MCCI significantly decreases. However, when the DCH is not considered, all of the molten debris remains in the pedestal, resulting in the occurrence of large scale MCCI.

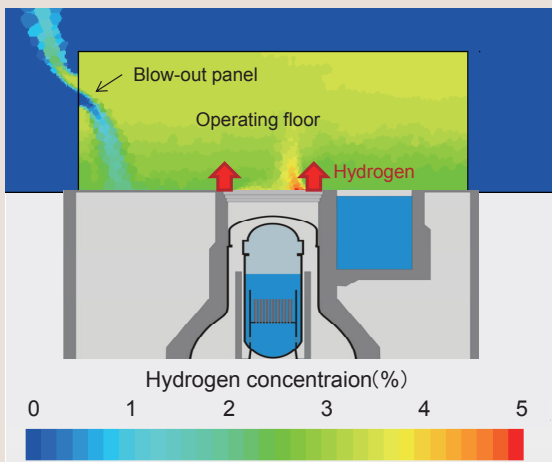


Fig. 3: Hydrogen behavior analysis in a reactor building

Behavior of hydrogen, which flows into the reactor building from the reactor containment in a severe accident, was calculated using a three-dimensional computational fluid dynamics (CFD) code. The lumped parameter model was expanded to cover the counter-current flow (upper figure), in which the gas is emitted through the upper half of a blow-out panel and enters from the lower half.

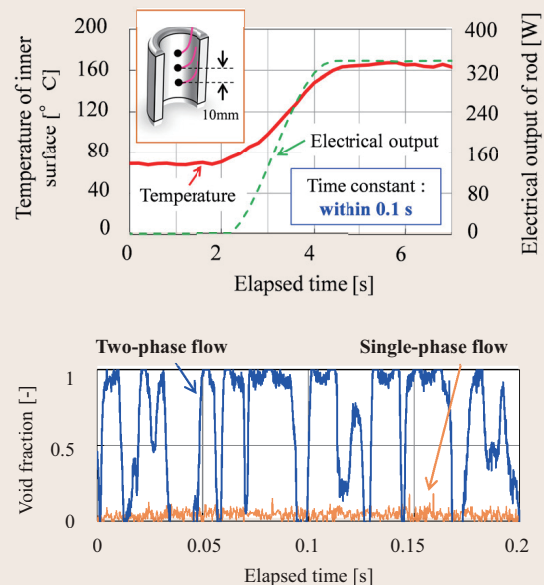


Fig. 4: Development of an RIA measurement method

A technology enabling measurement of void fraction and transient temperature in direct heating system which simulates RIA was developed. A wire mesh sensor covered with insulating material and a thermocouple which has balance circuit were constructed, and it has become possible to measure two-phase flow with a high degree of accuracy.

Assessment for the Effects of Natural Hazards on Nuclear Facilities

Background and Objective

Nuclear power is a base-load supply system which helps to suppress carbon dioxide emissions in our social economic system. However, the 2011 Fukushima accident revealed certain kinds of difficulties associated with managing NPP safely in times of crisis. The authority for safe operation of NPP has lost its reliability in the eye of the public, to the extent that all Japanese nuclear power plants are yet to return to service. The main cause of the 2011 Fukushima accident was the damage to the internal power

sources due to an inundation of the large-scale tsunami. Therefore, further precise assessment on catastrophic hazards and risks is needed to improve the safety operation of NPP.

Our research aims to unravel such catastrophic but infrequent processes, and to establish an assessment methodology for hazards and associated risks. The desired outcome is to contribute towards reducing a number of risks impacting upon the safe operation of NPP.

Main results

1 Strong motion seismology for assessment of probable asperity in a large active fault system

Strong motion seismology poses a difficulty because it is not possible to apply an empirical relationship of asperity*¹ on the rupturing process of multiple segments in a large active fault system. An empirical relationship involves determining position, size, and slip of asperity in a large magnitude earthquake. Our study aims to establish an assessment of probable asperity from

the surface length and displacement of active faults. Based on the 1992 Landers earthquake, USA, we have compiled position, size, slip of asperity and the surface profile of displacement of an active fault. As a result, we discovered a relationship between the characteristics of these parameters.*²

2 Source fault geometry estimated from balanced-cross section analysis

The edge geometry of deep source fault is an important characteristic to unravel the probable size of multiple fault-ruptures in an active fault system. This characteristic can be inferred from a balanced-cross section analysis of the source fault. Our analysis aimed to develop a 2D deep

geometric model of a source fault from the 2D seismic reflection profile at the offshore source fault of the 1964 Niigata earthquake. 3D geometry of a source fault was developed using a number of overlapped sections from the 2D fault model.*³

3 An empirical model of long-term magma discharge and a review of ash-fall models by numerical fluid dynamics

An empirical model of magma discharge over the past 50,000 years by the Esan volcanic complex (EVC) in northern Japan was established from volume and chronology. Because the EVC has been dormant for over 9,000 years without any major magmatic eruptions, if the model's assumption is accurate, the magma chamber beneath the EVC already contains a large volume of magma, to the extent that it could discharge a volume equivalent to its greatest discharge in the past.*⁴ Such a model

can be integrated into the assessment guideline of volcanic hazards, from which a more precise model can be established.

A number of ash tracking, dispersal and settling, and eruption column models were reviewed by means of numerical fluid dynamic techniques. We summarized the issue of ash-fall hazard processes onto electric facilities, and the issue of multi dimension models which require enhancement in future work.*⁵

*1 Asperity is a jog with high friction resistance on a fault plane. A large asperity is likely slipped during the occurrence of a large earthquake.

*2 Kuriyama and Sato (2013) Abstract for JSSJ 2013 Fall meeting.

*3 Kimura and Okamura (2013) Abstract for 2013 AGU Fall Meeting.

*4 Miura et al. (2013) GSA Bulletin, 125, 1503-1519, doi:10.1130/B30732.1

*5 Suto, Hattori and Toshida (2013) Wind Engineers, JAWE, 38, 416-425.

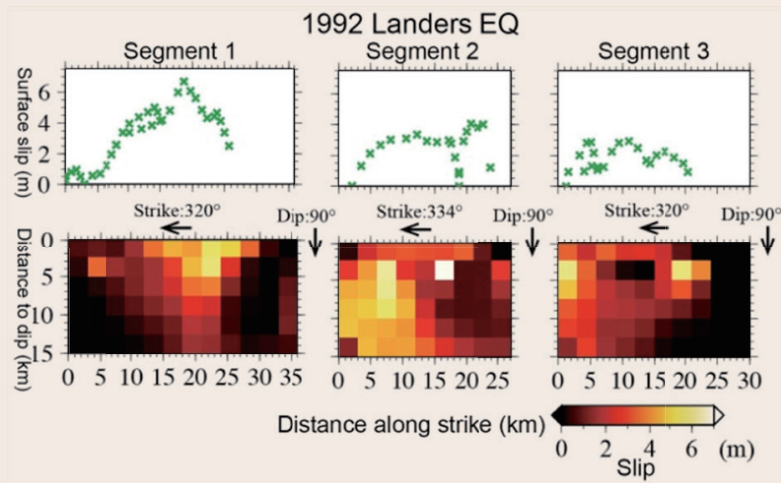


Fig. 1: Strong motion seismology for assessment of probable asperity in the large active fault system

Position, size and slip of asperity (Wald and Heaton, 1994), and the surface displacement profile (Sieh et al., 1993), in 1992 Landers earthquake, USA. The qualitative relationship between asperity and surface displacement is shown for each fault segment.^{*2}

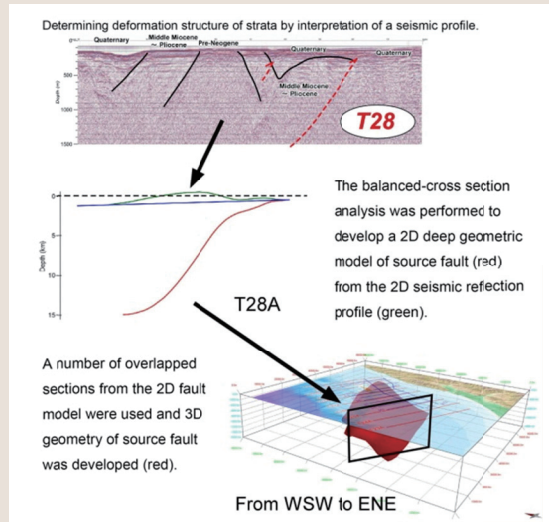


Fig. 2: Source fault geometry estimated from balanced-cross section analysis

3D geometry of the source fault of the 1964 Niigata earthquake can be obtained from a number of 2D fault sections through balanced-cross section analysis.^{*3}

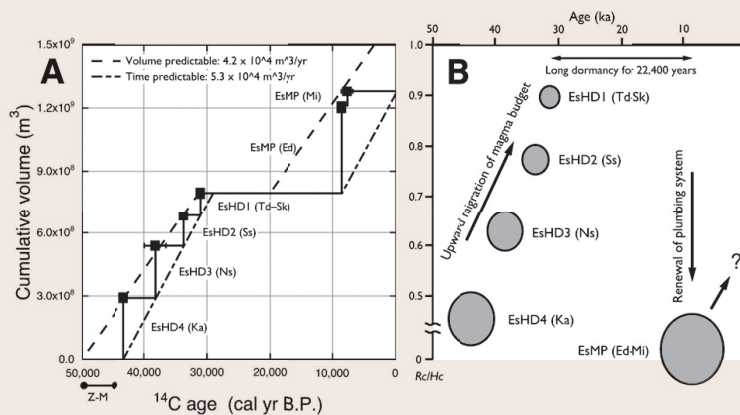


Fig. 3: An empirical model of long-term magma discharge

An empirical model of magma discharge was established from the discharged sequence of volume and chronology for the past 50,000 years at the Esan volcanic complex (EVC) in northern Japan.^{*4} A) Discharge diagram for the past 50,000 years at the EVC; B) Explanatory model of magma discharge using the upward migration of the magma batch.

Improvement of the Safety Assessment on External Natural Hazards for Nuclear Facilities

Background and Objective

The Fukushima Daiichi nuclear disaster has severely impacted upon the reliability of nuclear safety and social trust. Most nuclear power plants remain out of service for these reasons. Since nuclear power could play an important role in

the realization of a low carbon society, long-term shutdown should be avoided. In this project, safety assessment methodologies for nuclear power plants subjected to natural disaster are studied.

Main results

1 Evaluation of tsunami debris-induced risks

In order to establish the evaluation methods of tsunami debris-induced risks for NPPs, we developed simple criteria on generating/not-generating tsunami debris (Fig. 1), a new simple estimation method of tsunami debris impact load, and a probabilistic assessment approach

of debris impact by using a numerical debris tracking model. These methods enable screenings of tsunami debris-induced risk and make it possible to estimate external force caused by tsunami debris in the fragility assessment of NPP structures or instruments.

2 Installation of a Large-scale Tsunami Physical Simulator

The Large-scale Tsunami Physical Simulator, which is a large test flume able to be used for the fragility evaluation test of NPP structures or instruments in the event of a tsunami, was designed and installed (Fig. 2), and verification tests for operation of the facilities were carried out. The facility was able to generate tsunami-

inundation flow with a steep front and long-duration, as well as a fast and large-depth flow on a large scale. Using this facility, large-scale experiments can be carried out such as evaluations of tsunami hydrodynamic load, debris impact load, and damage mode of structures under tsunami-loading conditions.

3 Ultimate limit state of seismic isolators designed for light-water reactors based on full-scale break test*¹

To examine the applicability of a seismic base isolation system to nuclear power facilities, the ultimate limit state of full-scale seismic isolators was experimentally evaluated. For a series of the tests, lead rubber bearings designed for light-water reactors with 1600 mm diameters and 900

tons rated load, were constructed as specimens. It was demonstrated that the full-scale seismic isolators exhibited good ductility capacity and their ultimate state was well correlated by the results in the conventional small-scale tests.

4 Development of a collapse analysis program for reinforced concrete structures

Seismic performance of reinforced concrete structures has been judged based on failure of only one member in the conventional evaluation system. Also, a numerical analysis technique which follows the behavior after partial failure is expected to enable quantification of structural redundancy and elucidation of phenomena beyond design. As such, an FEM program is being

developed to simulate the experiment performed the year before last where specimens were loaded to collapse. Plate element with material nonlinearity of concrete and beam (rebar) element considering geometrical nonlinearity were implemented to the program and confirmed to function individually through trial (Fig. 4).

*¹ This research was conducted as a part of the national Japanese project "Development for Evaluation Methods of Seismic Isolation Systems" with the participation of Chubu Electric Power, Japan Atomic Power, Hokkaido Electric Power, Tohoku Electric Power, Tokyo Electric Power, Hokuriku Electric Power, Kansai Electric Power, Chugoku Electric Power, Shikoku Electric Power, Kyushu Electric Power, J Power, Toshiba, Hitachi-GE Nuclear Energy, Mitsubishi Heavy Industries, and the Institute of Applied Energy.

[1] T.Hiraki et.al: Development of a evaluation method for seismic isolation systems of nuclear power facilities (Part 9), Proc. on the ASME-PVP,2004.

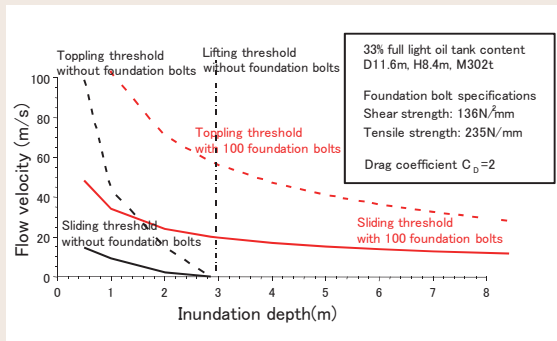


Fig. 1: Simple criteria on generating/not-generating tsunami debris

Relationships between flow velocity and inundation depth at sliding, toppling, and lifting thresholds for a light oil tank with (black) and without (red) foundation bolts are shown in the figure. The solid lines denote the sliding thresholds, the dashed lines denote the toppling thresholds, and the chain line denotes the lifting threshold. If the flow velocity and inundation depth around a target equipment are located lower than these lines, the target equipment is not slid, toppled, or lifted by the tsunami.

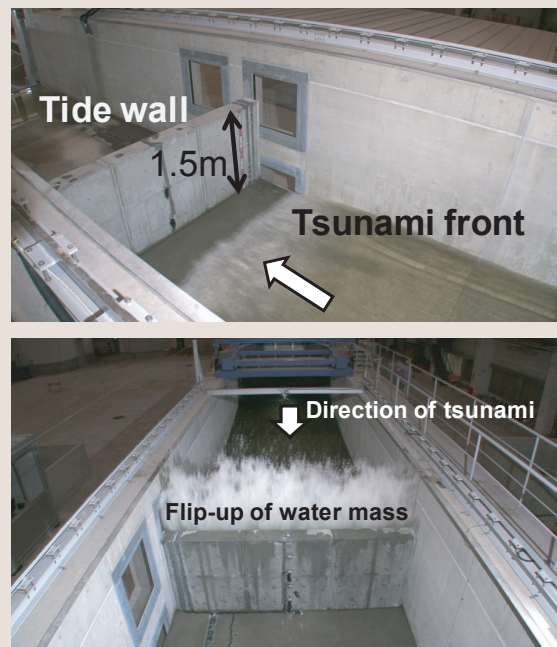


Fig. 2: An overtopping test of the tide wall by tsunami, using the Large-scale Tsunami Physical Simulator

The hydrodynamic force on a 15 m high tide wall was investigated. The top photo shows the flow just before the tsunami reaches the tide wall, while the bottom photo shows the flip-up of the water mass just after the tsunami strikes the wall. If the flow velocity and inundation depth are lower than these lines, the target equipment is not slid, toppled, and lifted.

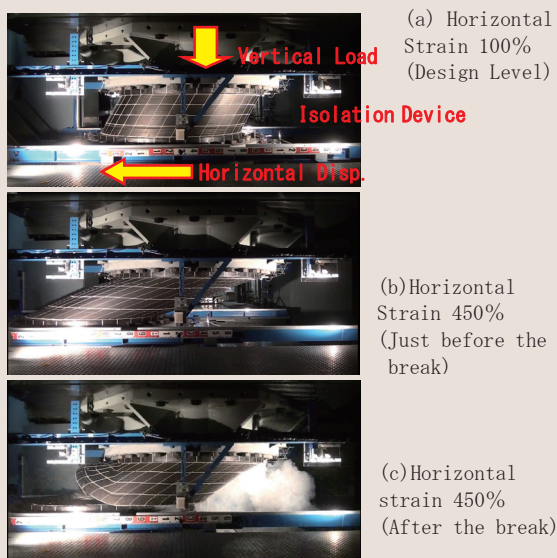


Fig. 3: Typical deformation of a full-scale seismic isolator under horizontal loading

In the typical load pattern, horizontal load was gradually applied to a specimen until its breaking under the constant vertical load corresponding to rated load (900 tons) as shown in Fig. 3. 13 specimens were tested under various loading patterns to evaluate the ultimate limit state. It was shown that full-scale seismic isolators exhibited good ductility capacity to have a large safety margin against an earthquake event exceeding design specifications.

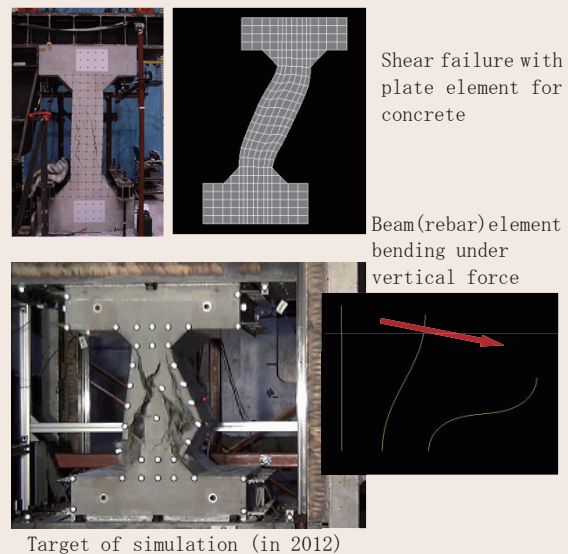


Fig. 4: Development of a collapse analysis program for RC structures

Components of the FEM program for simulation of collapse process have been developed as shown in the lower left picture. The Maekawa model, which has high precision for concrete and beam elements considering large deformation of rebar, was utilized in the program and its operation was verified.

Assessment of Radioactive Material Diffusion in the Environment and its Remediation Effectiveness

Background and Objective

In order to evaluate and continuously improve the safety of nuclear power plants, it is necessary to carry out preliminary assessments of the environmental impact of radioactive materials on the atmosphere and ocean in the case of severe accidents as well as the effectiveness of preventive measures against nuclear power plant accidents.

The target of this study is to develop techniques

for predicting the dispersion of radioactive materials into the atmosphere and ocean, as well as techniques for monitoring radioactive materials and assessing the migration of radioactive materials in marine organisms and forests. Through the development of these techniques, we aim to contribute to improving the safety of nuclear power plants via the assessment of environmental impact.

Main results

1 Prediction of atmospheric dispersion of radioactive materials emitted from nuclear power plants

The research team improved the atmospheric dispersion model to evaluate the deposition amount of radioactive materials emitted to the atmosphere during severe accidents, as well as to evaluate the level of external exposure associated with their deposition on the ground surface. The applicability of the model to the prediction of the atmospheric dispersion of radioactive materials targeting the

area within several ten kilometers of the power plant was verified (Fig. 1). In addition, the research team improved the resolution of a wide-area atmospheric transport model and compared the results obtained using the model with the measured values of field experiments. Reproducibility in terms of the grid resolution was also evaluated to identify any flaws in the model.

2 Developing assessment techniques for ocean diffusion of radioactive materials and transfer to marine organism

The oceanic dispersion of these radiocesium in the North Pacific was simulated by considering the direct discharge and the fallout of materials from the atmosphere. The simulation results were in good agreement with the monitoring results because the model can represent the subduction process into the intermediate layer (Fig. 2).^{*1} The simulation of radiocesium

transfer to the marine sediment estimated that the total amount in marine sediment was less than 5% of total amount in seawater.^{*2} The simulation of radiocesium transfer through the food chain, using initial seawater concentration and depuration rate, clarified the relationship between decrease profiles of seawater and marine organisms. (Fig. 3).^{*3}

3 Assessment of long-term environmental impact of radioactive material in trees

Radiocesium (¹³⁴Cs + ¹³⁷Cs) contamination, primarily derived from the Fukushima accident in March 2011, was observed in the leaves and twigs of 17 popular woody species in Japan at mid-growth season in the years 2011, 2012, and 2013. The general average of the radiocesium activities in leaves and twigs observed in 2012 were 64% and 110% of those observed in 2011, respectively, while those observed in 2013 were 19% and 28% of

those observed in 2011, respectively (Fig. 4). Thus, the radiocesium activities decreased with time, although the variation in amounts/rates of decrease with the species, sampling part, and position in each stand was not negligible. Particularly, ratios of radiocesium activity between current leaves and 1-year old leaves increased with time, suggesting a translocation of radiocesium from old tissues to newly developed ones. (V13008)

*1 TSUMUNE DAISUKE, et al., *Biogeosciences*, 10, 5601-5617, 2013.

*2 MISUMI KAZUHIRO, et al., The Oceanographic Society of Japan, Fall meeting, 2013 (in Japanese)

*3 TATEDA YUTAKA, *Isotope news*, 719, 2014. (in Japanese)

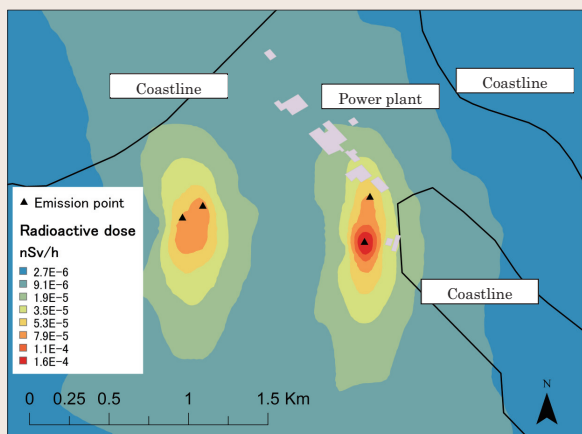


Fig. 1: Example of calculation using the atmospheric dispersion model

An experimental calculation for dispersion of radioactive plume from multiple emission sources was conducted using the data on the height of emission sources and meteorological conditions of surrounding areas in order to evaluate the level of external exposure to radioactive materials (e.g., Cs, I, and noble gas).

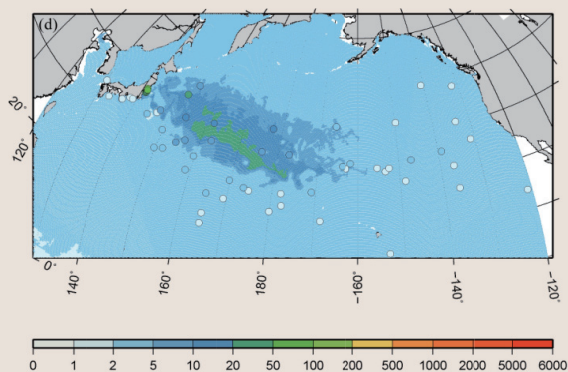


Fig. 2: ^{137}Cs concentration in surface layer of ocean in the North Pacific Ocean from Dec. 2011 to Feb. 2012

The ^{137}Cs concentrations in the ocean in the North Pacific Ocean from Dec. 2011 to Feb. 2012 obtained by simulation were in good agreement with the monitoring results. Color contours represent the simulation results, and color plots represent the monitoring positions and concentrations.

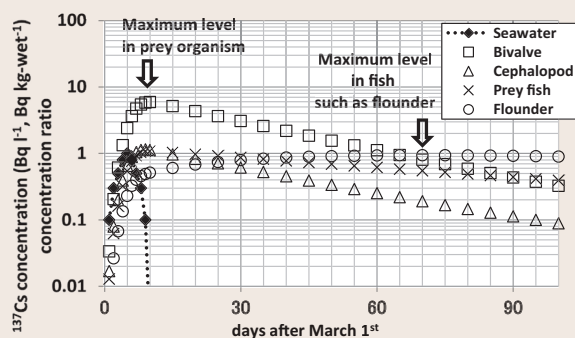


Fig. 3: Simulation of ^{137}Cs concentrations in seawater and marine organisms

The ^{137}Cs concentrations in biota (Bq kg^{-1}) were simulated under certain conditions of radioactive cesium concentration in seawater (increase during 5 days, decrease during 5 days after the 1Bq l^{-1} peak). The ratios of ^{137}Cs concentration in biota to the maximum seawater concentration (1Bq l^{-1}) are also shown on the vertical axis.

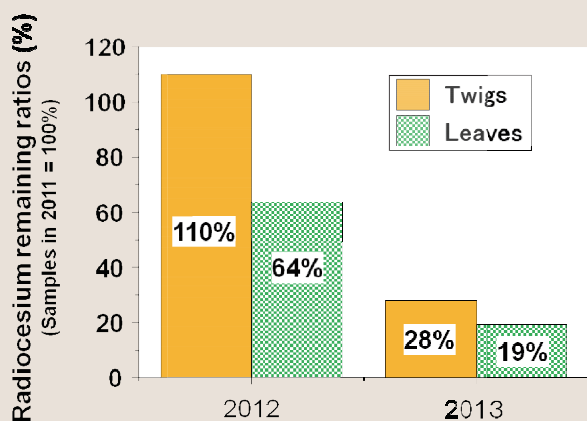


Fig. 4: Yearly transition of radiocesium activity in individual parts

Radiocesium activities in leaves ($n = 54-58$) and twigs ($n = 42-54$) of all stands/positions/species were averaged for each year samples. Then, the ratios for the averages of 2012 and 2013 against the averages of 2011 were indicated as their remaining ratios (%). Although the ratios were still high in 2012, particularly in twigs, these reduced to 20-30% in 2013. It is possible that the reduction is mainly due to washing by wind and/or rain; however, a translocation of radiocesium to newly developed tissues could also be observed.

Establishment of Methodologies to Evaluate Fires in Nuclear Facilities

Background and Objective

To obtain conformity on the new regulatory requirements for nuclear power plants, it is necessary to prepare fire prevention methodology with high accountability in accordance with the fire impact assessment guide enacted in June 2013. In addition, in order to reduce the risk induced by internal fire needed for the periodic safety review after recommencement of operations, continuous improvement of the fire hazard assessment and the fire prevention methodology is necessary.

In this project, we aim to evaluate the fire prevent methodology (fire extinguishing system, etc.) for nuclear power plants based on the fundamental fire tests and confirm its validity. In addition, to improve the accuracy of fire behavior prediction in accordance with fire source (such as, cable fire, oil fire and high energy arcing fault fire), we aim to integrate the fire hazard evaluation method and contribute to the establishment of scientific and rational countermeasures for fire prevention.

Main results

1 Establishing a construction method of tube-type automatic fire extinguishing system for cable tray fire

Among the countermeasures to reduce the internal fire impacts of nuclear power plants, installation of the tube-type automatic fire extinguishing system (Fig. 1) may be applicable as an automatic fire extinguishing equipment for cable tray fires. In order to establish an effective construction method for such a system, fire extinguishing tests were carried out using a cable tray attached to the metal lid with actual maximum width (1.8 m), and subjecting

the inflammable high-voltage power cables to an overcurrent of 2 kA class (Fig. 2) in vertical and horizontal orientations. As a result, fire extinction capability for the longest range of fire extinguishing equipment charged with the environmentally friendly halide fire extinguishing agent (50 m) was confirmed and a prospect of applicability for the actual installation obtained.

2 Clarification of limitations on the occurrence of High Energy Arcing Fault (HEAF) fires in high-voltage switchgear components

Successive fire due to a HEAF event in the high-voltage metal-clad switch gear*¹ was identified at the Onagawa nuclear power plant at the time of the Great East Japan Earthquake. As such, we tested full scale high-voltage metal-enclosed switch gear components (6.4 kV and 8.0 kV), and confirmed that the arcing energy below 25 MJ

did not induce the HEAF fire (Fig. 3), regardless of the arcing discharge position. Furthermore, we developed CFD (Computational Fluid Dynamics) code to predict damage to the metal enclosure and the zone of influence by pressure and gas emitted from a broken enclosure, thus confirming its applicability to the fire hazard assessment.

3 Establishment of an efficient methodology to predict air temperature in a compartment fire by the fire model FDS

In fire impact assessments for fire compartments, to establish the extent of fire impact and estimate the firing time or damage time of important safety equipment, the representative fire model FDS (Fire Dynamics Simulator)*² is applicable for the detailed evaluation of compartment fires with complicated configurations however analysis accuracy is highly dependent on input conditions. As such, we evaluated the accuracy

of a fire model, FDS, for a fire plume from combustible liquid and a natural convection from a high-temperature vertical wall, and found that the air temperature in a compartment fire could be reproduced accurately by appropriately setting the pyrolysis conditions of the fire source or computational grid-spacing condition (Fig. 4) (N13010).

*1 Installed in the metal enclosure with a protective relay (such as circuit breakers) and high-voltage bus to protect and control the power system.
*2 A CFD model developed by NIST (National Institute of Standards and Technology) in the US, which primarily simulates heat and substance transport in fire fields and enables evaluations of spatial distributions of physical quantities such as air temperature.

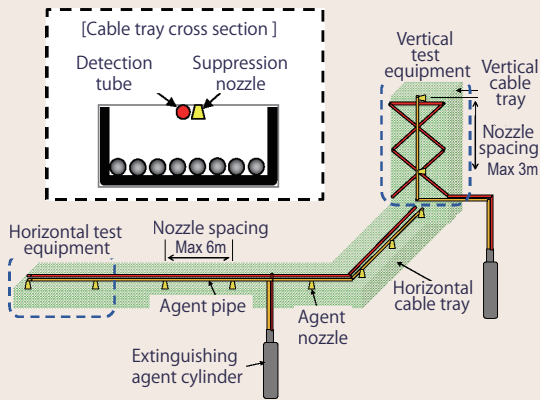


Fig. 1: Example of a tube-type automatic fire extinguishing system for cable tray fires

A tube-type automatic fire extinguishing system is composed of a fire extinguishing agent cylinder, detection tube, pipe and valve for agent injection, etc. Immediately after the burst of the polyamide detection tube containing pressurized nitrogen gas due to the heat of the flame (activation temperature: 180°C), the pneumatic cylinder valve for fire extinguishing agent (Novec1230: liquid at room temperature, boiling point 49°C) will be activated. The suppression agent will be injected through the nozzles into the designated fire area and induce a suppression effect over the combustion reaction and a cooling effect. Moreover, as this system can detect fires automatically without any power source, the capability of fire extinguishing even in the event of a power failure can be assured.

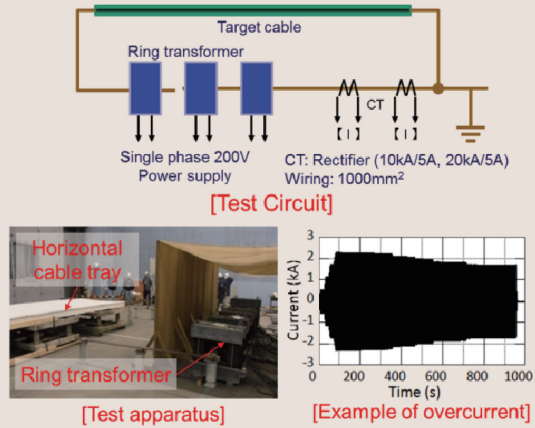


Fig. 2: Cable fire test apparatus with the overcurrent system

Using the overcurrent test equipment installed in high power short-circuit testing facility at the electric power engineering research laboratory (Yokosuka area), cable fire extinguishing tests subjected to six times the allowable current (2 kA) were carried out using flammable high-voltage power cable (6.6kV-CV-3C-150sq). In these tests, one target cable was continuously energized by ring transformers to reproduce the cable fire. By using a cable tray attached to a metal lid of actual maximum width (1.8 m) covered with a heat resistance sheet, an ensemble which simulates the end of the extinguishing agent pipe system, we performed fire extinguishing tests in horizontal and vertical orientations and confirmed that use of 50 m of tube-type automatic fire extinguishing system was the longest possible coverage.

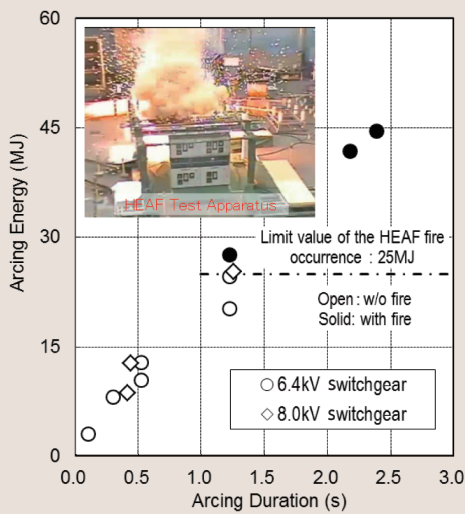


Fig. 3: Arcing energy measured in HEAF tests using high-voltage switchgears and the limitations of fire occurrence

We measured arcing energy* using two types of high-voltage switchgears (test voltage 6.4 kV and 8.0 kV, three-phase three-wire system, copper bus conductor) under a condition with short circuit current around 20 kA and durations from 0.1 to 2.2 sec. When the arcing energy did not exceed 25 MJ, a successive fire was not identified, regardless of the arcing discharge position (VCB room or bus-bar room).

*Hot gas heated in the metal enclosure due to arc flash will be emitted out of the enclosure or to adjacent enclosure, and has a potential to damage surrounding equipment.

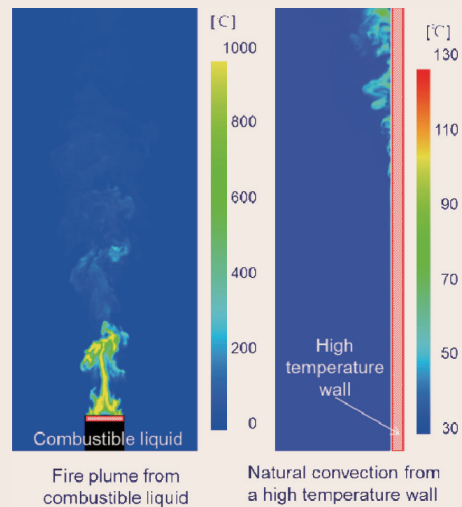


Fig. 4: Example of simulation of the fire plume using a fire model FDS

The FDS fire model gives spatial distributions of physical quantities, such as temperature, velocity, oxygen concentration, as well as their temporal variations. As shown in the figure on the left, concerning grid spacing for accurately predicting a fire plume from combustible liquid (Ethanol, pan diameter 30 cm), the condition of $\Delta < D^*/20$ (D^* : characteristic fire size, Δ : grid spacing) could be applied. Moreover, as shown in the figure on the right, for a natural convection from a high temperature wall, unsteady flows near walls were accurately predicted under the grid-spacing condition of $\Delta \eta < \text{approximately } 0.6$ (η : similar variable for laminar boundary layer).

Quantitative Evaluation of Low-Dose Radiation Risk and its Reflection on Radiation Protection

Background and Objective

The radiation exposure to workers in nuclear facilities, and to the public from environmental contamination caused by nuclear accidents are characterized as prolonged low-dose-rate exposures. Epidemiological research studies of residents in high background radiation areas suggest the existence of a dose-rate effect with no increase in radiation risks at a low-dose-rate, unlike the high-dose-rate radiation exposure. Understanding biological mechanisms of the dose-rate effect could contribute to the establishment

of reasonable protection criteria, and relieve public concern towards radiation exposure. Furthermore, the accuracy of dose evaluation underlying radiation risk assessment is also an important issue.

This project aims to reflect the dose-rate effect in radiation protection systems by elucidating its biological mechanisms through experimental studies, and to develop dose evaluation methods to reduce uncertainties in radiation risk assessment.

Main results

1 Developing an experimental system for radiation effect on tissue stem cell to elucidate mechanisms of the dose-rate effect

Cancer is considered to be initiated by an accumulation of lesions in tissue stem cells (TSC^{*1}). TSCs in normal tissues maintain their function in groups (TSC pools). In the case of low-dose-rate radiation exposure, damaged and undamaged TSCs would be intermingled in TSC pools. If damaged TSCs can be excluded by competition between damaged and non-damaged TSCs, it can be assumed that lesions in TSCs caused by radiation would accumulate less in TSC pools at low dose-rate exposure. We tackle explorations to confirm this hypothesis, in which these mechanisms could explain the dose-rate effect.

To study the competition in detail, we developed a novel *in vitro* assay using organoid^{*2} formation from intestinal TSCs (Fig. 1) and showed the number of organoids as an index of survival rates of TSCs after 0-4 Gy exposure (Fig. 2 left). By using this system, we quantitatively clarified that organoid-forming TSCs irradiated with X-rays at doses ≥ 2 Gy acquired increased organoid-regenerating capacity (Fig. 2 right). Thus we demonstrated that the *in vitro* assay can quantitatively analyze behaviors of intestinal TSCs after radiation exposure and it is useful to verify the dose-rate effect by competition between TSCs^[1].

2 Estimating aging characteristics of radiation-counting efficiency for clearance inspection^{*3}

In the case of clearance inspection for materials used at nuclear facilities, it is necessary to estimate low level radioactivity, so enhancement of the precision of radioactivity estimation is an important issue. One important factor of estimating low level radioactivity is the effect of corrosion products generated on alloys due to aging. If radiations are shielded by corrosion products, it is necessary to evaluate the effect of corrosion products for radiation measurement to avoid underestimation of contamination.

In this study, acceleration tests of corrosion products growth were performed using carbon steel and stainless steel coupon specimens which were contaminated with either ²⁴¹Am or ⁶⁰Co.

The relationship between amount of corrosion products and decrease of radiation-counting efficiency was obtained (Fig. 3). In order to investigate the growth of corrosion products on alloys in an actual warehouse environment, coupon specimens were placed in warehouses of nuclear facilities for over one year (Fig. 4). These results made it possible to estimate the decrease of radiation-counting efficiency in an actual warehouse environment. For waste contaminated with uranium, we also made the appropriate estimation available for uncertainties due to aging characteristics, taking into account the difference of the alpha particle energy between ²⁴¹Am and ²³⁸U [2, 3].

*1 Cells which tissue-forming cells originate in. They are also considered as origins of cancer because of their proliferative characters.

*2 Three-dimensional structure of several kinds of functional cells derived from TSCs which shows a cell arrangement similar to living organisms.

*3 Confirmation of radioactivity concentration of materials with radioactivity concentrations below the level which requires treatment as a radioactive material.

[1] YAMAUCHI, M. et al., J Radiat Res, 55(2), 381-390 (2014).

[2] ICHIJI, T. and KAWAMURA, H. Jpn. J. Health Phys. 48(4), 171-179 (2013).

[3] ICHIJI, T. and KAWAMURA, H. Jpn. J. Health Phys. 48(4), 200-205 (2013).

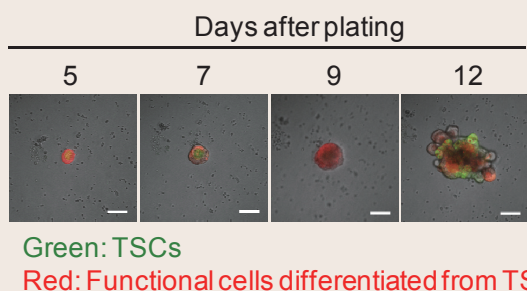


Fig. 1: Organoid formation from intestinal TSCs

Pictures of organoids formed *in vitro* from intestinal cells containing TSCs isolated from mice intestines. The green color represents TSCs while the red color indicates cells derived from TSCs. Projections similar to crypts which exist in the roots of villi in small intestine were formed after 12 days of culture. At the bottom of the projections, green cells, which represent TSCs, were observed, in a similar manner to the distribution *in vivo*.

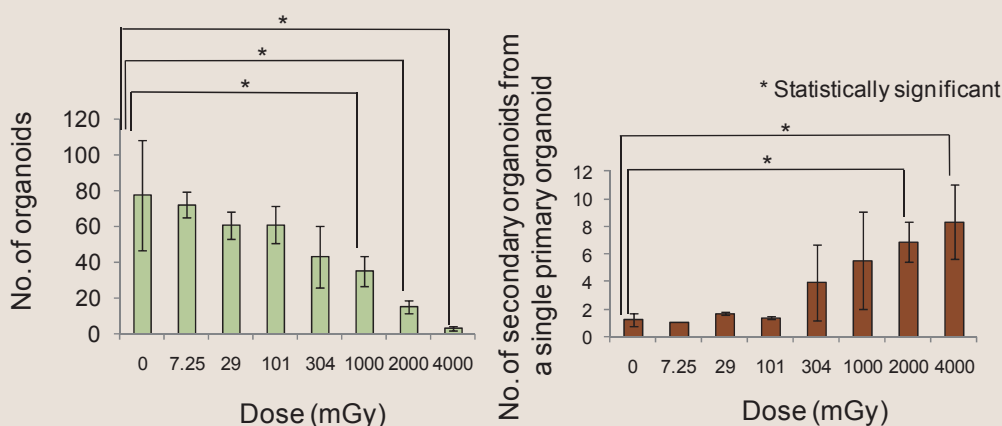


Fig. 2: Assessment of radiation effects using the organoid assay

The number of organoids after radiation exposure was observed (left). Because each organoid is formed from a single TSC, the efficiency of organoid formation represents a survival rate of TSCs after exposure. Significant decrease was observed after 1 Gy (1000 mGy) compared with non-irradiated control. There have been no quantitative data on the tissue-regenerating capacity of surviving TSCs for the repair of wounded tissues after radiation exposure. Then, the primary organoids formed in the experiments shown at the left were dissociated and they were passaged to allow secondary organoid formation to assess organoid-regenerating capacity (right). The number of secondary organoids produced from a single primary organoid was measured, and quantitatively clarified to increase with radiation dose.

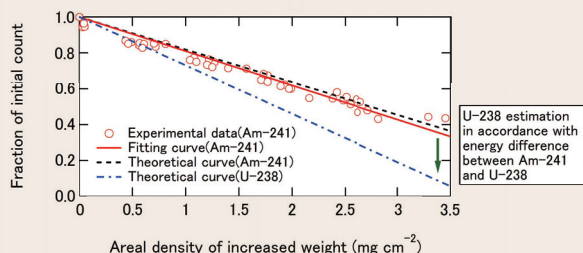


Fig. 3: Decrease in radiation-counting efficiency caused by corrosion products on alloy (experimental data and theoretical values)

This figure shows the result of the decrease in radiation-counting efficiency of carbon steel samples, where ^{241}Am was dropped. Experimental data show good agreement with the theoretical values. Using the theoretical curve which was calculated taking into account the difference of the alpha particle energy between ^{241}Am and ^{238}U , it will be possible to estimate the decrease for ^{238}U in the radiation-counting efficiency caused by corrosion products.

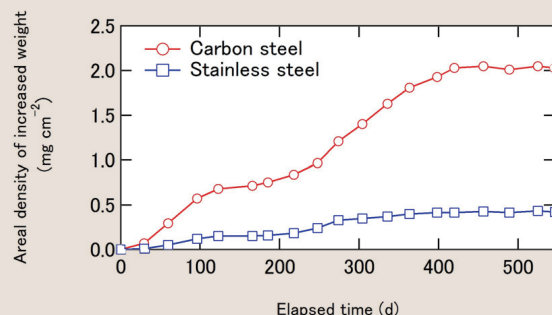


Fig. 4: Amount of corrosion products on alloys placed in the warehouse environment at the nuclear facility

Carbon steel and stainless steel coupon specimens were placed in a warehouse environment at a nuclear facility and the amount of corrosion products generated on coupon specimens was measured. Using the data illustrated in Fig. 3, it is assumed that radiation-counting efficiency may drop to 40-50% of the initial value for carbon steel, which was contaminated by ^{238}U and elapsed over 500 days.

Development and Systematization of Long-term Safety Assessment Technologies for Radioactive Waste Disposal

Background and Objective

As storage capacity of the low-level radioactive waste (LLW) in nuclear plants is growing tight, the licensing safety of pit and sub-surface disposal require review based on a planned schedule. Moreover, in regards to high-level radioactive waste (HLW), the Japanese government is engaged in various efforts such as investigating direct disposal, securing safety in the future, the systemization of site selection and so on.

In this project, R&D of LLW disposal aims to develop methods to evaluate hydraulic conductivity and to evaluate migration characteristics of engineered barriers in order to build a reliable technology. R&D of HLW disposal aims to develop methods to evaluate the residence time of groundwater and to select cementitious materials for the different components in a disposal facility.

Main results

1 Hydraulic conductivity test for Ca-type bentonite-sand mixture

Ca-type bentonite-sand mixture will be used in low-level radioactive waste disposal facilities. A hydraulic conductivity test of soils has been standardized in JIS, but the JIS method is not applicable to low permeable soils such as bentonite. This study improved the JIS method

for Ca-type bentonite-sand mixture. It became possible to evaluate the saturation of specimens before permeation, and to discuss the effect of plugging by fine particles (Fig. 1). It is expected that this report will contribute to new standardization (N13005).

2 Evaluating gas migration characteristics of compacted Ca-bentonite mixture

Since the gas permeability of Ca-bentonite mixture is low, it is necessary to investigate the effect of gas pressure generated mainly by the chemical interaction between aluminum and the alkaline component of cement. Thus, gas migration tests together with their numerical simulation were

conducted using CRIEPI's code. As a result, it was revealed that the in-situ gas breakthrough pressure is thought to be smaller than the gas breakthrough pressure measured by the gas migration test due to the difference in stress caused by different boundary conditions.(Fig. 2)(N13011).

3 Estimating residence time of groundwater contaminated by drilling fluid

Understanding the migration of groundwater is required for safety assessment of HLW and the residence time of groundwater (RTG) is useful information for this. RTG can be assumed by radiocarbon (^{14}C) in the dissolved natural organic matters (NOM). However it is frequently

contaminated by artificial organic matters (AOM) added in drilling fluid. The separation method between NOM and AOM has been established. This method has enabled the correct estimation of RTG by using ^{14}C in NOM. (Fig. 3) [1]

4 Investigation of the methodology used in selecting cementitious materials for the different components in the underground facility

The objective of this study is to list and sort the required characteristics of cementitious materials for each component in the facility, in order to provide input for determining material selection methodology. When deriving the required characteristics of cementitious materials for each component, physico-chemical properties were investigated that will fulfill required operational functions and minimize effects on the safety

function of the disposal system due to alteration or degradation. Based on these investigations, step changes in the state of the disposal system are identified, including the bedrock around the drifts, by considering alteration or degradation of the cementitious material. Significant components for ensuring safety function can be identified by specifying the step changes in the state of the disposal system. (Fig. 4)(N13009)

[1] Nakata, K., Kodama, H., Hasegawa, T., Hama, K., Iwatsuki, T., Miyajima, T., Journal of Hydrology, 489, pp.189-200, 2013.

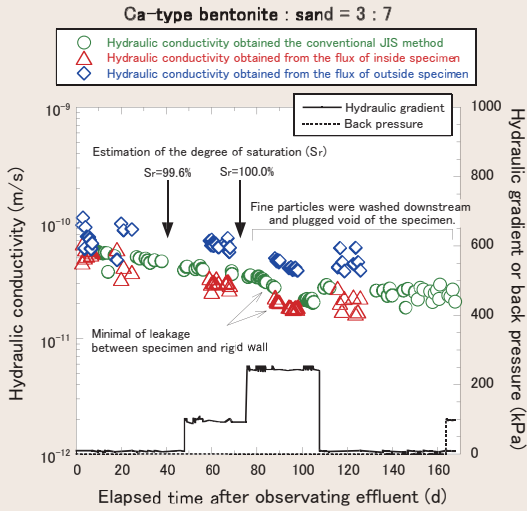


Fig. 1: Experimental result of a hydraulic conductivity test
 The slight decrease in hydraulic conductivity after saturation was determined to be caused by the clogging of fine particles. Measuring the flux of inside specimen showed that the conventional JIS method was substantially applicable to Ca-type bentonite-sand mixture.

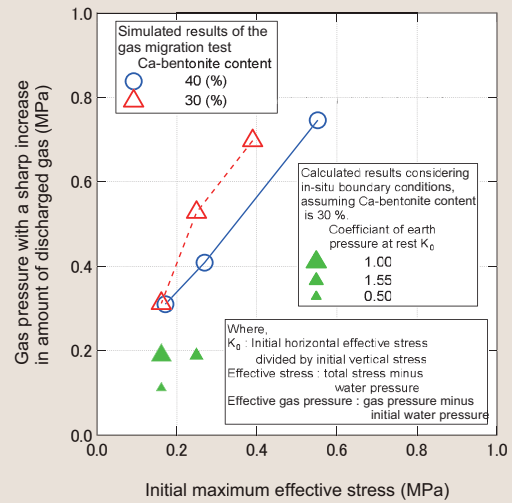
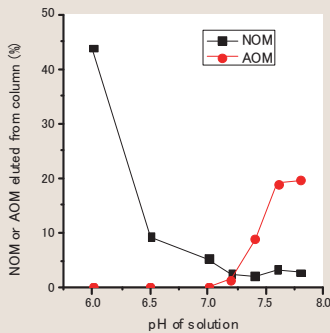
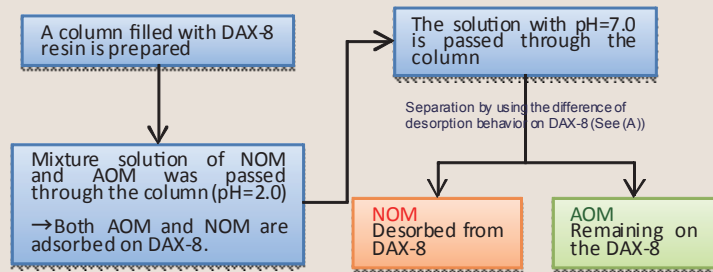


Fig. 2: Gas pressure with a sharp increase in amount of discharged gas
 In-situ gas pressure with a sharp increase in amount of discharged gas is smaller than that evaluated by laboratory tests because of difference in initial stresses and reaction forces from surroundings.



(A) pH vs amount of eluted organic matter



(B) Flow chart of separation between NOM and AOM

Fig. 3: Separation between NOM and AOM and measurement of ¹⁴C in NOM

Separation of natural organic matter (NOM) and artificial organic matter (AOM) has been achieved by using their respective differences in sorption and desorption behavior on DAX-8 resin.

Mechanical plug periphery: Slack of hydraulic plug, back filler, and bed rock progress by leaching leaving aggregate

Upper buffer periphery: Slack of buffer and bed rock progress by leaching leaving aggregate

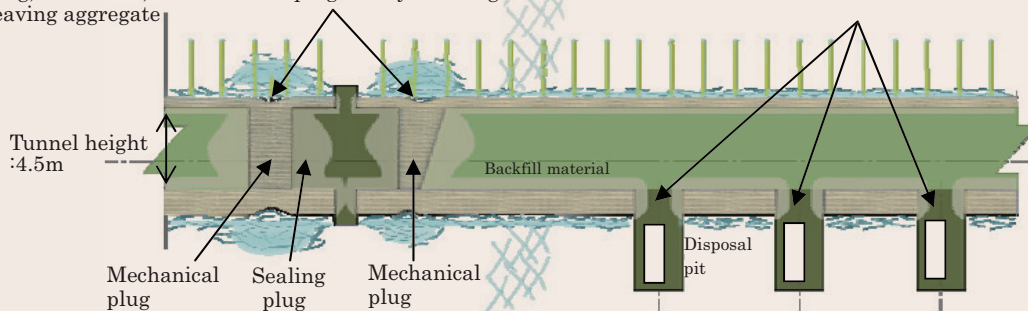


Fig. 4: Trial estimation on mechanical and chemical state transition of HLW underground facility

Due to the progression of leaching of ions from cement hydrated phase in concrete, surrounding area of the mechanical plug and buffer will loosen. Considering such a long-term state transition, the material and mechanical design of concrete components should be made a priority issue.

Development of Long-Term Storage Management Technologies for Spent Fuel

Background and Objective

The interim storage of spent fuels generated from nuclear power plants until they are reprocessed is necessary. Furthermore, it is important to prepare for an increase in storage amount and an extended storage period. Many dry interim storage facilities using metal casks exist in countries around the world, including Japan. It is also necessary to evaluate the safety of post-storage transport, taking into account aging of the components during the storage period. The

early realization of interim storage facilities using concrete casks is demanded in Japan from an economical point of view.

In this project, we aim to develop an evaluation method for confinement of metal casks taking into account its aging. For the practical use of concrete cask technology, we aim to improve countermeasures for stress corrosion cracking and the investigation method for welding of canisters*1.

Main results

1 Development of an evaluation method for the long-term sealability of metal gaskets

To obtain the data necessary to validate the long-term sealability evaluation method of metal gaskets, we performed relaxation tests using test flanges with metal gaskets^[1]. The outer liner of the gasket is made of silver and we used gaskets with two different cross section diameters for

the tests. The results obtained from the data of 50,000 hours show that the residual linear load of the gasket and Larson-Miller parameter (LMP) have good correlation (Fig. 1). This development of the evaluation method contributes to the long-term storage of spent nuclear fuel.

2 Proposal of a draft revision for the Japan Society of Mechanical Engineers (JSME) concrete cask code

Defects may occur in the initial welding layer of the primary lid of the canister when the primary lid is welded under moist conditions. To understand the effects of moisture in welding, we performed a welding test. The results showed that unstable flow rate of back shield gas and insufficient oxygen control (less than 5%) lead to

the occurrence of obvious defects in the initial welding layer (Fig. 2). We made a revision draft for the JSME code regarding concrete casks*2 including our research results in 2013. The proposal of this draft revision contributes to practical use of concrete casks in Japan.

3 Development of prototype devices for remote measurement of salt attached to canisters

The measurement of salt attached to a canister is a promising inspection method for monitoring the occurrence of SCC at the surface of the canister during storage of spent fuel. Laser-induced break down spectroscopy (LIBS) is a candidate salt measurement method, however, remote measurement is an important issue in terms of inserting the LIBS devices into the narrow

space such as the space between the canister and a concrete body. In this study, we developed a compact device comprised of optics for LIBS and a drive unit for vertical movement (Fig. 3). The performance test results showed that salt can be detected by LIBS in the narrow space when the distance from the laser device to the measurement points was around 22 m (H13004)

4 Development of a monitoring system for helium leakage from canister

We propose a monitoring system which uses the temperature difference between the top and bottom of the canister as a helium leak sensor for the canister in storage. In order to analytically evaluate the change of this temperature difference during the leakage of helium gas from the canister, an unsteady state

thermal hydraulics model has been developed which considers the change in density of helium gas (Fig. 4) (N13008).

Hereafter, we will verify the model and establish the evaluation method for sealability of the canister, so as to contribute to practical use of concrete casks in Japan.

*1 A cylindrical container made of stainless steel which contains spent nuclear fuel and is placed in a concrete cask

*2 JSME, Code for Construction of Spent Nuclear Fuel Storage Facilities (JSME FBI-2003)

[1] A. Bèziat, M. Wataru, K. Shirai et. AL., 17th International Symposium on the Packaging and Transportation of Radioactive Materials, August, 2013

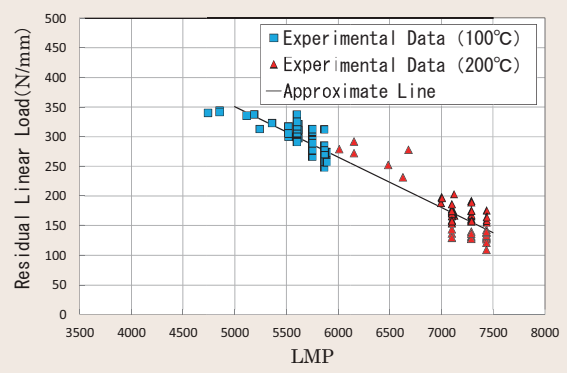


Fig. 1: Relation between residual linear load of metal gasket and LMP

This figure shows the test results with a metal gasket 6.2 mm in diameter. X axis is the LMP. The LMP is shown as follows; $LMP = T^*(C + \log(t))$ where T (K) is absolute temperature, C is material constant, t (h) is time. l_1 is assumed for C. Y axis is residual linear load of the metal gasket. Residual linear load at 100 and 200°C and the LMP have good correlation. The results with a diameter of 8.4 mm are similar. This was a combined study between CEA (France), GNS (Germany) and CRIEPI. The tests will continue for 100,000 hours and finish in 2015.

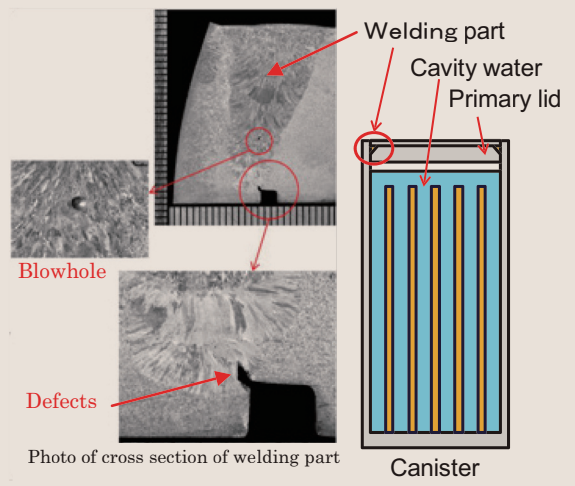


Fig. 2: Relation between residual linear load of metal gasket and LMP

The primary lid of the canister is welded under moist conditions because the cavity water is heated by the decay heat of spent nuclear fuels. We performed the welding test using a small test plate made of SUS304L (diameter: 50 cm, thickness: 12.6 mm). The defects in the initial layer of welding occur if the back shield gas decreases and oxygen gas concentration in argon gas exceeds 5%. These results show that it is necessary to enhance training of welders and inspectors regarding welding under most conditions and perform a welding procedure test using a full-scale mock-up before commencing the practical welding process. We added these results to the draft revision for the JSME code.

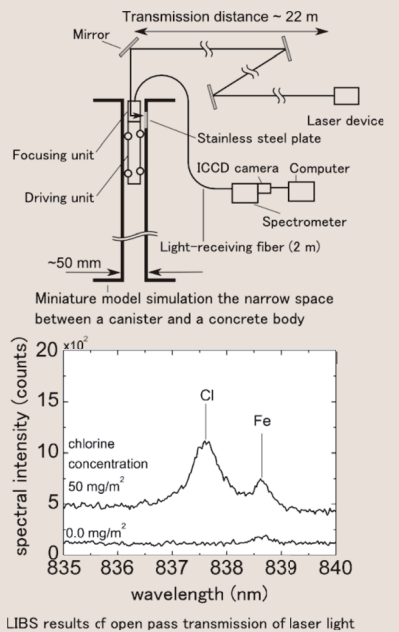


Fig. 3: Remote measurement test using a miniature model simulating the narrow space between a canister and a concrete body

The remote measurement of salt attached to canister material has been performed by inserting LIBS devices, which have laser light focusing and a light-receiving function, into a miniature model simulating the narrow space between a canister and a concrete body. The results showed that the chlorine emission spectrum was measured when the distance from laser device to the measurement points was about 22 m, and suggest that salt concentration can be measured by remote LIBS.

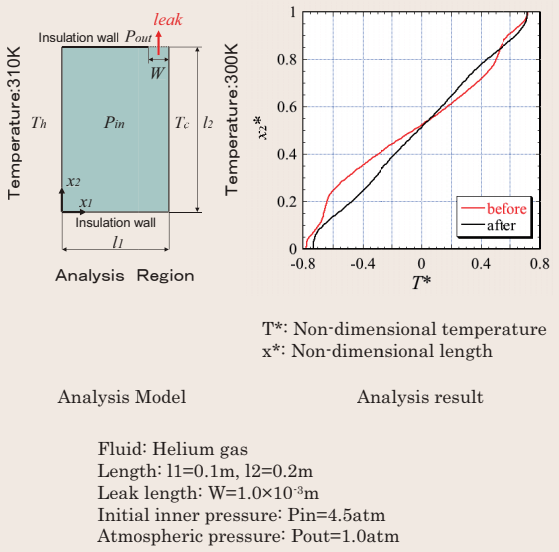


Fig. 4: Results of a helium leak analysis for cavity flow

The characteristic of the present model considers the non-conservative method of the governing equations for the compressible fluid problem. We confirmed a valid solution was obtained for the problem of helium leaks from rectangle cavities. Hereafter, we will make a 3D model to simulate the complex structure of the inner canister in order to apply this method to a real cask.

Fluid: Helium gas
 Length: $l_1=0.1m, l_2=0.2m$
 Leak length: $W=1.0 \times 10^{-3}m$
 Initial inner pressure: $P_{in}=4.5atm$
 Atmospheric pressure: $P_{out}=1.0atm$

Development of Prediction Methods for Meteorological and Climatic Impact on Power Facilities

Background and Objective

Disasters have occurred at a higher frequency, associated with super typhoons, rapidly-developed low pressure systems, localized heavy rainfall/snowfall or tornado wind blasts, etc. There is concern that global warming could possibly be related to the occurrence of extreme events.

In this project, we aim to assess the variety of hazards for meteorological phenomena and oceanography, and to evaluate the impact of global warming. For this purpose, a long-term high-resolution meteorological database

is produced. This database is anticipated to be utilized as fundamental data for considering each hazard during the design of electric power facilities. Another important issue is the development of techniques that are needed for preventing the occurrence of damage or supporting the quick restoration of damaged components. A forecasting method for severe storms up to a week in advance and their associated highly-convenient systems will then be developed for various lead-times.

Main results

1 Development of a high resolution, long-term weather and climate database

The numerical weather forecasting and analysis system, NuWFAS, has been improved as a regional climate model for applying to a long-term regional climate prediction around Japan (Fig. 1). Through a physical downscaling with this model and two global reanalysis datasets provided by the European Centre for Medium-range Weather Forecasts (ECMWF), a database, CRIEPI-RCM-Era2, was developed by compiling the hourly product of downscaling during the

period from FY1958 to FY2010 (N13004). The database is composed of meteorological variables including surface wind, temperature, and precipitation from surface to 20 km aloft with a horizontal resolution of 5 km. The fine spatiotemporal resolution is good enough to use for the practical purposes of evaluating the impact of extreme weather conditions on electric power equipment, in particular distribution facilities (Fig. 2).

2 Short-range rainfall forecasting for prevention of hydropower facility disasters

A radar data assimilation system developed based on VDRAS*¹ can assimilate routine observation data from domestic Doppler weather radars in order to improve the accuracy of the initial condition of a numerical weather prediction (NWP) model. This assimilation technique results in more accurate forecasts of rainfall and wind fields for heavy rainfall cases, even if it is difficult to forecast such

cases by only using the NWP model (Fig. 3). In the line of research, a short-term rainfall prediction system was developed, in which the product from very short-range (up to 2 hours ahead) nowcasting based on the extrapolation of sequential radar echo images and the product from short-term (up to 6 hours ahead) rainfall forecasting using NuWFAS are combined.

3 Assessment of storm surges and high waves for the design of seaside power plants

A model to predict and estimate a storm surge due to a typhoon was constructed using ROMS*². The sea level elevation and duration of the storm surge predicted by the model are consistent with the tide gauge observations (Fig. 4). These results confirmed that the model (including a conceptual typhoon model using atmospheric pressure, the radius of the region where winds over 25 meters per second, and

traveling speed of typhoon) allowed us to estimate the impact of the storm surge due to a typhoon. The database of ocean waves around the Japanese coast, CRIEPI-OWCM05, was also developed by the ocean wave model using CRIEPI-RCM-Era2 as physical wind forcing. This database is useful to evaluate the impact of high waves on the design of seaside power plants.

4 Assessment of the impact of tornadoes on the design of nuclear power plants

Regions prone to supercell tornadogenesis were specified from a map based on CRIEPI-RCM-Era2 (Fig. 5). This map is useful in determining the regions to be considered for hazard assessment. The probabilistic method developed can estimate an exceedance hazard curve from past observations. The design wind speed estimated is used for assessing the behavior of tornado missiles. Furthermore, the maximum of the missile speed,

and the horizontal and vertical travelling distances can be assessed by a code called TONBOS (Fig. 6). As a countermeasure to mitigate the impact load of a tornado missile, a method for the construction of high-strength metal mesh was also proposed, as well as a design for an energy absorption method (N13014). These research results have been used to assess the safety of nuclear power plants according to the new national regulatory standard.

*1 Variational Doppler Radar Assimilation System developed by the National Center for Atmospheric Research.

*2 Regional Ocean Modeling System has been developed by Rutgers University and UCLA and other academic institutions.

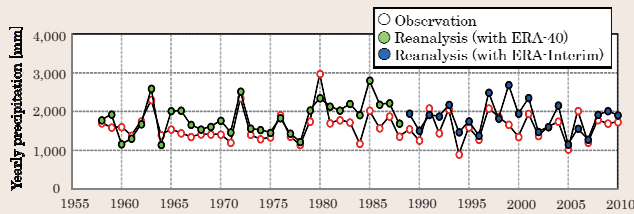


Fig. 1: Temporal variation of yearly precipitation over 53 years
 ERA-40 and ERA-Interim reanalysis datasets provided by ECMWF are used for this 53-year reproduction run. This result indicates that numerical errors do not accumulate with time and that yearly accumulated precipitation reproduced is in good agreement with observations.

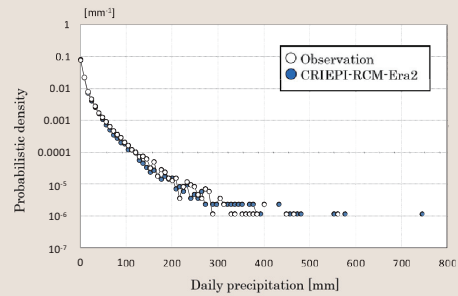


Fig. 2: Probability density distribution of daily precipitation

The probability density pattern from the obtained database is compared with the one from observation. It is suggested that this database is sufficiently accurate for the hazard analysis of extreme weather events.

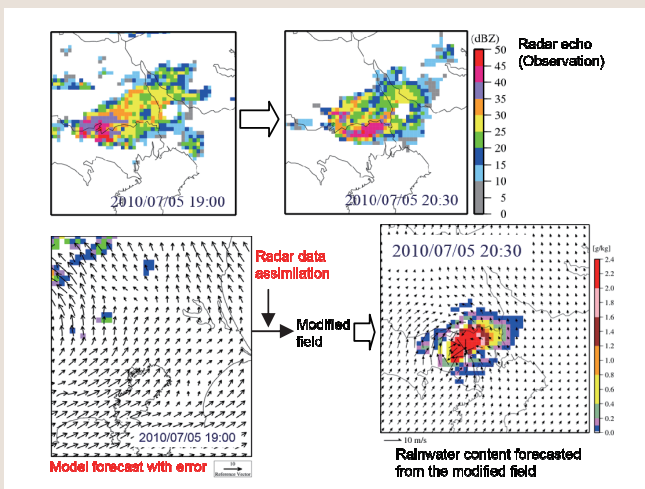


Fig. 3: Improving the accuracy of short-range rainfall forecasting using NCAR VDRAS

Errors in the initial condition and forecasting result of the meteorological model make forecasting of torrential rainfall difficult. Modification of the initial field or the forecasted field by assimilating four-dimensional radar data during a time window can enhance the capability of forecasting such severe storms.

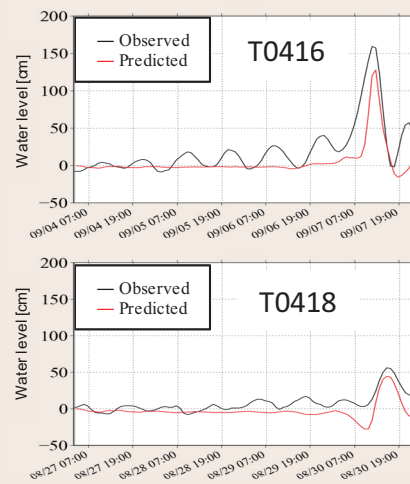


Fig. 4: Comparison of predicted and measured sea level changes of storm surges

The sea level changes of storm surges caused by the 16th and 18th typhoons in 2004 are compared with tide gauge measurements. With the exception of the semi-diurnal oscillations, predicted sea level changes agree with the measurements.

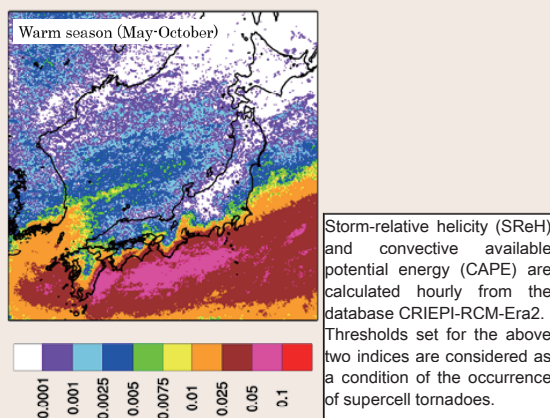


Fig. 5: A map of probabilistic likelihood of the occurrence of F3 and larger tornadoes [%]

An analysis is made of the frequency that both thresholds are exceeded, set for two indices relating to vorticity transported to cloud and atmospheric instability. The result suggests that the frequency tends to increase over coastal areas on the Pacific side and around Kyushu. Regions with high frequency include almost all locations where F3 tornadoes occurred.

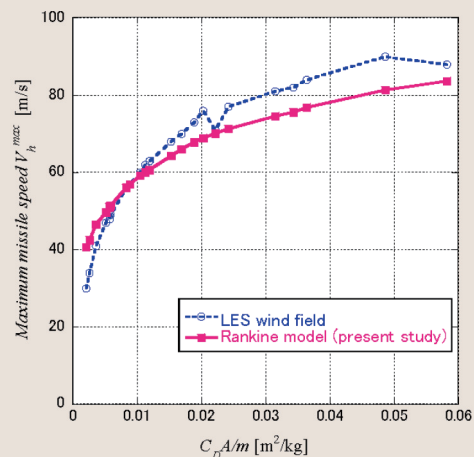


Fig. 6: Example of the maximum missile speed assessed under the two wind fields

The maximum travelling speed of a tornado missile, which begins to travel from a location 40 m above the ground level, depends on the material property represented by a drag coefficient C_D , cross section A , and mass m . The effect of the wind field is relatively smaller than the material property.

Establishment of Protective Measure Technologies against Wind and Snow Damage of Overhead Transmission and Distribution Facilities

Background and Objective

In December of 2005, severe snowstorms on the coast of the Sea of Japan caused damage to overhead transmission facilities including the partial collapse of transmission towers due to the weight of heavily accreted snow, short circuiting of transmission lines caused by galloping*1, and the failure of electrical insulators, (flashover) due to heavily accreted snow containing sea salt. After the occurrence of snow-related damage, CRIEPI started a ten-year research project from FY2007 to FY2016 on damage to overhead transmission facilities caused by severe snowstorms. This

project is conducted in cooperation with electric power companies.

In the first phase (from FY2007 to 2011) of this project, field observations were mainly conducted in order to elucidate the physical processes of snow-related damage and to examine current measures against it. The second phase of the project commenced in FY2012 to propose effective countermeasures against snow-related damage using practical analysis and prediction methods. Applicability of the research results to distribution facilities is also investigated.

Main results

1 Continuous operation of field observation and consolidated data management systems

Field observation data related to meteorological conditions of snow-related damage and effectiveness of countermeasures have been obtained in seven sites across Japan. Data management systems for storing practical examples of snow-related damage and their meteorological conditions have been continuously

operated and 223 new practical examples*2 have been added to the database. These data are used for to elucidate the meteorological conditions of snow-related damage, examine its prediction methods, and evaluate effectiveness of countermeasures.

2 Evaluation of a thermodynamic model for snow accretion on electric wires

CRIEPI has recently developed a dynamic snow accretion simulation code for overhead transmission lines, named SNOVAL-dyn. Further improvement of the SNOVAL-dyn has been made by incorporating a thermodynamic model with heat exchange between the air and snow sleeve, solar radiation, Joule heating of the conductor, etc., which makes it

possible to calculate the liquid water content of the snow sleeve as well as cohesive and adhesive forces (Figures 1, 2). This simulation enables us not only to evaluate the snow accretion process including snow melting and snow shedding, but also to improve the accuracy in predictions on accreted snow mass by a known simple snow model.

3 Detailed elucidation of the flashover mechanism of snow-accreted insulators

In order to evaluate the effect of time-variation in snowstorm and snow conductivity on flashover, high-voltage tests were performed under artificial snowstorm conditions in a climatic laboratory. The process of partial discharge propagation until flashover was observed for an energized 33 kV long-rod insulator under snowstorm conditions. As a result, it was found that the higher the snow conductivity, the greater the discharges on the snow-accreted insulator were. However, too much

discharge activity prevented snow accretion on the insulator. This led to snow melting or snow shedding. To conduct further study, new facilities to conduct similar high voltage tests were prepared in the Yokosuka Area. Also, as shown in Figure 3, the generation of fine ice particles with well-defined conductivity in the form of artificial snow was possible. We will continue to observe the flashover phenomena of snow-accreted insulators in detail and develop a high-voltage test method.

4 Construction of a new full-scale test facility for snow-storm damage to overhead transmission lines (abbreviated to "Kushiro test line")

For field observation of galloping and wet-snow accretion on conductors and insulators, full-scale test facilities for snow-storm damage to overhead transmission lines has been newly constructed in Kushiro city, Hokkaido, and operation commenced (Figure 4). The test facility consists of two phases of four-bundled conductor, five phases of single conductor, insulators for observation of snow

accretion, and various meteorological instruments. Using these facilities, field observation data related to meteorological conditions of snow accretion and galloping are acquired. Effects of loose spacers on galloping and of snow resistant rings and counterweights against snow accretion are also examined.

*1 Self-excited oscillation of conductors due to wind and accreted snow or ice. If the amplitude becomes large or the oscillation continues, the phenomenon causes short circuiting or facility failure through fatigue.

*2 Practical examples of short circuit accidents, and damage to electric facility such as supports and conductors due to icing

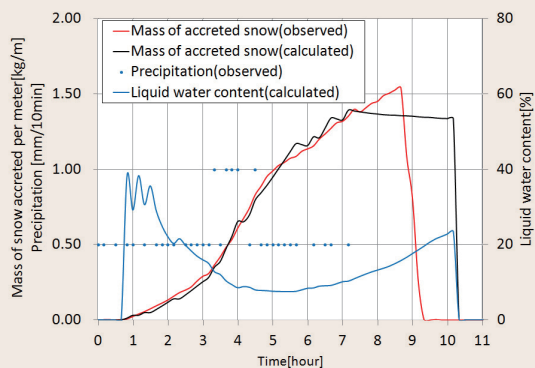


Fig. 1: Time change of mass for accreted snow and liquid water content calculated by SNOVAL-dyn

Using the meteorological data of a wet snow event, the mass of accreted snow calculated by SNOVAL-dyn is compared with that observed on a short conductor sample supported by wire ropes. The SNOVAL-dyn incorporating a thermodynamic model enables us to calculate the liquid water content of snow sleeve, as well as to determine the start time of snow accretion and the snow shedding time.

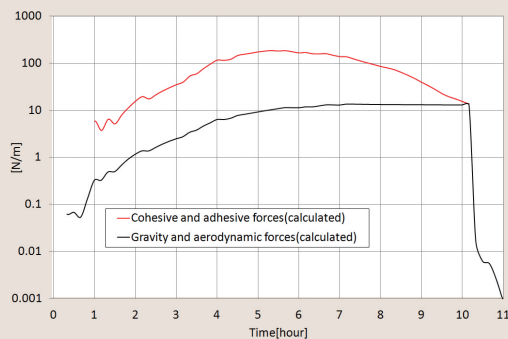


Fig. 2: Time change of cohesive and adhesive forces, and gravity and aerodynamic forces

The cohesive force between the snowflakes as well as the adhesive force between the surface of electric wire and the snowflakes are a mathematical function of the liquid water content of snow sleeve. The snow shedding time in Figure 1 is determined from the point where gravity and aerodynamic forces exceed the cohesive and adhesive forces, which is the intersection between the red and black curves.

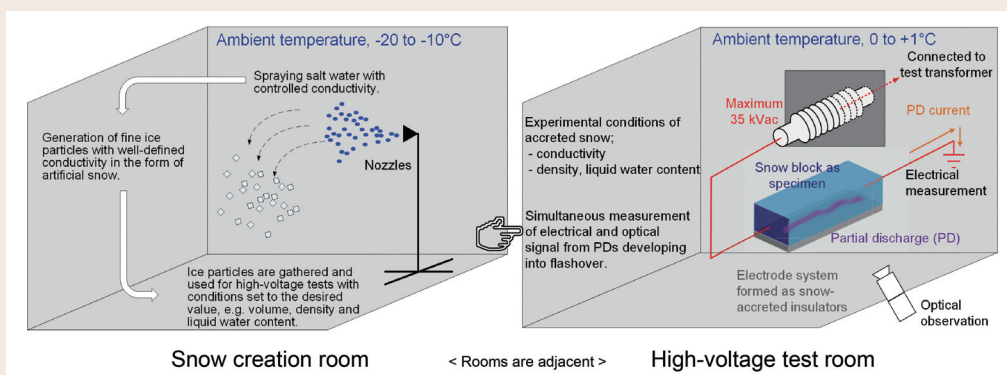


Fig. 3: Overview of snow generation and high-voltage test using the new facilities

New test facilities to conduct further experiments were prepared in the Yokosuka area. These facilities consist of two adjacent rooms used for snow generation and high-voltage tests on snow-accreted specimen. Simultaneous measurement of electrical and optical signal from PD provides important information to clarify flashover mechanisms on snow-accreted insulators.

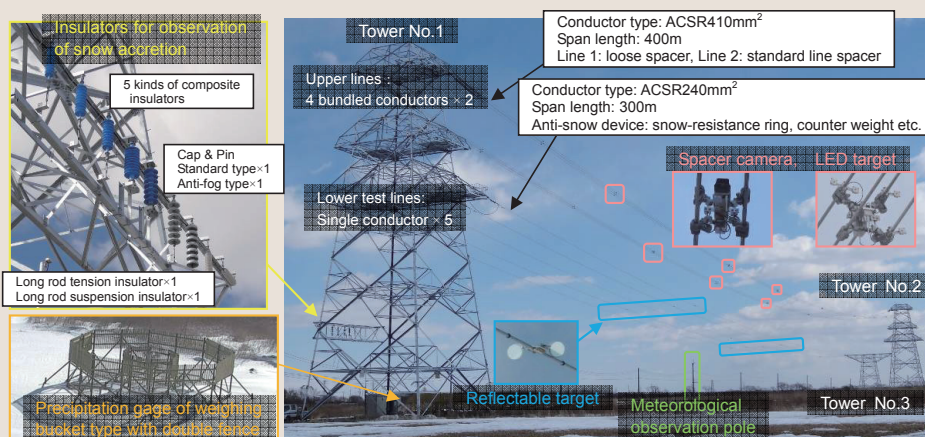


Fig. 4: Full-scale test facilities for snow-storm damage to overhead transmission lines

Meteorological data are acquired by using various kinds of instruments installed in towers and poles. The dynamic behavior of overhead wires is observed by using a tension meter and angle meter, with targets installed in conductors, infrared ray projector, network cameras, spacer cameras. Moreover, insulator specimens were also installed to compare their snow accretion property as well as a precipitation gage, which can measure precipitation with high accuracy under strong wind conditions.

Development of Lightning Risk Management Schemes

Background and Objective

We have carried out studies of lightning protection design for transmission lines, substations and distribution systems and established lightning protection schemes for these apparatuses. However, introduction of ICT (Information and Communication Technology) in power systems such as smart meters and capacity of renewable energy sources such as wind power and solar power will increase in the future. Therefore, lightning protection methods for these facilities are required

in addition to those for conventional power apparatuses.

In this project, we will develop a lightning risk assessment procedure for various power apparatuses and establish lightning protection guidelines for facilities using ICT considering their electro-magnetic immunity. We will then utilize these lightning protection guidelines for the rational lightning protection design of power systems.

Main results

1 Investigating characteristics of lightning strikes to extremely high structures

We installed a wide-band lightning current observation system on Tokyo Skytree, the height of which is 634 m, to clarify lightning current characteristics and characteristics of lightning strikes to extremely high structures such as UHV transmission lines. Observation using this system commenced in 2012*1. It was considered that upward lightning mainly occurred on such high

structures, but two years of observing the Tokyo Skytree revealed that it is subjected to downward lightning as well as upward lightning (Fig. 1). This phenomenon is due to the difference in weather conditions when the tower is struck by lightning. The cumulative distribution of crest values for lightning striking the tower is similar to those previously reported (H13012).

2 Acceleration of 'VSTL REV' and its application to lightning surge analysis of a reinforced-concrete building

We have developed a surge simulation code, VSTL REV, which is based on the numerical electromagnetic computation method in order to predict surge phenomena of three-dimensional structures such as buildings and grounding structures such as grounding grids. In 2013, using the parallel and GPU (Graphics Processing Unit) computing techniques, we made it possible to execute the VSTL REV on GPU-based parallel computers to accelerate the VSTL REV calculation. We confirmed that the improved VSTL REV enables a surge simulation more than forty-times faster in

comparison to a conventional CPU-based simulation. As an example of a surge simulation using the accelerated VSTL REV, we calculated electromagnetic fields inside a real-scale reinforced-concrete building in case of direct and indirect strikes. These calculated results reveals that the concrete and structures of the building such as walls influence the electromagnetic fields inside the building significantly and it is possible to reduce these electromagnetic fields by installing a grid-like shielding inside the building (Fig. 2)(H13009).

3 Evaluation of immunity characteristics for IP equipment installed in power stations

To establish immunity test methods suitable for IP (Internet Protocol) equipment installed in power stations, each bit packet was observed during LAN packet transmissions. The electric fast transient / burst (EFT/B) noise was applied to the power port and the signal (Ethernet) port of switching hubs to observe their effect on data transmission quality by measuring packet losses. It was observed that the interference

to the LAN packet transmission has different aspects for the power port application and the signal port application (Fig. 3). That is, for the power port application, the packet losses occurred in synchronization with each pulse of the burst, while for the signal port application, synchronization was not observed and losses increased as the applied voltage of the noise elevated.

*1 Collaborative research by CRIEPI, University of Tokyo and Tobu Tower Skytree Co. Ltd.

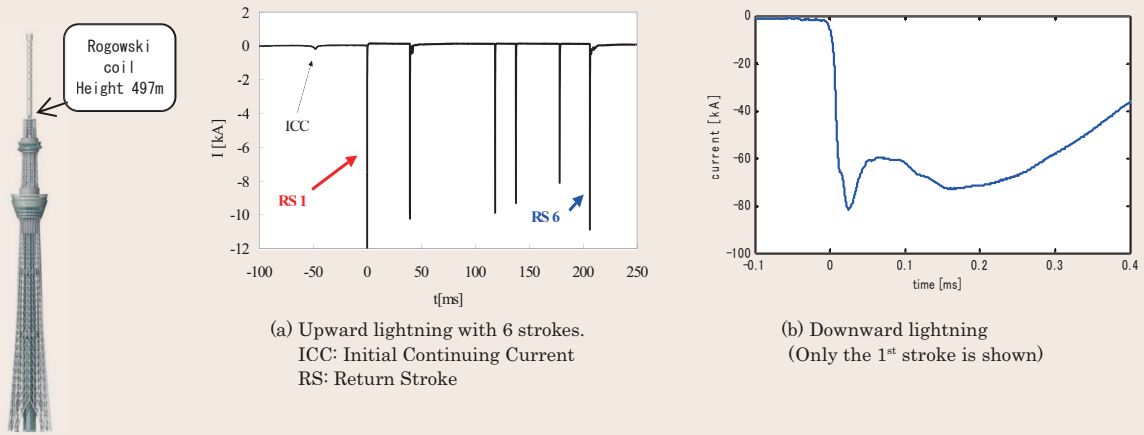


Fig. 1: Examples of current waveforms of upward and downward lightning

In the case of lightning in summer, a lightning flash often contains several strokes. The rise time of a current waveform is in the order of micro-seconds as shown in Fig. 1 (b).

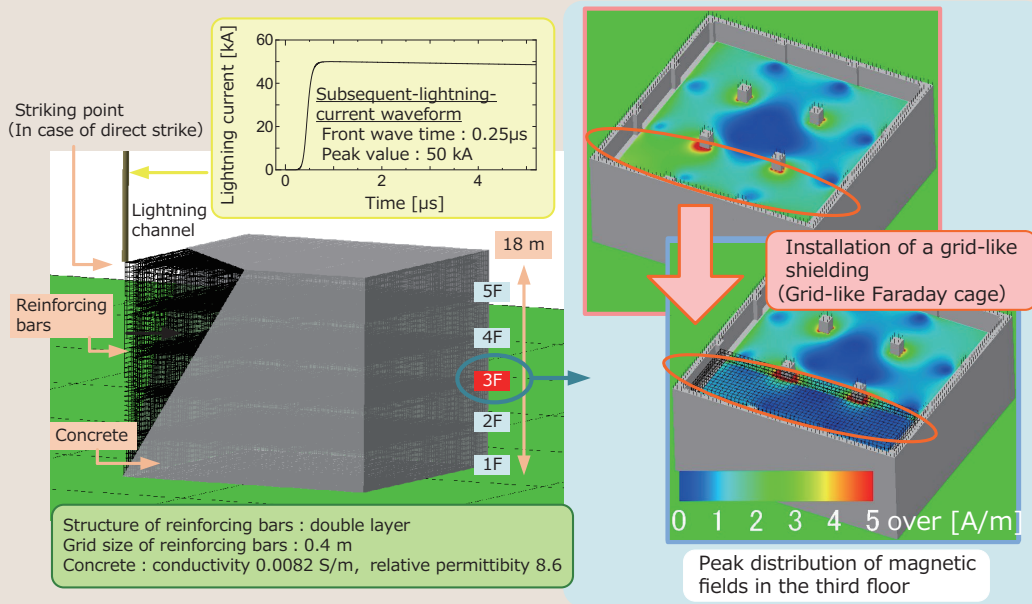


Fig. 2: Analysis of electromagnetic fields inside a reinforced-concrete building struck by lightning

Modeling a building of which the roof is struck by lightning, we calculated electromagnetic fields inside the building and confirmed the effectiveness of a grid-like shielding installed in the building against the electromagnetic fields.

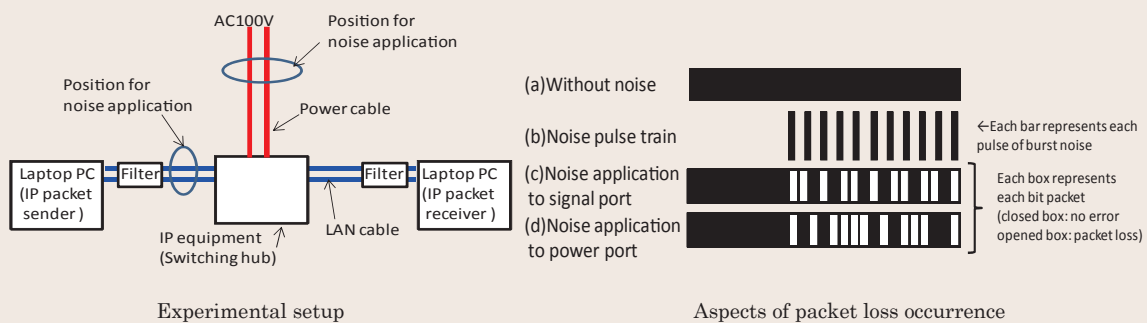


Fig. 3: Aspects of packet loss occurrence for burst noise application to power port and signal port of IP equipment

For the power port application, the packet losses occurred in synchronization with each pulse of the burst, while for the signal port application, synchronization was not observed and the losses increased as the applied voltage of noise elevated.

Well-functioning Electricity Market and Network Neutralization

Background and Objective

In Japan, discussion is underway on institutional design for government policy to reform the electricity industry. In order to make this reform beneficial for society, it is important to identify the risks in institutional changes and to present measures to mitigate such risks. The evaluation of cases in other countries where the electricity industry has been restructured to introduce more competition in the industry would be beneficial

in helping Japan learn lessons regarding the implementation of such a reform program. In this project, we aim to contribute to Japan's successful implementation of the reform by revealing the underlying risks in institutional design of the electricity market and network considered for the reform through our analyses of electric restructuring cases in overseas countries.

Main results

1 A Comparative Analysis of Capacity Mechanisms in the US and Europe

We investigate various capacity mechanisms*¹ introduced or proposed in the U.S. and Europe (Fig. 1). In the U.S., there is a centralized capacity market in the Northeast and bilateral capacity market in California. The bilateral capacity market suffers from a lack of transparency while the centralized capacity market has a risk of price distortion caused

by complex institutional design. In Europe, aiming for a single European electricity market, centralized capacity market is to be introduced in UK while a decentralized capacity market is pursued in France. In addition, there are other types of capacity mechanisms, and as yet, the best practice is unclear.

2 Evaluation of Transmission Unbundling in Germany

We investigated the issues in transmission unbundling in Germany. Two electric power companies are now unable to control the transmission business strategically as a result of choosing "legal unbundling" by transforming their transmission system operators into ITO*² with a strict code of conduct (Fig. 2). This makes it, in effect, very similar to ownership unbundling. Such stricter forms of unbundling are not required

for distribution system operators, over which the holding company still has strategic control. After unbundling the transmission, it is becoming more difficult to coordinate siting of generation and transmission planning, which is likely to lead to an inefficient transmission network. It is important for Japan to consider how to coordinate generation and transmission planning, when unbundling the electric power companies.

3 Issues in Competition Review and Regulated Price in Liberalized Electricity Market

We investigated issues in assessments of electricity retail market competition conducted by the U.K. energy regulator (Ofgem) for 15 years. It became difficult to assess the competition appropriately with indicators such as market shares and switching rates. Ofgem has been relying more on qualitative indicators, such as consumer surveys, though we found that developing appropriate indicators is a complicated task for the regulator (Fig. 3). In addition, determinants of choice between regulated tariffs

and market-based tariffs were analyzed based on a questionnaire survey targeting residential customers (Fig. 4). Residential customers are not likely to choose market-based tariffs when regulated tariffs requiring approval by a regulator is emphasized. On the other hand, it would be effective to allow customers to return to regulated tariffs even after they choose market-based tariffs, in order to induce customers to switch to market-based tariffs.

*1 Mechanism to ensure generation adequacy
*2 Independent Transmission Operator

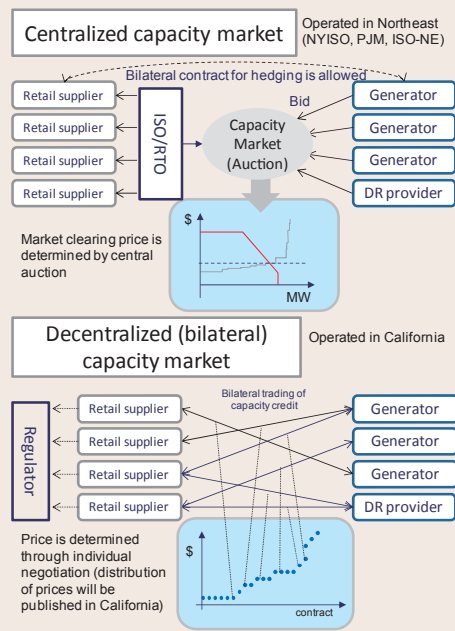


Fig. 1: Categorization of Capacity Market in the United States

In the US, there are two types of capacity market: Centralized capacity market in the Northeast and bilateral capacity market in California. Considerable risk in market design exists for centralized capacity market where price is determined by central auction. Lack of transparency is one of the problems in bilateral capacity market. It is worthwhile to start with a simple bilateral capacity market and gradually improve operation.

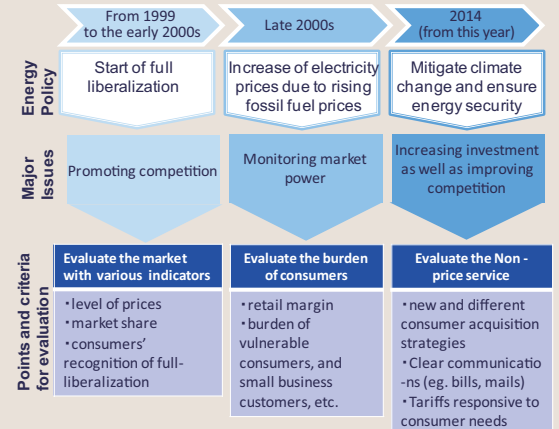


Fig. 3: Transition of electricity retail market competition assessment

In the UK, to assess the electricity retail market, the energy regulator has used not only quantitative indicators, such as market shares and switching rates, but also qualitative ones, such as consumers' experiences. In the late 2000s, as the fuel prices rose dramatically, the energy regulator tried to estimate retail margins, though accurate estimation was apparently difficult. These days, Ofgem has been facing the challenge of developing the qualitative indicators, for instance, new and different consumer acquisition strategies of retailers under vast investment requirements dictated by energy policy. In the near future, the competition assessment of the electricity retail market will be introduced in Japan too. However, as far as we can ascertain from the UK cases, developing appropriate indicators is a complicated task for the regulator under high energy cost.

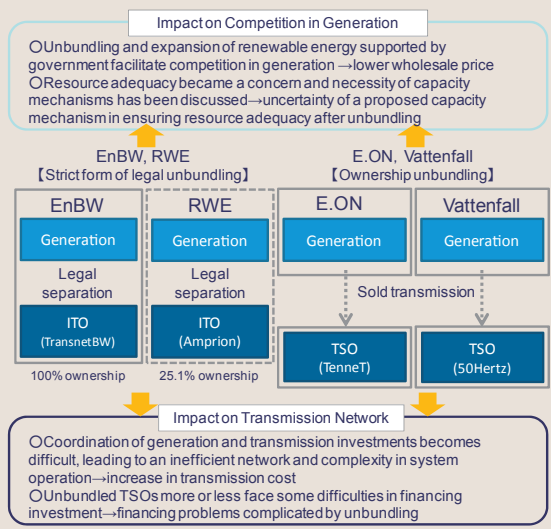


Fig. 2: Current status and issues in transmission unbundling in Germany

In Germany, coordination between generation and transmission investments has become difficult as a result of unbundling, leading to an inefficient network investment and complexities in system operation. In addition, unbundled TSOs face difficulties in financing investment to a varying extent, and unbundling complicates the problem of financing. Competition in generation has been facilitated thanks to a large amount of renewable energy, but capacity shortage in the future is a cause of concern and it is crucial to have an effective capacity mechanism.

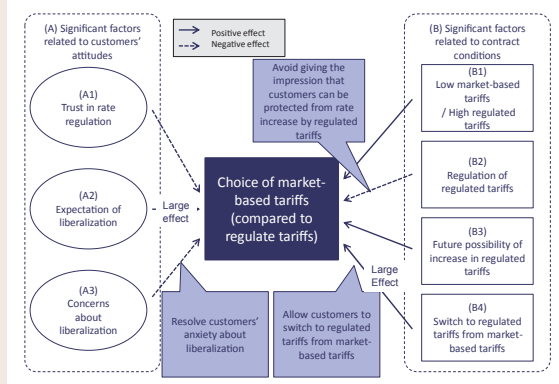


Fig. 4: Determinants of choice between regulated tariffs and market-based tariffs

The results of a survey targeting Japan's residential customers showed that (A) their attitudes and (B) contract conditions would affect their choices. (A) Effect of customers' attitudes: customers who anticipate electricity rate would decrease due to liberalization are likely to choose market-based tariffs (A2). On the other hand, customers who are concerned that they might not be protected against increases and fluctuations in retail electricity price are unlikely to choose market-based tariffs (A3). (B) Effect of contract conditions: Residential customers are not likely to choose market-based tariffs when customers are aware that regulated tariffs need to be approved by the regulator (B2). On the other hand, customers are likely to choose market-based tariffs when customers are allowed to return to regulated tariffs from market-based tariffs.

Analyses of Energy Saving and Environment Institutions from an Economics and Energy Security Perspective

Background and Objective

Nations are considering new proposals for an international framework governing greenhouse gas emissions after 2020. The agreed deadline for this is 2015 and Japan is considering its domestic emission reduction policy.

We will assess the effectiveness of policies

(voluntary approach, energy efficiency policy, renewable energy policy, emission trading and so on) based on empirical analyses of policy implementation. We will propose a national greenhouse gas mitigation policy in harmony with the economy and energy security.

Main results

1 Analysis of electricity saving activities and energy efficiency programs

We conducted a questionnaire and interviews targeting households and firms to analyse their electricity saving activities, perceptions, and persistency after the summer of 2011 (Y13010) (Y13014). The results show that, while the overall activity level of saving electricity was lowered in 2013 compared to the 2011 level, reduction rate of electricity use from the 2010 level has been maintained at around 10%. It is also shown that the cumulative impact of high-efficiency equipment might be compensating the

moderated behaviors (Figures 1 and 2).

We also conducted an evaluation of subsidy programs for energy efficiency (Y13028). Based on a questionnaire to firms which participated in subsidy programs, we estimated the levelized costs per energy saved by the programs, and found that the subsidy programs were mostly cost-effective when compared to the avoided costs and carbon emission prices, although the freerider rates were estimated to be rather high at around 50% to 60%.

2 Evaluating the Feed in Tariff of renewables in some European countries and Japan

The Feed in Tariff (FIT) makes renewables low-risk investments by securing a long-term fixed FIT price, which has led to large expansion. However, FIT has met with criticism due to its increasing cost burden, most notably with regard to so called PV bubbles. According to European countries' experiences, the causes of the PV bubbles were (1) short lead time of PV projects, (2) limited price monitoring by government agencies and (3) excessively high

FIT prices. We find that the solutions to these problems, which have since been put into action, were to frequently reduce the FIT prices, restrict capacity, and retroactively cut the FIT price for existing plants (Table 1). Therefore, given the early experiences with FIT in those countries, Japan needs to pay attention to efficiency when implementing FIT (Y13031).

3 Assessing the effectiveness of voluntary approaches

Using a survey of approximately 1,000 firms in Japan, we find that the establishment of the Voluntary Action Plan (VAP) by Japanese sector associations influenced its member companies to take proper action against climate change. What is more, we find that the VAP significantly promotes the pro-environmental behavior of small and medium-sized companies, which typically face severe energy efficiency barriers owing to relatively smaller capacity to access information.

We conclude that an important role of voluntary approach is not restricting CO₂ emissions, but rather establishing proper institutions within industries to distribute well-becoming information and encourage business pro-environmental activities as far as economically justifiable. Based on these facts, we recognize the success of voluntary approach is best understood by focusing on tangible activities rather than focusing on quantitative outcomes.

4 Analysis of international negotiations on climate change

We analyzed views of countries at negotiations on post-2020 international climate regime (Figure 3). As a result, we found that developed countries and some developing countries generally support a hybrid system in which all countries nationally determine their emissions reduction targets and actions after international consultation on an

ex-ante draft of them, while China, India, and other like-minded developing countries insist that developed countries should set its target in a top-down manner and developing countries can keep discretion to decide their actions in a bottom-up manner (Y13020).

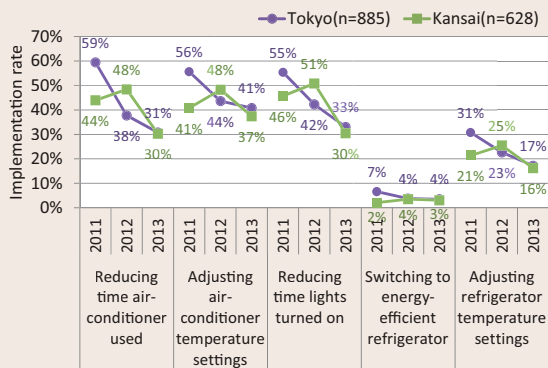


Fig.1: Implementation rates of electricity saving measures in the residential sector

Implementation rates are on a downward trend in 2013, while electricity consumption in the summer after weather adjustment remained below approx. 10% of the 2010 level. The statistical analysis shows that cumulative impact of buying new appliances accounts for about 3% in 2013. With regard to persistence, it is necessary to carefully understand the downward trend of behavior-based impact.

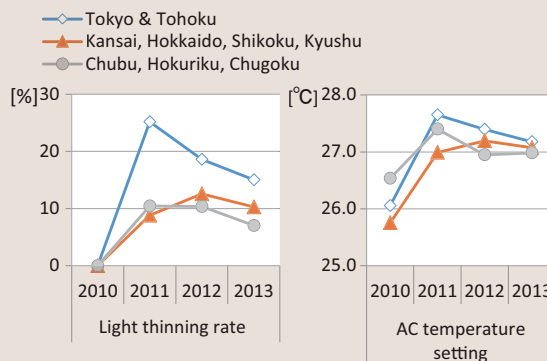


Fig. 2: AC temperature setting and light thinning rates in office buildings for the summers of 2011 through 2013

The overall activity level of saving electricity was lower in 2013 compared to 2011. However, saving activities such as limiting use of lighting and air conditioning were still persisting. The figure to the right shows that the average temperature setting in office buildings was still 1 degree C above the 2010 level in summer 2013. Similarly, the figure to the left shows the rate of light thinning was maintained at around 10% even in summer 2013. It is implied that similar levels of activities and reductions could be sustained at least in the next few years if other factors remain unchanged.

Table 1: Preventing the PV bubbles

Selected European countries have implemented the modified FITs that frequently reduce the FIT prices and restrict capacity to solve the PV bubbles.

	Frequent reduction of the FIT prices	Restrict installed capacity
Germany	Revised every month since May 2012	2.5 GW/year
Italy	Revised every month to 6 months since June 2011	6.8 billion euro/year since Aug. 2012
Spain	Revised every 4 months since April 2010	0.5 GW/year in 2009 0.47 GW/year in 2010
France	Revised every 4 months since 2009	1 GW/year since 2013
UK	Revised every 4 months since 2010	1.06 billion pounds from 2011 to 2014

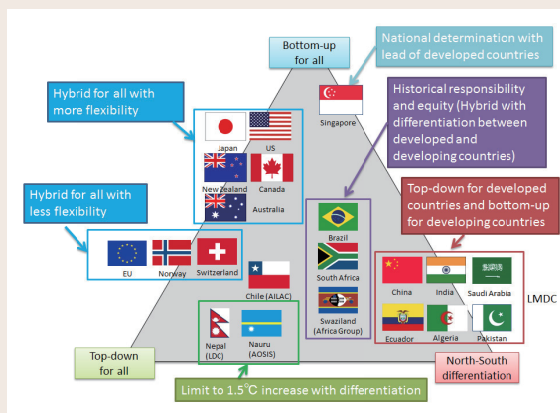


Fig. 3: Views of countries on post-2020 international climate regime

Developed countries generally support a hybrid system that is applied to all countries. Brazil and South Africa propose a hybrid system with differentiation between developed and developing countries. Like-minded developing countries including China and India insist on a top-down system for developed countries and a bottom-up system for developing countries.

Scientifically and Economically Rational Scenarios for Reducing CO₂ Emissions

Background and Objective

Although we do not have a clear outlook for the national energy policy, reduction of CO₂ emissions is a major international issue, as it was before the Great East Japan Earthquake. New scientific findings related to global warming, which form the basis of emissions reduction (including inevitable uncertainties) should be considered in a rational plan of emissions reduction. Based on the latest technology trends and their potential risks, we need to select an appropriate direction for development of low-carbon technology which

can lead to emissions reduction.

This study synthesizes our knowledge of climate science and low-carbon technologies to forecast a long-term target of CO₂ emissions reduction while considering technology availability and economic feasibility. The study thus aims to contribute to the establishment of a long-term national energy policy. We also conduct a preliminary assessment of various risks regarding carbon capture and storage (CCS) to discuss the future adoption of CCS technology.

Main results

1 Implications of new findings from climate science for the long-term target

Regarding the Working Group I (climate science) contribution to the Fifth Assessment Report (AR5) of the Intergovernmental Panel on Climate Change (IPCC), published in September 2013, we have clarified and examined key issues from the perspective of long-term targets. This report shows, for the first time, an approximately linear relationship between the globally averaged temperature increase and cumulative CO₂ emissions since pre-industrial times, which has

been confirmed in our climate model (Fig. 1). However, the proportional constant for the relationship between temperature increase and cumulative CO₂ emissions strongly depends on climate models, which means that the relationship between the climate stabilization target (the upper limit of the temperature increase) and cumulative CO₂ emissions is inconclusive.

2 Analysis of long-term CO₂ emissions targets using an integrated assessment model

Our integrated assessment model (named BET), referenced by the Working Group III (mitigation) contribution to the IPCC AR5, is a tool for evaluating economically optimal emission pathways while considering the cumulative CO₂ emissions targets under energy resource constraints and global scenarios of population and economy. Using this model, key mitigation characteristics for cumulative emissions that are compatible with the 2°C target* have been analyzed. The model results show that the

target requires promotion of electrification and global deployment of technologies for biomass use combined with CCS, and that the emission pathways in 2050 are strongly affected by biomass resource constraints (Figures 2 and 3). Thus, the long-term CO₂ emissions reduction target should be continuously assessed with sufficient flexibility along with the development of low-carbon technologies as well as findings from climate science.

3 Comparison of potential risks to the environment and human health induced by low-carbon technologies

The introduction of CCS in coal-fired power plants in Japan will continue to be discussed in the future, therefore the role of CCS in low-carbon technologies should be clarified. Considering this, we have developed a life cycle assessment method for power generation technologies in terms of the risks they pose to the environment and human health, and conducted an assessment of coal-fired plants with CCS, photovoltaic, and geothermal power generation (Fig. 4). The results

show different characteristics for each technology: for example, the introduction of CCS leads to an increase in the environmental load relative to conventional coal-fired power generation, for all the impact categories except global warming. Considering the wide range of risks to the environment and human health, the introduction of low-carbon technologies should be examined more carefully.

* This is the target that limits the global average temperature increase to 2°C relative to pre-industrial levels. It was documented in the agreements (Cancun Agreements in 2010) in the Conference of Parties to the United Nations Framework Convention on Climate Change. 2°C is considered as an aspiration goal rather than an obligation.

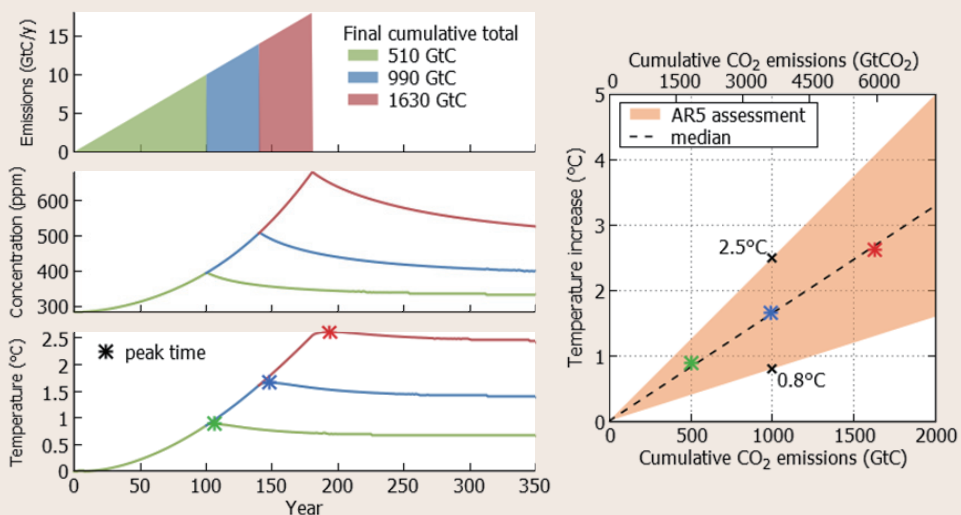


Fig.1: Relationship between the cumulative global CO₂ emissions and global average temperature increase

Results from the computation of the CO₂ concentration and temperature increase for increased emissions when the annual emissions increase by 0.1 GtC consecutively for 100, 140, and 180 years, followed by zero emissions. The IPCC Fifth Assessment Report (AR5) assesses 0.8 to 2.5°C for the temperature increase per 1000 GtC with 66% probability (color-shaded region in the right panel). The dotted line in the right panel indicates the upper limit of the emissions for achieving a given temperature target with 50% probability. Emissions in GtCO₂ are 3.67 times higher than in GtC (the amount of carbon alone).

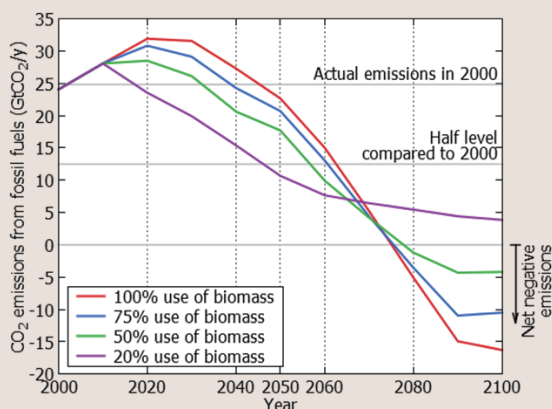


Fig. 2: CO₂ emissions pathways from fossil fuels compatible with the 2°C target

Fig. 2 shows the CO₂ emissions pathway scenarios that enable us to achieve the 2°C target computed with four different constraints for available biomass resources. As shown in Fig. 3, an increase in electrification rates is necessary in all scenarios. In addition, net negative emissions in the future require not only innovative technologies, such as heat pumps, electric vehicles, and hybrid freight vehicles, but also CO₂ removal technologies, such as biomass use combined with CCS.

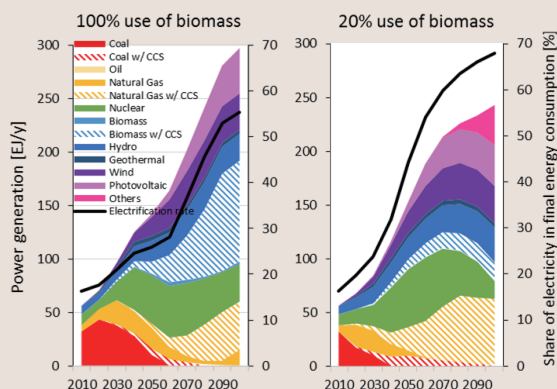


Fig. 3: Transition of the global power generation mix (left axis) and electrification rates (right axis) compatible with the 2°C target (EJ=10¹⁸J)

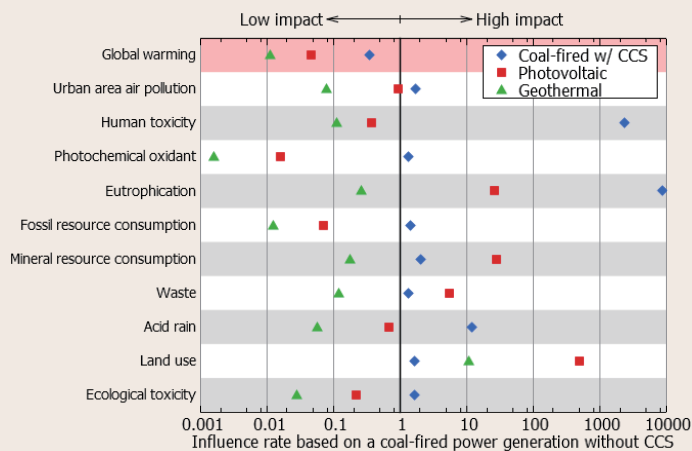


Fig. 4: Comparison of categorized environmental and health impacts throughout the life cycle of low-carbon power generation plants

The assessment results show the environmental impacts for each technology relative to conventional coal-fired power generation. The introduction of CCS in coal-fired plants increases the environmental impact in all the categories except global warming. The impact of photovoltaic power generation is noticeable in the category of mineral resource consumption among others, which is caused by manufacturing of solar panels. The impact of geothermal power generation is relatively low except in the category of land use.

Structural Integrity Evaluation of Reactor Pressure Vessels and Core Internals

Background and Objective

In order to accomplish the safe and stable operation of LWR plants, we will enforce the technical basis for structural integrity of reactor pressure vessels (RPVs) and core internals through

better-understanding of various degradation mechanisms together with the development and the improvement of evaluation methods. In this project, we have conducted the following research.

Main results

1 Improvement in the method for integrity evaluation of irradiation embrittlement in RPV steels

Microstructural observation of a weld material cut out from a RPV of the Greifswald reactor in Germany was carried out using atom probe tomography (APT), which enables observation at an atomic level. Although the material was fabricated

in accordance with the German standard differing from the Japanese one, the formation of small solute atom clusters due to irradiation was confirmed (Fig. 1). The results will be utilized for the analysis of Japanese decommissioned reactor materials.

2 Evaluation of irradiation effects on microstructural changes in stainless steels

Grain boundary segregation is one of the causal factors of irradiation-assisted stress corrosion cracking (IASCC). The segregation in a type 304 stainless steel irradiated up to 5.5 dpa*, at which the materials in commercial reactors are deteriorated,

was investigated using APT. Both in a grain and at a grain boundary, segregation was observed (Fig. 2). Based on the APT observation, we will elucidate the effects of the segregation on IASCC.

3 Development of a practical application technique for the Master Curve evaluation

We developed the Master Curve testing and evaluation technique using miniature specimens machined from surveillance specimens. The fracture toughness based on the miniature specimens was equivalent to that of larger specimens (Fig. 3). We

conducted an international round robin test and ensured the reliability of the technique. We will codify the new testing standard in collaboration with the related organizations^[1].

4 Adequacy of stress intensity factor solutions for nozzle corner cracks

Japanese code^[2] requires structural integrity for the supposed cracks in nozzle corners. We examined the applicability of the stress intensity factor

solution in the code through a comparison with a finite element analysis result and ascertained that the solution gave reasonable prediction (Fig. 3).

* dpa (displacement per atom): A unit corresponding to the number of displacements per atom in the material due to irradiation.

[1] M. Yamamoto, et al., Sixth International Symposium on Small Specimen Test Techniques, 2014

[2] Japan Electric Association Code, "Method of Verification Tests of the Fracture Toughness for Nuclear Power Plant Components," JEAC4206-2007.

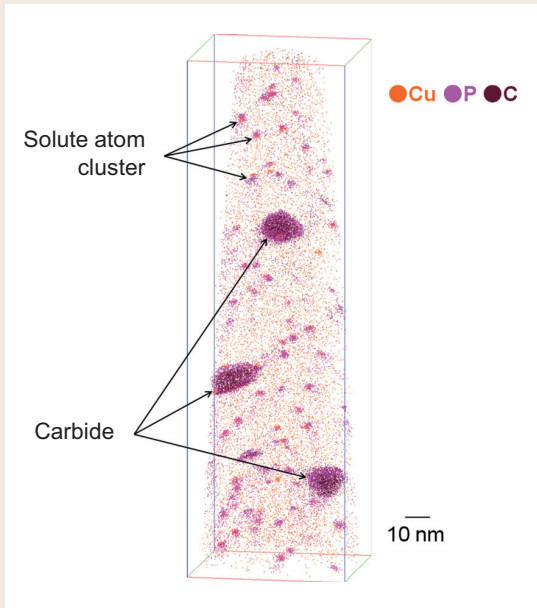


Fig. 1: Atom map of RPV weld material from a decommissioned commercial plant

This is the result of the APT observation of a weld material cut out from the RPV of the Greifswald Unit 4. The formation of solute atom clusters with the segregation of copper and phosphorous due to irradiation can be confirmed. Fine carbides and phosphorous segregation to the surroundings of the carbide are also observed.

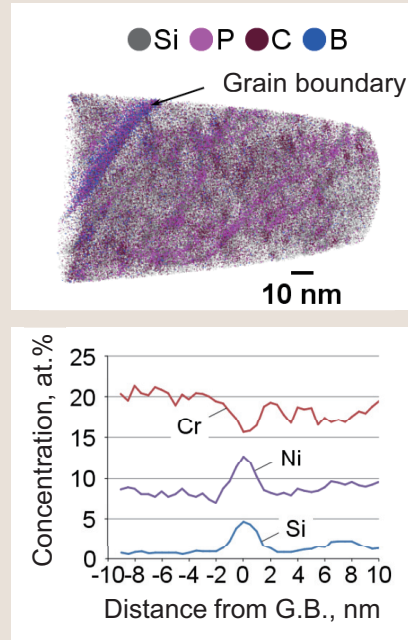


Fig. 2: Atom map (top) and result of grain boundary (G.B.) analysis (bottom) of irradiated type 304 stainless steel

This is the result of APT observation of type 304 stainless steel irradiated to 5.5 dpa. The segregation of nickel and silicon and the depletion of chromium at the grain boundary as well as the segregation of silicon, phosphorous, and carbon in the grain can be observed.

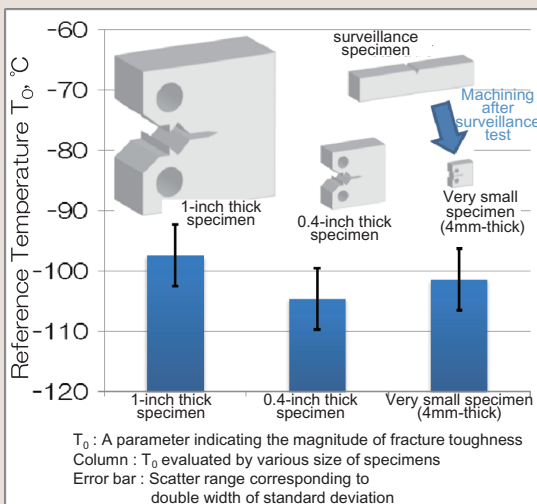


Fig. 3: Comparison of reference temperatures obtained from miniature and larger specimens

This compares the reference temperature (an index indicating the magnitude of fracture toughness in dimension of temperature) among various specimens. The reference temperature obtained from miniature specimen was equivalent to that of the larger specimens.

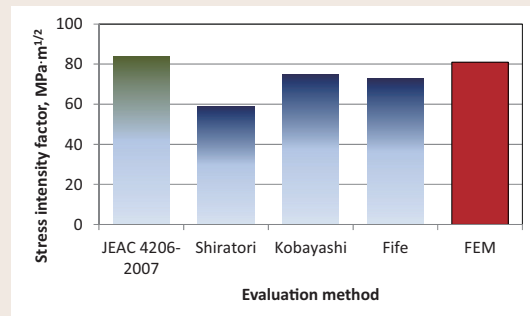
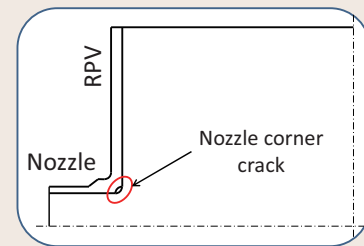


Fig. 4: Comparison of stress intensity factor solutions for nozzle corner crack

Compared with the finite element analysis result, every solution gives adequate stress intensity factors. The solution in JEAC4206 can treat membrane stress only, whereas the other solution can consider complex stress distribution at nozzle corner.

Integrity of Components and Piping in Nuclear Power Plants

Background and Objective

Flow Accelerated Corrosion (FAC) and Liquid Droplet Impingement Erosion (LDI) are pipe degradation phenomena managed by utilities with pipe wall thickness measurement based on JSME technical rules. There are expectations regarding optimized allocation of inspection resource for this management, with development of an accurate mechanistic prediction method for FAC and LDI as described in the revision plan of the JSME rules.

There is discussion currently underway relating to elimination of rolled steels for general structure (SS steels) from the JSME material code. Such SS

steels are widely used in power plants. Rolled steels for building structures (SN steels) is a possible candidate to be included in the JSME material code as an alternative to SS steels. However, to apply SN steels to nuclear power plants, it is necessary to standardize them based on evaluation of detailed material properties.

In this project, we develop a prediction method of pipe wall thinning able to be applied to actual plants. We also evaluate mechanical properties of SN steels for standardization.

Main results

1 Verification of Pipe Wall Thinning Prediction Software, FALSET, with Water Single-Phase Flow Pipeline Data

Pipe wall thinning prediction software, FALSET, is being developed for its application to the FAC/LDI prediction methods for wall thinning management in actual power plants. FALSET was verified with FAC data in condensate and feedwater lines (water single-phase system), and its prediction accuracy

was confirmed to be within about 10% of error for residual thickness (Fig. 1) (L12403). Following further verification and revision with power plant data, FALSET is expected to be introduced to wall thinning management rules and used practically as a management tool.

2 Modeling for FAC prediction in Steam-Water Two-Phase Flow

For the modeling of FAC in steam-water two-phase flow conditions, such as extraction and drain lines, an evaluation method was developed for the assumed specific hydraulic condition, i.e. annular flow. This method showed considerable accuracy for the liquid film behavior created on the inner wall of a pipe (Fig. 2) (L12008). As for water chemistry factor, a calculation method for liquid film pH was

studied, including the gas-liquid distribution effect of pH agent (Fig. 3) (Q11025). Considering these differences from water single-phase flow condition, the FAC prediction method will be extended to two-phase flow condition, and applied to the FALSET software after certain verification with power plant data.

3 Evaluating Tensile Properties of 'Safety-Conscious' SN Steels at High Temperature

SN steels is expected to be used for support structures in nuclear power plants as an alternative to SS steels. Comprehensive tensile properties of SN steels were compiled at high temperature so that they can be incorporated into the JSME material

code. The effect of temperature on the tensile properties was similar in spite of the different origins, material types, or plate thicknesses (Fig. 4). The effects of strain rate as well as the contents of P and S were also small (Q13009).

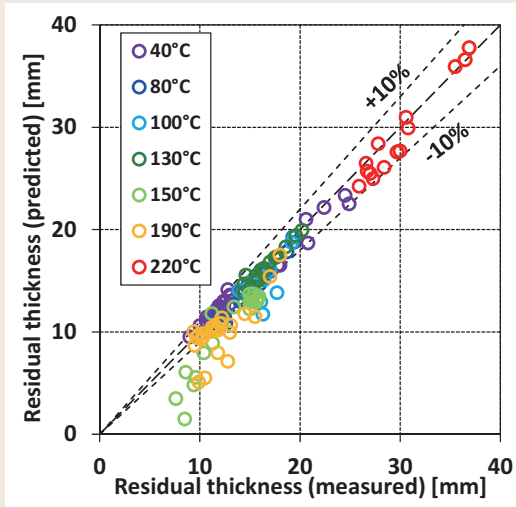


Fig. 1: Comparison of the measured residual wall thickness with that predicted by FALSET for water single-phase flow pipeline

Excluding some underestimated conservative data, FALSET demonstrated a prediction accuracy within approximately 10% of error for residual wall thickness of 160 elbows in condensate/feedwater pipelines of a PWR

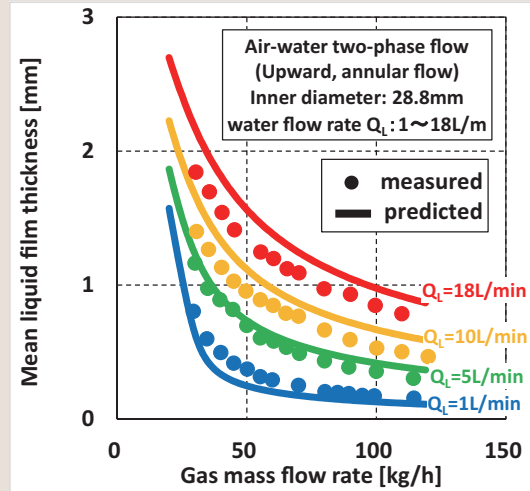


Fig. 2: Evaluation of liquid film thickness in gas-liquid two-phase annular flow

With the developed analysis method, experimental data of liquid film behavior (mean thickness) from a previous study⁽¹⁾ can be quantitatively predicted.

(1) T. Ueda, S. Nose, Trans. JSME, 39, 325 (1973)

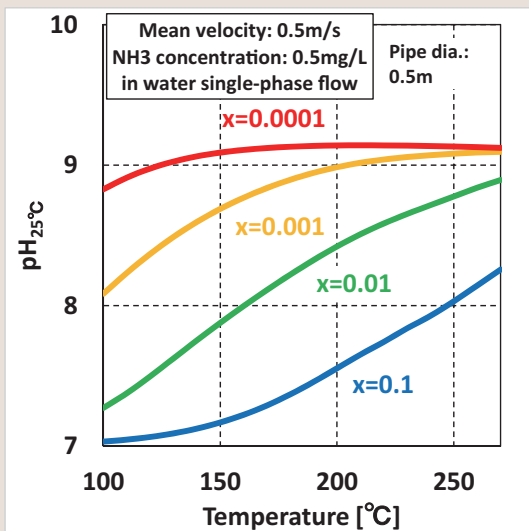


Fig. 3: pH evaluation with gas-liquid distribution of pH agent in a two-phase flow condition

Considering the distribution behavior of pH agent (ammonia: NH_3) to gas/liquid phases, pH value in the liquid film can be simply evaluated in terms of temperature and steam quality (x).

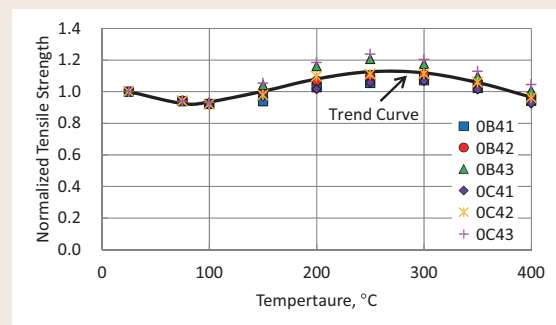


Fig. 4: Effect of temperature on tensile strength for SN steels

Tensile strengths at high temperature are normalized by those at room temperature. OB41 to OB43 and OC41 to OC43 use different steels (SN400Bs and SN400Cs) with a thickness of 40 mm, respectively. The different types of steels has different contents of P and S; nevertheless, the effect of temperature is presented by a unique line.

Assessment of Cable Insulating Performance Used in Nuclear Power Plants

Background and Objective

Evaluating the insulating performance integrity of instrumental and control cables used in containments is important to establish safe and stable operation of nuclear power plants. Heat and radiation, along with their synergic effects, have to be adequately considered on the basis of in-service aging states to implement technically reliable

aging prediction on polymeric insulating materials. The aim of the present study is to investigate and improve the lifetime evaluation method to consider several factors under normal plant operation conditions. This is undertaken through analyzing the aging trend of service-used cables.

Main results

1 Confirming integrity through analysis of service-used cables

Short available service duration is predicted based on an accelerated aging test for some kinds of frame-retardant ethylene propylene rubber insulations*¹. Analysis on mechanical properties such as elongation at break and on chemical properties such as micro infrared spectroscopy as

well as oxidation induction time were carried out for the corresponding service-used cable insulations in the present study. The result depicted in Fig. 1 shows that their integrity is secured even 24 years after installation (operation duration: 16 years).

2 Statistical data analysis of service-used cables

Statistical analysis was conducted for elongation at break values*² obtained for the service-used cable insulations*¹. Service period used for the analysis was evaluated assuming that the cables were used under the same condition, 60°C and 10 mGy/h, since the actual environments were different for each of the cables. A regression curve was obtained

to reveal the aging trend under normal operation conditions. The curve was then used as a reference and each mechanical data was extrapolated to estimate their service duration*³. The result (Fig. 2) shows that the predicted available service duration based on accelerated aging tests is much shorter than the reference one (H13002).

3 Wear-out artificial additional aging for service-used cable

An additional thermal aging test based on wear-out approach*⁴ was performed for the service-used cable insulation (Fig. 3). The mechanical aging trend observed during the test was slower than the one predicted from the acceleration aging

result in the ACA project*¹ (Fig. 4)*⁵. Moreover, by performing a recovery analysis using a logistic function it was quantitatively suggested that aging slows down.

All the analyses conducted above show that the prediction using the acceleration aging test reported in the literature*¹ is too conservative.

*1 Japan Nuclear Energy Safety Organization, JNES-SS-0903, 2009 (Assessment of Cable Aging for Nuclear Power Plant, ACA project)

*2 Y. Eguchi, 2012 Equipment Qualification Technical Meeting, San Antonio, TX, 2012

*3 Criterion on elongation at break is set to 70%, and service duration is estimated for the actual operation period to reach this value.

*4 A methodology to estimate the material lifetime from the relation between the operation period and wear-out time to reach the criteria.

*5 N. Fuse et al., IEEE Tech. Meeting on Dielectric and Electrical Insulation, DEI-14-42, Tokyo, 2014.

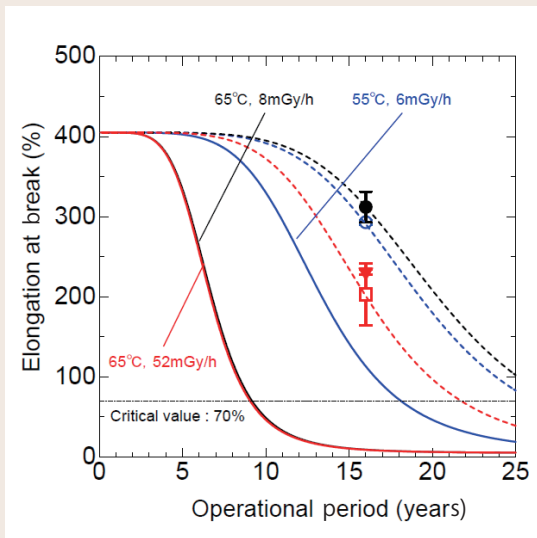


Fig. 1: Comparison of aging trends in service-used cables and aging prediction by the ACA project

Several instrumental analyses were conducted on service-used cables in order to evaluate their integrity. Discrepancies between the prediction by the ACA project (solid curves) and the actual aging trend (broken curves) are clearly shown.

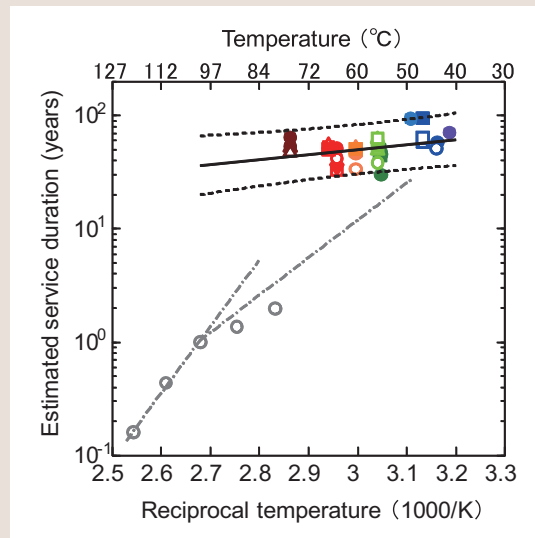


Fig. 2: Service duration estimated for cables used in nuclear power plants and their temperature in an Arrhenius plot

Colored plots are the duration estimated for each service-used cable. Their regressed result is shown in a black solid line, and the two broken curves represent 95.4% prediction band. Gray open symbols are the result of an acceleration aging test performed by the ACA project.

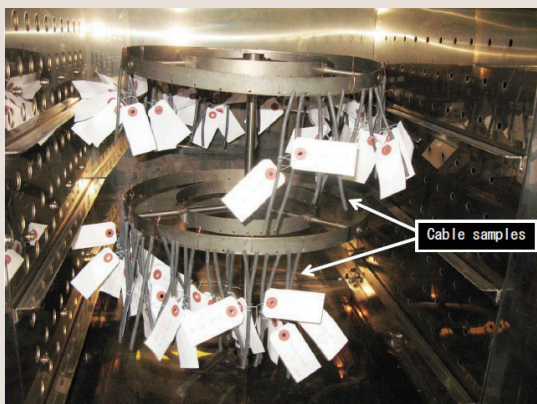


Fig. 3: A thermostatic oven during the wear-out additional aging test

Additional heat aging is performed on service-used cable insulations at 110°C. The test meets the Japanese Industrial Standard to use a gear oven with air ventilation every hour. Conductors are removed from the samples prior to the test.

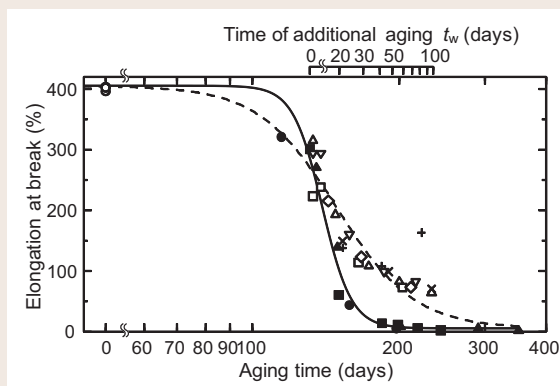


Fig. 4: Comparison of the mechanical aging trend during the wear-out test to that predicted based on the ACA project result

The solid plotting with a regressed curve indicates the prediction based on ACA project result. The open circles are the value for un-degraded samples. The other open symbols and their regressed curves represent the wear-out testing result of service-used cables.

Research of Advanced Nondestructive Evaluation

Background and Objective

For the sake of appropriate maintenance and securing the safety of electric power facilities including nuclear power facilities, the nondestructive inspection of defects in metals used in such facilities is important. In this project, optimum NDE technologies are

developed for important components related to the safety of light-water reactors to enhance the operation safety of light-water reactors. Meanwhile, standardization and implementation of a PD system*¹ for these technologies are also taken into consideration.

Main results

1 NDE method development for fatigue cracks in embedded foundation bolts

Wave propagation in bolts was simulated to develop an ultrasonic phased array technology*² for inspection and sizing of fatigue cracks in the embedded foundation bolts of nuclear power plants. Numerical results show that two peaks can be observed in the curve of echo intensity versus refraction angle. One of the peaks corresponds

to the vicinity of crack tip and strongly depends on crack depth. This phenomenon is also verified by experiments. A conservative method for depth sizing of fatigue cracks is proposed by making use of this peak. The deviation between actual depth and determined value is smaller than 2 mm.

2 Elucidating initiation and growth behavior of stress corrosion cracking for low carbon stainless steels

A series of creviced bent beam tests for low carbon stainless steel was conducted to clarify the initiation behavior of SCC on PLR piping. The tests revealed that distribution of crack depth initiated on the CBB*³ specimen does not depend on a strained surface condition. In addition, the number of cracks greater than 20 μm depth (correspond to

average depth of single grain) gradually increase with testing time in the early stage, then increase rapidly, as shown in Figure 2. The results indicate the possibility that crack depths greater than 20 μm is caused by coalescence of small cracks. Therefore, further investigation on the coalescence process is needed. (Q13008)

3 Effectiveness of the PD qualification system

PD Center has conducted PD examination of SCC depth sizing for nuclear power plant piping based on PD qualification code NDIS0603 of JSNDI*⁴. The result (44 out of 89 persons passed from March 2006 to January 2013) indicates that the passed

candidates can size SCC depth with high accuracy (Fig. 3)^[1]. This means the PD qualification system improved the reliability of crack depth sizing and contributed to the management and maintenance of nuclear power plants.

[1] H. Shohji et al., E-Journal of Advanced Maintenance Vol.4 (2013) 125-132

*1 Qualification and certification of personnel for performance demonstration of ultrasonic testing systems

*2 A technology possibly fires ultrasonic waves with different directions and focus positions by controlling transmission and reception timing of each individual elements in a phased array transducer.

*3 Environmental acceleration testing method by introduce crevice to the bended specimen.

*4 The Japanese Society for Non-destructive Inspection

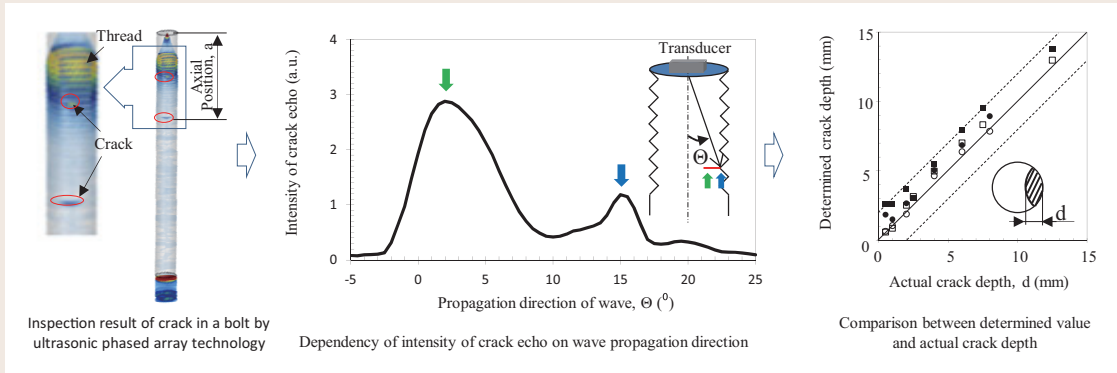


Fig. 1: Inspection and sizing method of cracks for embedded foundation bolts

It is possible to observe two peaks corresponding to the corner and the vicinity of a crack in a bolt when it is inspected by ultrasonic phased array technology (These two peaks overlap for a shallow crack). The peak resulted from the vicinity strongly depends on crack depth, therefore, the position of this peak can be used to determine crack depth.

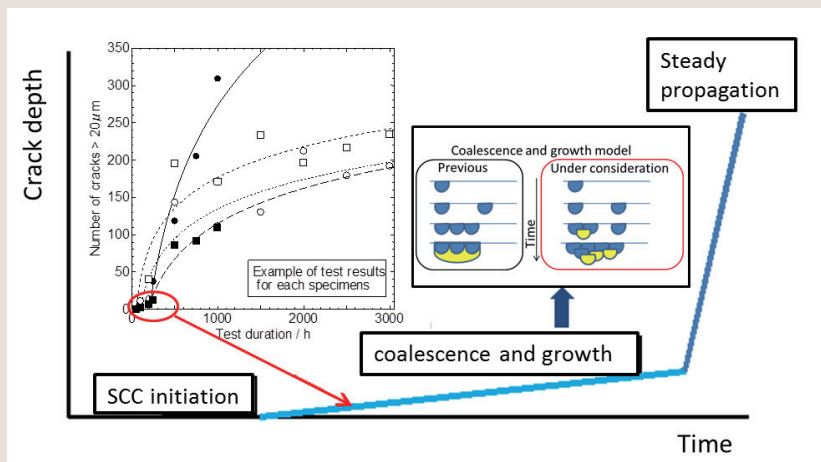


Fig. 2: Time dependence of crack depth (greater than 20 micrometers) for low-carbon stainless steel

Number of cracks greater than 20 mm in depth obtained by CBB tests for low-carbon stainless steel gradually increase at first, then increase rapidly. Previous model based on the coalescence process then growth is not able to explain the behavior of early stage. The results indicate the step by step coalescence and growth in early stage. Detailed investigation on coalescence and growth process is needed to clarify the SCC initiation and propagation behavior.

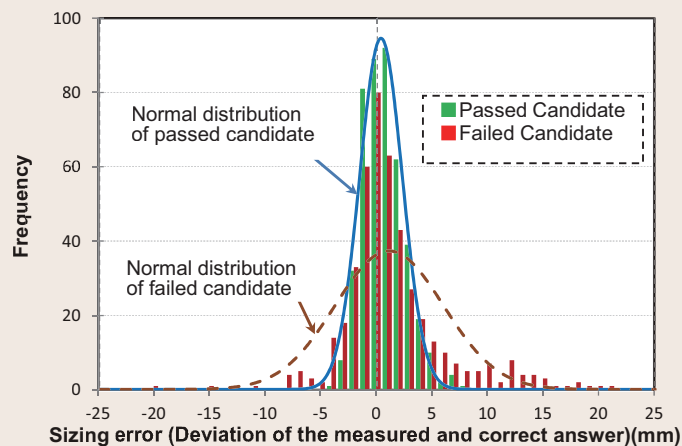


Fig. 3: Analysis of the PD examination results

The passed candidate can measure SCC depth in high accuracy (Average error: 0.33 mm, standard deviation: 1.92 mm). For a failed candidate, the average error is 1.05 mm and standard deviation is 4.87 mm.

Development of Life Assessment Technology for High Temperature Structural Components of High Chromium Steels

Background and Objective

Ultra-supercritical (USC) pressure thermal power plants supply power with high efficiency and large capacity. However, troubles caused by creep damage have occurred in various types of welded joints in the large-diameter high chromium steel pipes of such plants. Such troubles adversely affect the stable operation of USC thermal power plants. The establishment of highly reliable diagnostic

technologies for high-temperature equipment made of high-Cr steel is required as a preventive measure. In this project, we aim to develop diagnostic techniques for assessing creep damage in girth welds and nozzle stub welds of the high-Cr steel pipes, which are both welds vulnerable to creep damage, and to apply the technologies to the on-site maintenance and operation of facilities.

Main results

1 Creep damage mechanism of 12Cr steel pipe girth welds

In order to clarify the creep damage mechanism of high-Cr steel girth weld, a creep test was performed under superimposed condition of an internal pressure and a bending load. The specimen was a large-diameter pipe with the dimensions of actual piping made of 12Cr steel with girth welds. The creep test was interrupted to inspect the specimen when its deformation rate increased rapidly. A

surface crack was observed in the girth weld where axial tensile stress was applied due to the bending load (Fig. 1). Detailed observation of cross-sections of the girth weld in the specimen revealed that creep cracks initiated inside the wall thickness of the pipe and the cracks propagated along the fine-grained heat-affected zone (HAZ) of the base metal.

2 Nondestructive inspection and life assessment of girth welds in 12Cr steel pipe

To establish maintenance technology for high-Cr steel girth welds, ultrasonic nondestructive testing (UT) was carried out on the 12Cr steel pipe welds before the pipe was cut. Creep cracks were indicated over a wide area in the girth welds of the pipe wall thickness. This result was in good

agreement with the observation of cross-sections of the girth welds, demonstrating the applicability of UT (Fig. 2). Using the analytical life estimation technology developed by CRIEPI, the creep life of the girth welds was successfully predicted with a high accuracy on the basis of the strain criterion.

3 Factors affecting creep life of 9Cr steel welds

To develop a highly reliable diagnostic technique for high-Cr steel welds, various factors affecting the creep life of 9Cr steel welds were experimentally investigated. It was found that the creep life becomes shorter as the angle between the fusion

line and the stress direction, which is equal to 90 degrees minus the groove angle in welding joints, becomes smaller (Fig. 3). This suggests that the groove angle should be considered in the assessment of welds.

4 Assessment of remaining creep life of re-welded portions of 9Cr steel

A 9Cr steel weld subjected to creep damage was re-welded so that a groove edge in the re-welding was made in the initial weld metal. In a creep test performed after the re-welding, it was found that the remaining creep life was much shorter than that with no re-welding. In the creep test, a crack was generated from the HAZ, which was formed in the weld metal by the re-welding, whereas cracks are generated from the fine-grained HAZ in the base

metal in the case of normal 9Cr steel welds. Finite element creep analysis was conducted by modelling each material property in the re-welded portion. As a result, strain concentration was found to occur in the HAZ of the weld metal (Fig. 4). This result suggests that numerical analysis can be an effective tool to assess the remaining creep life of re-welded portions which usually have a complex shape.

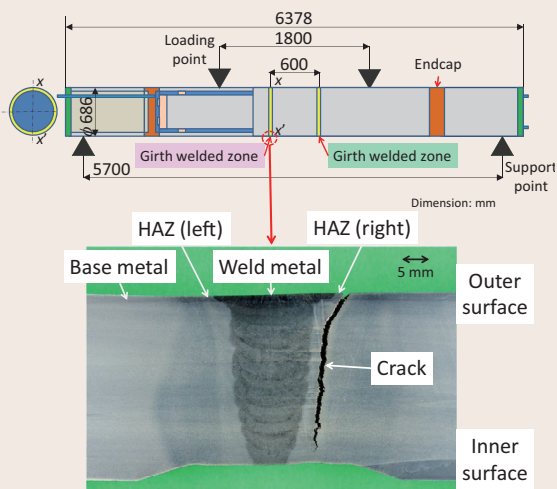


Fig. 1: Cross-section of a girth weld in 12Cr steel pipe after creep test

After a creep test at 650°C for approximately 8,000 h, propagation of a macroscopic crack was observed along the fine-grained HAZ of the girth weld where tensile stress due to bending was applied.

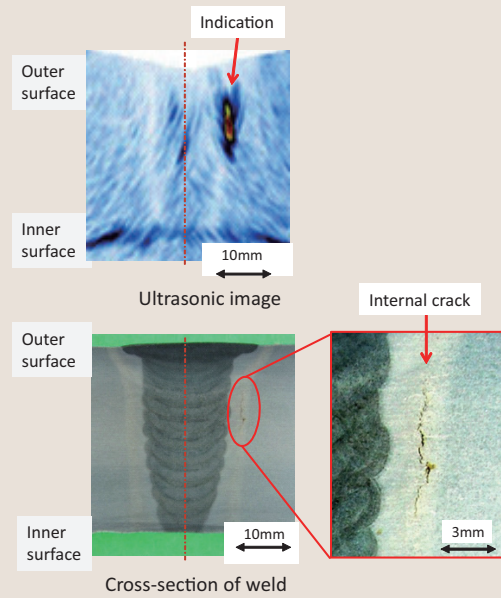


Fig. 2: Applicability of ultrasonic testing

Internal cracks in girth welds of 12Cr steel pipe were successfully detected by ultrasonic testing.

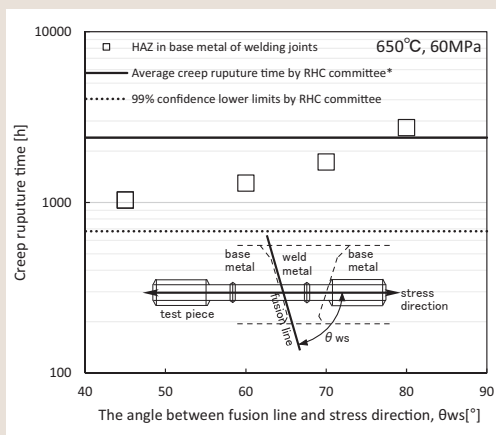


Fig. 3: Factors affecting creep life of 9Cr steel welds

The creep life decreases as the angle between the fusion line and the stress direction, which is equal to 90 degrees minus the groove angle, reduces.

*RHC committee: The Committee on Review on Reliability of High Temperature Strength Enhanced Ferritic Steels for Fitness-for-Service of Thermal Power Components

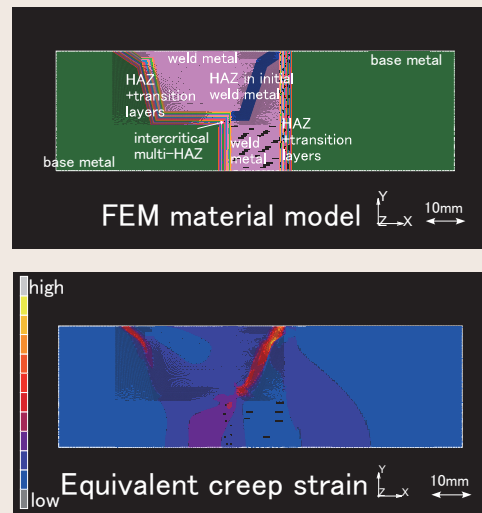


Fig. 4: Finite element creep analysis of a re-welded portion of 9Cr steel

Finite element analysis for a re-welded portion of 9Cr steel was conducted based on the modeling of each material property. Strain concentration was found to occur in the HAZ formed by the re-welding within the weld metal, where a creep crack was observed in an experiment.

Development of Comprehensive Assessment Techniques for the Impact of Thermal Power on Atmospheric Environment

Background and Objective

Japan's dependence on thermal power generation and interest in the generation of geothermal power, which is renewable and can be stably supplied, have been increasing concurrent with the long-term stoppage of nuclear-power-plant operation. Prompt and low-cost assessment of the environmental impact from the construction, extension, and replacement of thermal and geothermal power plants has been required. Thermal power plants are suspected to be the emission sources of secondary-air-pollution-precursors, such as particulate matter

with a diameter of 2.5 μm or less (PM_{2.5}) and photochemical oxidants. Thus, some measures from a scientific viewpoint will likely be demanded in the future. The objective of this research is to develop a method and a tool (software) for easy, rapid, and inexpensive assessment of atmospheric environments. In addition, an assessment method for secondary air pollution is developed to clarify the impact of emission sources and contribute to the formulation of rational measures against the emission of these agents.

Main results

1 Development of an atmospheric environmental assessment support tool for thermal power generation

The research team developed an atmospheric environmental assessment support tool applicable in a wide range of tasks from preliminary environment impact assessment to the preparation of assessment reports for the construction, extension, and replacement of thermal power plants. When source conditions (*e.g.*, position and height of stacks, specifications of emission gas) are input, the dispersion of emission gas in the atmosphere is calculated to draw a distribution of the concentration of the dispersed emission gas on a map. In addition,

the support tool automatically acquires publicly available environmental concentration data to enable easy assessment of the impact of the emission gas on the surrounding environment. Furthermore, the support tool can calculate the dispersion of the emission gas from multiple sources then automatically determine particular meteorological conditions and geographical properties that may cause a high concentration of emission gas using source information and geographical data (Fig. 1) (V13020).

2 Development of a dispersion prediction numerical model for atmospheric environmental assessment of geothermal power generation^{*1}

The research team has begun developing a numerical model that can replace the wind tunnel experiments generally used in dispersion prediction to speed up the time taken for atmospheric environmental assessment of geothermal power generation and reduce the associated cost. The research team constructed a simplified model that is applicable to a relatively simple geography

and developed its prototype model for rapid numerical analysis. For a detailed model that covers complicated geography and the effect of reactor buildings, the results of the calculation using the model were compared with those of wind tunnel experiments to determine the precision of the turbulent-flow model used as the base model and to clarify the problems of the developed model (Fig. 2).

3 Development of an assessment method for impact of emission source on secondary air pollution

Ozone is a secondary air pollutant synthesized in the presence of nitrogen oxide and organic compounds. It is also closely related to the generation of PM_{2.5}. As an assessment method of the impact of the emission source on ozone concentration,^{*2} the applicability of a high-precision and high-sensitivity analysis method^{*3} and a tracer tagging method^{*4} with low calculation cost was compared. The result indicates that the latter overestimates the impact of the emission source on the environment close to the source compared with the former. When a

similar analysis was carried out by introducing a concept that considers ozone depletion (potential ozone^{*5}), the results obtained using the above two methods were in good agreement. From this finding, the tracer tagging method was demonstrated to be an effective assessment method for impact of the emission source on ozone concentration (Fig. 3). The achievement of this research will be utilized to assess the impact of thermal power generation on secondary air pollution.

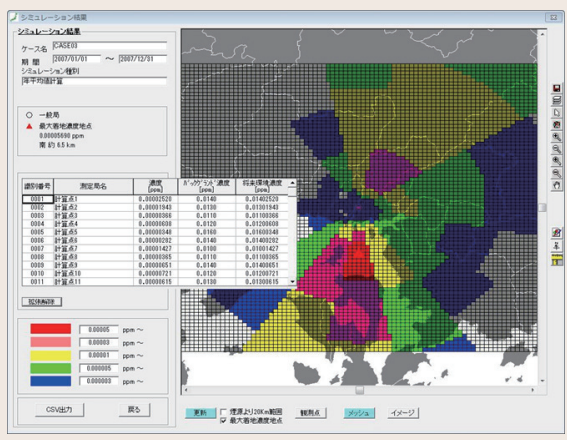
*1 Jointly developed with New Energy and Industrial Technology Development Organization (NEDO).

*2 Index of the percentage impact of emission source in surrounding areas (countries) on atmospheric ozone concentration measured at assessment target points. This index is useful in developing efficient measures against the emission source.

*3 Method of calculating the extent of impact from the response (sensitivity) of atmospheric concentration with respect to the emission of precursors.

*4 Method of calculating the extent of impact by tagging emitted precursors and tracing their activities.

*5 Ozone disappears by chemical reaction with nitrogen monoxide to generate nitrogen dioxide. During this reaction, the concentration of potential ozone (= ozone + nitrogen dioxide) is maintained.



- ### Main functions
- Coupled with geographic information system (GIS)
 - Operation using graphical user interface
 - Import of meteorological data from Japan Meteorological Agency and related agencies
 - Correction of wind velocity depending on altitude
 - Determination of atmospheric stability and its conversion depending on altitude
 - Determination of particular meteorological conditions
 - Dispersion equations (puff and plume models)
 - Automatic import of environmental concentration
 - Setting of multiple stacks in one area
 - Polymerization calculation of annual mean and daily mean

Fig. 1: Display of results obtained using an atmospheric environmental assessment support tool

The results of dispersion calculation with an input of the calculation period and smoke-source conditions are displayed on a map. The color contour indicates distribution of annual mean concentration and the triangle indicates position of maximum ground concentration. The locations of air pollution monitoring stations around the smoke source and related data are automatically extracted from a public database of the National Institute for Environmental Studies to tabulate the current environmental concentrations.

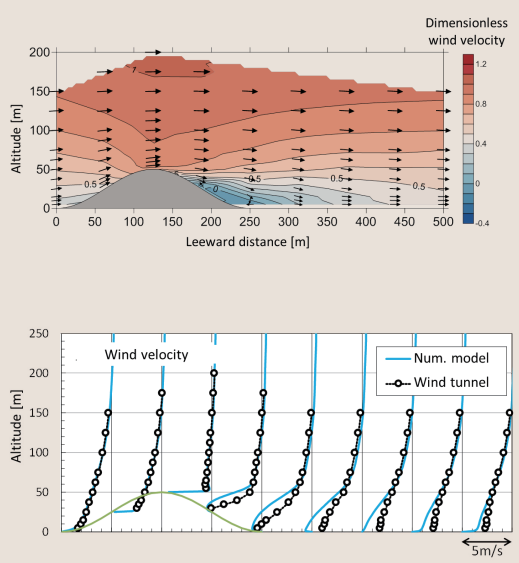


Fig. 2: Result of wind tunnel experiment (upper) and result obtained using atmospheric dispersion numerical model (detailed) for geothermal power generation (lower)

A detailed model is currently being developed using a turbulent-flow model as a base model to reproduce a complicated atmospheric current. When the result of the calculation using the model is compared with that of the wind tunnel experiment with simple geography, the general turbulent-flow model tends to underestimate the wind velocity in the main flow direction at the back of the target geography.

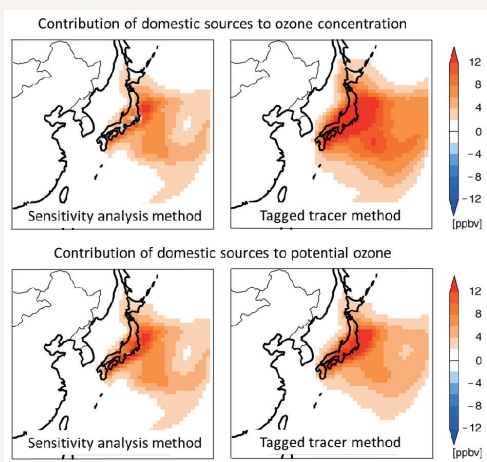


Fig. 3: Impact of domestic emission source analyzed by a high-precision and high-sensitivity analysis method and tracer tagging method

The impact of the emission source that caused a high ozone concentration exceeding the atmospheric environmental limit in springtime was evaluated. The impact of the emission source on ozone concentration in the surrounding vicinity evaluated by the tracer tagging method (upper right) tended to be larger than that evaluated by the high-precision and high-sensitivity analysis method (upper left). By introducing the concept of potential ozone, this tendency was markedly suppressed and the agreement between the results of the two methods improved (lower). Domestic emission sources include all manmade sources such as power plants and automobiles.

Development of Technologies for Supporting Construction and Maintenance of Power Plants with Consideration to Biodiversity Conservation

Background and Objective

According to the Environmental Impact Assessment Law amended in 2011, the assessment of biodiversity impact must be conducted in the planning stage, and the results of environmental conservation measures must be published. In addition, wind-power generation was added as a new target project regulated by the Law. Furthermore, introduction of regulatory biodiversity offsets*¹ and assessment of the environmental

impact of power plants on marine ecosystems have been discussed at government level and technological developments is needed so as to adapt to such new regulations and systems. The target of this research is to develop useful technologies related to biodiversity assessment and conservation to help enable the smooth construction, renewal, and operation of power plants.

Main results

1 Developing a method for estimating inhabitation likelihood of principal animal and plant species*²

The environmental impact assessment in the planning stage should be carried out using a simple method based on existing data. Principal animal and plant species listed in Red Data Books (RDBs) are targeted, however, existing data on their distribution were mostly insufficient for the impact assessment at the range of planned project areas for power plants. The research team developed a method for estimating the inhabitation likelihood

of principal species in target project areas using existing data on animal distribution and vegetation maps of the surrounding areas (Fig. 1). By this method, it is possible to narrow down the number of principal species likely to be inhabiting planned project areas from among the many principal species found in a wider range indicated by existing data (V13004).

2 Development of a technique for estimating the biomass of seaweed beds

Among the marine ecosystems, seaweed beds are high bio-productive, and thus provide key habitats for various organisms. Assessing the biomass of seaweed beds during a flourishing period is a necessary element of impact assessment, but it is time-consuming and costly to carry out diving surveys. The research team developed a numerical model for estimating the biomass of seaweed beds during a flourishing period using publically

available data (e.g., amount of solar irradiance, water temperature, transparency) provided by a public institution, and verified the validity of the model through comparison with observed values (Fig. 2). The developed model enables mapping of the biomass of seaweed beds in target marine regions, reducing the time and cost of impact assessments.

3 Development of a simple survey technique for flying birds

The impact of wind-power-generating facilities on flying birds should be incorporated in environmental impact assessment due to growing public concern regarding the collision of birds with wind-power-generating facilities. To obtain the data required for such an impact assessment, flying birds have been observed manually, however, this requires considerable effort and suffers large observation error. Using the system for monitoring flying birds developed in FY2012, the research team developed software for obtaining images of the flight path of

an individual bird simultaneously recorded from two different directions using two cameras so as to produce 3D stereo-imaging of the bird flight path. This 3D imaging software for flying birds enables the acquisition of accurate data on their routes and altitudes, which are difficult to measure manually (Fig. 3). The validity of this software will be demonstrated through comparison with the results of future field surveys with the aim of reducing human labor required in the impact assessment on birds.

*1 When the ecosystems in the project areas cannot be satisfactorily preserved, the negative impact of power plants on the ecosystems in the project areas can be mitigated by creating and developing similar ecosystems at other sites.

*2 Principal species refer to the Species designated by the laws and regulations of the government and municipalities as being critically endangered or easily affected by changes in the environment.

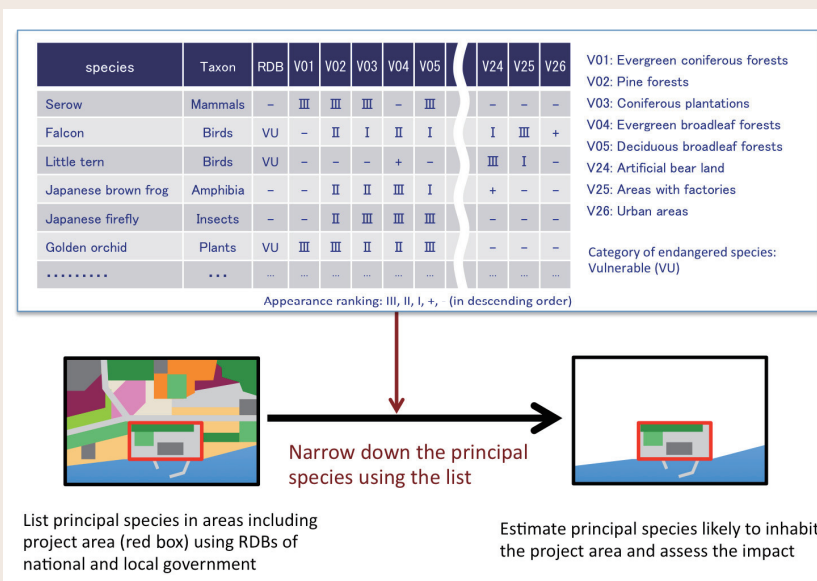


Fig. 1: Method of estimating likelihood of inhabitation of principal species

The presence/absence of principal species in 26 vegetation cover types, including pine forests and areas with factories, was examined and a list of principal species for estimating the likelihood of their inhabitation in each area was developed on the basis of the survey results of principal species reported in 49 previous nationwide power plant assessments (upper table). Number of species targeted in an impact assessment were narrowed down from among the many principal species by comparing the list with a vegetation map (lower figures).

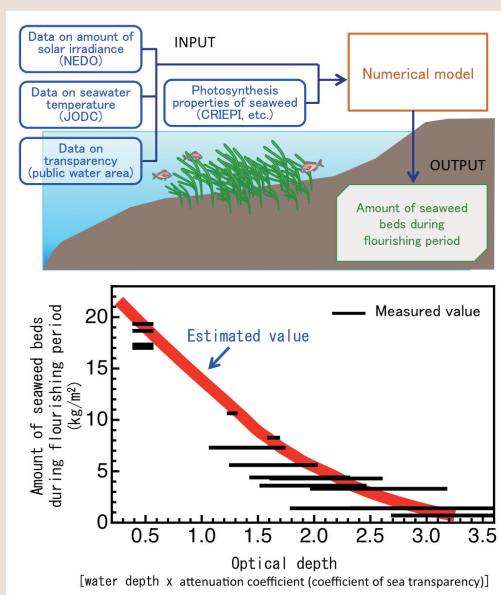


Fig. 2: Numerical model for estimating biomass of seaweed beds

Environmental data, such as the amount of solar irradiance, seawater temperature, and transparency, are entered into the model to calculate the amount of seaweed beds during a flourishing period (upper figure). The ecosystem of *Ecklonia cava* beds has been surveyed in detail in Japan (Kanagawa, Shizuoka, and Mie). The biomass of *E. cava* beds during a flourishing period (the maximum at each depth in each site) obtained by the survey were compared with estimated results, confirming that the amount of seaweed beds can be estimated using the developed model (lower figure).

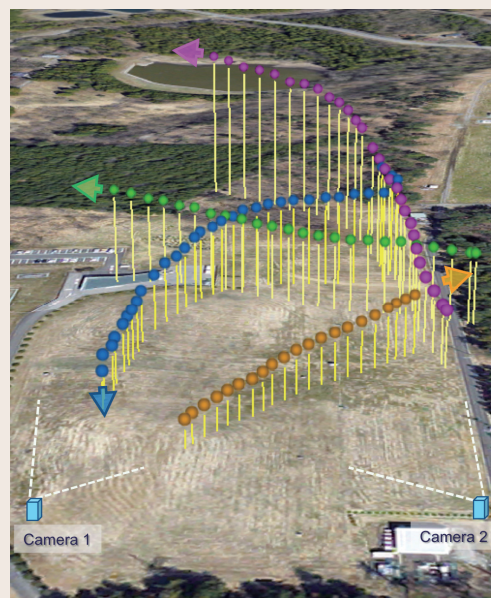


Fig. 3: Stereo-imaging determination of flight paths

The routes and altitudes of individual flying birds can be measured from video footage simultaneously recorded using two cameras. (Filled circles of each color and yellow lines represent the flight path and altitudes of individual flying birds, respectively.) It is possible to accurately assess how birds fly in the vicinity of rotating wind turbines and increase the reliability of estimations on the collision of birds with wind turbines.

Synthesis System of Numerical Analysis for Current and Sediments in Rivers and Reservoirs

Background and Objective

In order to plan and judge an operation of sediment pass-through on hydropower dam reservoirs, it is necessary to consider the condition of the riverbed in the downstream of a dam and the influence on fishes. As such, the method of predicting sediment deposition in rivers and reservoirs is required in order to evaluate its influence and to operate rational dam sediment management. However it is difficult to make sufficiently accurate predictions of the behavior of sediments which are supplied from forests and deposited in rivers and reservoirs due

to being unable to accurately estimate the erosion amount of river bed and stream banks.

In this project, a system predicting watershed sedimentation and water quality was developed based on a highly precise flood prediction model and a synthesis system of numerical analysis combined with a system of rainfall intensity and discharge prediction, then a practical method of sediment transportation prediction will be offered to each electric power company.

Main results

1 Estimation of sediment yield from upstream mountains

The amount of sediment expected from new collapses was estimated from quantified topographic change over four years using laser-profiler data to evaluate the sediment generation from a wide upstream area of dams (Fig. 1). On the other hand, the applicable condition of one of the popular cropland soil erosion assessment models,

EUROSEM, to forests was confirmed through analysis of temporal change of turbid water and surface runoff at forest slope. Furthermore, we began observation and analysis of the actual soil erosion at a forest floor in dam basin by installing power-supply-free systems to measure soil erosion (Fig. 2).

2 A development of evaluation method for slope stability with heavy rainfall

An evaluation method for slope stability with heavy rainfall developed in FY2012 (N12014) was applied to a slope field collapsed by the typhoon with the largest recorded rainfall. This was done in order to estimate slope stability change with a varying amount of cumulative precipitation.

The result of the estimation showed that the total safety factor of the slope dropped and evaluated to be a slope failure during a time between 70 hours and 100 hours after the calculation and that the evaluation was approximately consistent with the real phenomenon (Fig. 3).

3 Construction of a system for measuring sediment transportation in rivers and reservoirs in real time

In order to clarify the dynamic state of sediment in the downstream of a dam, instruments able to observe the water quality of the river and the reservoir in real time were developed. These instruments require no electrification system as they utilize a solar panel and battery power, thereby making long-term observation possible. After such instruments were installed at 7 locations from a hydropower dam to a river mouth, continuous observation of water quality data began (V13007).

The acquired data is transmitted to the server in our office by the mobile phone communication network. Data is stored automatically and water quality of the river can be seen from a remote location (Fig. 4). This instrument system has a function to sample the river water automatically if the preset turbidity is exceeded or an order is given from a remote PC. The human labor otherwise required to perform this observation can be decreased by using this system.

4 Synthesis System of Numerical Analysis for flood and sediment transportation

The watershed sedimentation in rivers and reservoirs at the time of a flood and the riverbank erosion effect due to a decrease in water level of reservoir were estimated using the predicted sediments flow analysis program (C-HYDRO-2D). Change in water temperature and DO over several days was able to be predicted by combining a

water quality prediction system with this program. Operation of the whole prediction system for the rainfall intensity, discharge, and water quality was checked from this verification, and completion of a synthesis system of numerical analysis for sediment level and turbidity is expected.

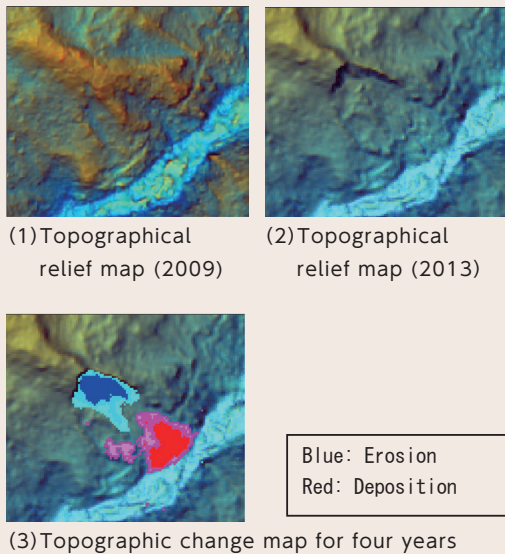


Fig. 1: Estimation of sediment production and deposition by Laser profiler

Laser profiler data of from 2009 and 2013 has detected a new landslide located far from the road. We will conduct a field survey to estimate the sediment production and deposition by the this landslide.

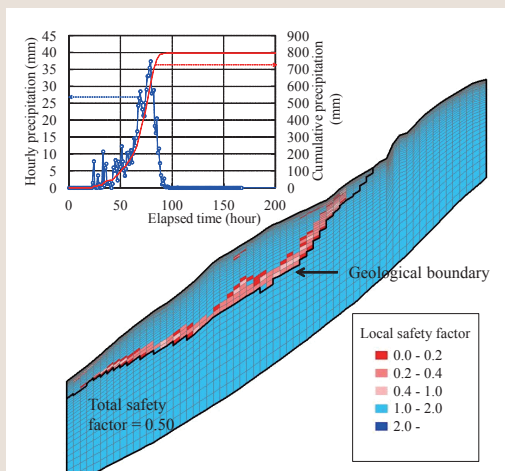


Fig. 3: Calculated results of mechanical stability for a slope field with heavy rainfall (100 hours after the calculation, total amount of rainfall was 800 mm)

Local safety factors in geological boundary between debris and bedrock decreased due to the rainfall infiltration and area of low safety factor connected 100 hours after the beginning of the calculation. Total safety factor of the slope was calculated as 1.25, 1.06 and 0.50 of the initial condition, 70 hours and 100 hours after the calculation, respectively by using the distribution of the local safety factors. This result showed that the slope collapsed during a time between 70 and 100 hours after the calculation.

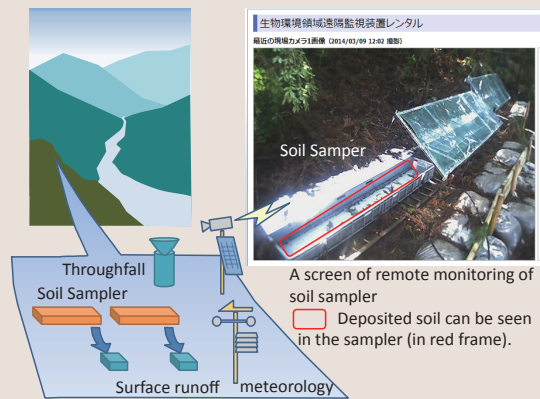


Fig. 2: Outline of the soil erosion measuring system

The soil erosion measuring system we had developed (V11030) consists of the multiple soil samplers, the surface runoff meter and the meteorological station including rain gauges. In this study, rational decision of maintenance and data-collection timing has been made possible by remote monitoring of the soil samplers using webcams.

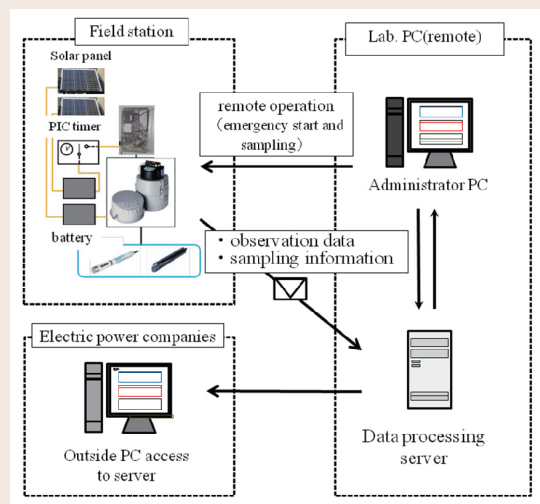


Fig. 4: Outline of the system for measuring sediment transportation in real time

Developed GUI software to facilitate real time monitoring of water quality. As a result, a large amount of data transmitted from seven points can be processed. Moreover, the execution and cancellation of water sampling are possible while checking data on a remote PC.

Development of Maintenance Technologies for Aged Power Transmission and Distribution Facilities

Background and Objective

The development of systematic maintenance technologies is important in order to successfully standardize maintenance and renewal work on aged power equipment, as well as consider the cost-

benefit performance. In this research project, we improve our degradation diagnosis method and our ability to gather degradation data, then establish support methods of facilities for renewal.

Main results

1 Abnormality diagnosis of a power transformer by FRA

We have been developing a degradation detection program to detect transformer wires abnormalities using FRA (Frequency Response Analysis). Currently, a technique is applied to shunt reactors with winding structures similar to transformers with power company members^[1] and we succeeded in

detecting winding abnormality of the equipment as shown in Fig. 1. After dismantling the shunt reactor, we discovered the abnormality, thus confirming the applicability of the FRA method in detecting abnormalities in shunt reactor structure.

2 Insulation diagnosis of XLPE and OF cables

We have been measuring the breakdown strength of used 20-60 kV XLPE (cross-linked polyethylene insulated) power cables supplied by Japanese power companies and the water tree degradation level, that determines the breakdown strength of the cables, has been measured. After accumulating data, we plan to develop an estimation method for the remaining life of those XLPE power cables considering their usage conditions and cable structures.

As for OF (Oil Filled) cable joints, recently it has become very important to determine their

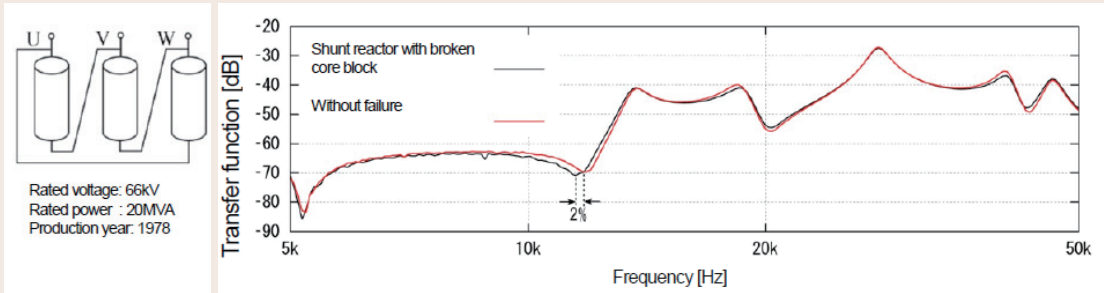
degradation mechanisms because PD (Partial Discharges) traces are detected in the replaced cables without any detection of PD by gas analysis. We began PD measurement tests of OF cable joint models with defects as shown in Fig. 2 (a). We clarified the PD process of the model from the voltage application to the final breakdown. We discovered it was possible to detect the extent of degradation through trend management of PD occurrence frequency, duration and electrical discharge load (Fig. 2)(H13014).

3 Degradation diagnosis of rust and surface paint of power equipment

We are trialing THz (tera-Hertz) wave to measure rust under the opaque anticorrosion coating and develop a deterioration degradation method for coated steels of power equipment. THz wave has the advantage of being easily absorbed by the

rust of the material surface. We found that this measurement method could also be applied to the deterioration degradation of metal under paint coats of equipment installed near the sea (Fig. 3)^[2].

[1] S. Miyazaki et. al., IEEJ, B-Society Convention Paper No.405, 2013
[2] N. Fuse, et. al., IEEJ, IIS-13-64, 2013

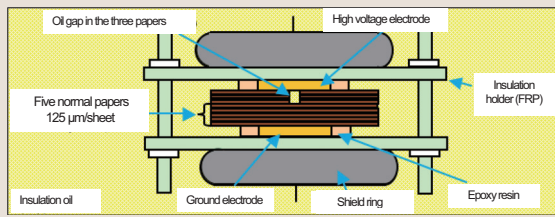


(a) Specification

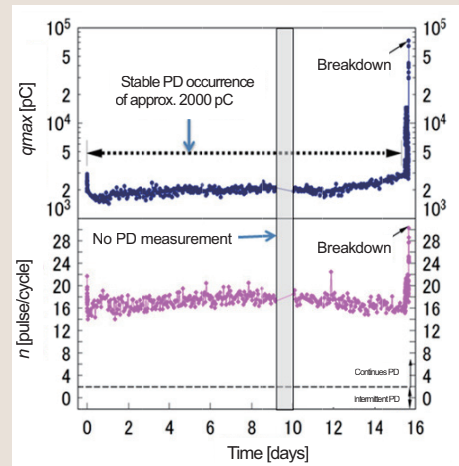
(b) FRA analysis results

Fig. 1: Abnormality detection of a shunt reactor

The measurement result of a shunt reactor is shown. A downward peak at 12 kHz shifted to lower frequency due to the occurrence of an abnormality. This abnormality was confirmed by dismantle analysis of the reactor. This result confirms the validity of FRA method as a detection method for shunt reactor abnormalities.



(a) Oil-paper model specimen with gap defects



(b) Time dependence of PD characteristics

Fig. 2: PD measurement with an OF cable model specimen

A PD occurrence of over 2000 pC was observed with a sheet specimen under continuous alternating voltage application condition. With this experimental result, we found that the potential for breakdown can be estimated by the PD magnitude after it exceeds approx. 2000 pC.

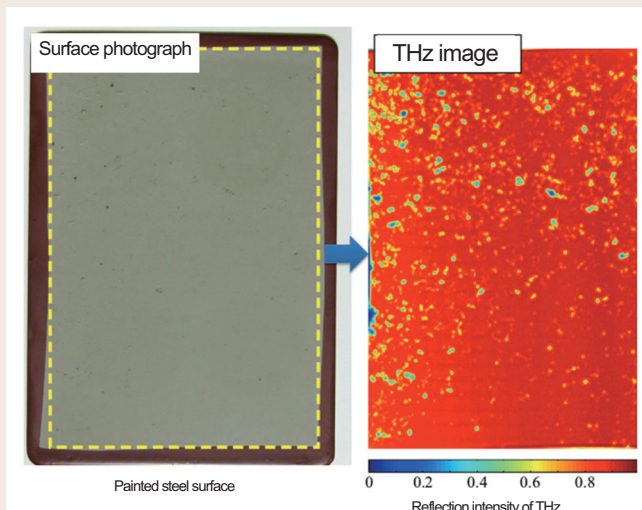


Fig. 3: THz analysis of paint polyurethane coated steel surface

THz imaging was carried out on the surface of a 9 cm × 12 cm painted steel plate. A THz wave was projected onto the surface at a perpendicular angle while reflection intensity and time were measured. While the surface photo (left) does show a small amount of degradation, the THz image is capable of detecting degradation with much greater clarity. The THz image was normalized by the intensity of the projected signal. A reflection intensity of 1 indicates full reflection, while that of zero corresponds to complete absorption. The closer the intensity is to zero, the higher the extent of degradation.

Development of Soundness Assessment Techniques for Aged Overhead Transmission Steel Towers

Background and Objective

The aging of overhead transmission steel towers constructed during Japan's high economic growth (almost two full decades beginning from 1954) has progressed rapidly, giving rise to a need for the standardization of their repairing and rebuilding, which must also be performed with efficiency. Meanwhile, in the 2011 Tohoku Earthquake, larger accelerations than those observed in the Southern Hyogo prefecture earthquake of 1995 were observed, therefore, it is also necessary to gain an understanding of the seismic performance of steel towers against high-level earthquake ground motion.

In order to contribute to the efficiency and rationalization of maintenance for aging overhead transmission steel towers, this project aims to develop comprehensive diagnostic methods for their soundness, including a remaining life assessment considering corrosion and fatigue, a more efficient corrosion inspection method and a foundation stability assessment. In addition, we aim to clarify the seismic margin of steel towers considering elastic-plastic behavior against high level earthquake ground motion.

Main results

1 Observation and mapping of corrosive environmental factors

For quantitative evaluation of corrosion factors in inland areas, devices for measuring corrosive environments were installed on an existing transmission tower (Narita-shi, Chiba-ken) and observations begun. Moreover, an annual averaged map of airborne sea salt (in the Kanto region) was made by trialing the super high resolution meteorological simulation database for 53 years

(CRIEPI-RCM-Era2) created by the Numerical Weather Forecasting and Analysis System of CRIEPI (NuWFAS) and the simulation code of sea-salt transport (NuWiCC-ST). The predicted amount of annual averaged airborne sea salt using the NuWFAS data reproduced qualitative variation in the observed amount of deposited sea-salt (Fig. 1).

2 Evaluation of effects to inner corrosion of steel pipe for transmission towers: horizontal or diagonal arrangement to the ground

Steel pipes placed horizontally or diagonally to the ground to simulate horizontal and diagonal brace of an actual transmission tower, were exposed at Yokosuka coastal testing field. Several ACM (Atmospheric Corrosion Monitoring)^{*1} sensors were inserted into these steel pipes in the longitudinal direction to evaluate their internal corrosion rate. It appeared that the ACM

sensors in the diagonally-arranged pipe showed a higher corrosion rate than that of the horizontally-arranged pipe (Fig. 2). The results acquired in this study will be utilized for the estimation of corrosion rate of each part and site of transmission tower and the identification of the parts and sites which need preferential maintenance inspection (Q13007).

3 Surveys and database construction for the current corrosion states of aging steel towers

In order to identify the current deterioration states of aging steel towers mainly caused by corrosion, 41 steel towers installed in 25 transmission lines were surveyed from a coastal to mountainous area in Japan. The survey results showed typical corrosion states in that, corrosion in the coastal area was mainly caused by sea salt while that in the mountainous area was mainly caused by fog and

dewfall. As a result, typical corroded environmental conditions for steel towers were specified. Based on the survey results, a database for ageing steel towers was constructed. The database includes not only the actual corrosion survey results, but also meteorological environment information and the basic design condition of steel towers, making it a useful tool for effective maintenance action.

4 Observations of pile foundation of steel tower and ground around foundation

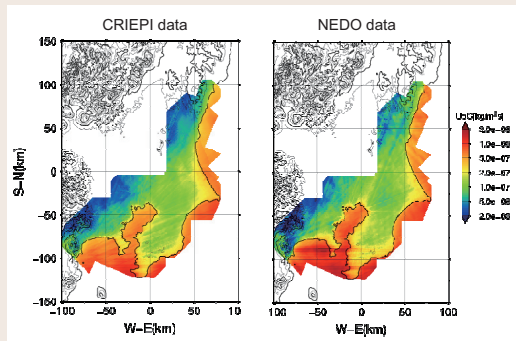
In order to clarify the earthquake behavior of steel tower pile foundation, a seismometer above the foundation and strain gauges of the pile top were installed in the full-scale test facilities for snow-storm damage to overhead transmission lines at Kushiro-shi, Hokkaido (Fig. 3). Time-dependent changes of the strain gauges in the construction phase of the tower were observed prior to the

dynamic observation.

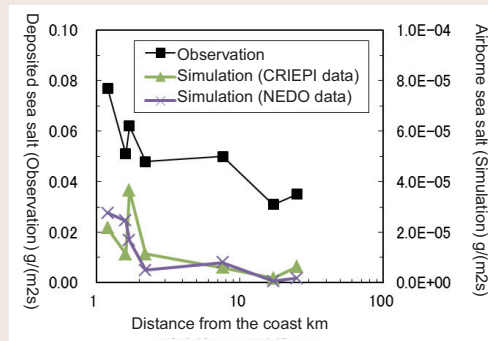
Measurement was carried out by setting up a developed borehole inclinometer with FBG optical fiber sensors^{*2} on a slope (Saikai-shi, Nagasaki-ken) where the mechanism of behavior was unclear. By setting up these sensors, we will acquire the basic data for the development of stability evaluation method for tower foundations.

*1 Sensor for measuring the corrosion rate of metal in a given environment.

*2 This inclinometer can measure subterranean displacement at a 20 cm pitch, which is more accurate than conventional measurement techniques.



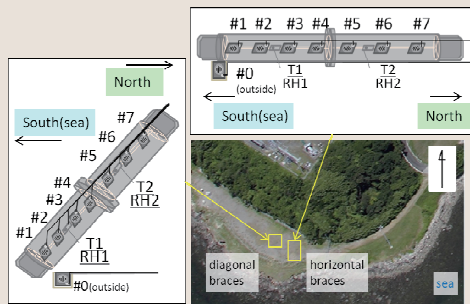
(a) Annual-averaged map of airborne sea salt (the Kanto region)



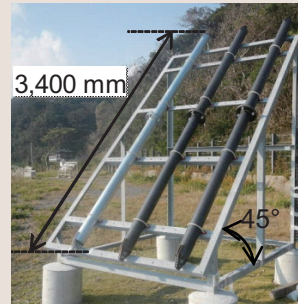
(b) Comparison with observation data (measured values using ACM sensors by TEPCO)

Fig. 1: Trial production of an annual-averaged map of airborne sea salt

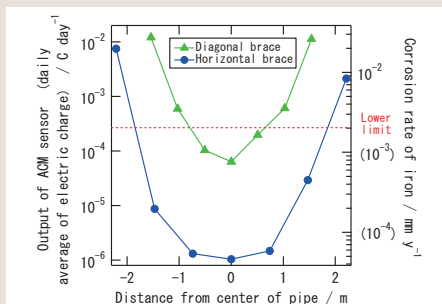
Airborne sea-salt maps were made based on occurrence frequencies of wind velocity at sea taken from the meteorological database for 53 years simulated by NuWFAS (CRIEPI data) and the existing database simulated by LAWEPS (NEDO data). In comparison with observed values of deposited sea salt and predicted values of airborne sea salt, the map using CRIEPI data was found to more precisely reproduce qualitative variation than the map using NEDO data.



(a) Schematic diagrams of ACM sensors arranged in horizontal and diagonal braces arranged at Yokosuka coastal testing field.



(b) Photo of diagonal braces arranged at a testing field.



Lower limit in the figure shows the minimum effective value to calculate corrosion rate.

(c) Corrosion rate of inside horizontal and diagonal braces in June, 2013.

Fig. 2: Result of exposure test: horizontal and diagonal braces

Simulated horizontal and diagonal braces were arranged at a coastal testing field. Seven ACM sensors were arranged in both pipes at a regular interval in a longitudinal direction. An ACM sensor was also arranged outside the pipe. The sensors in the diagonal brace showed larger values than the ones in the horizontal brace. Particularly in the center, quite a significant difference in values for the diagonal and horizontal cases was observed. It is presumed that this difference depends on the inflow of corrosive substance into the steel pipes.

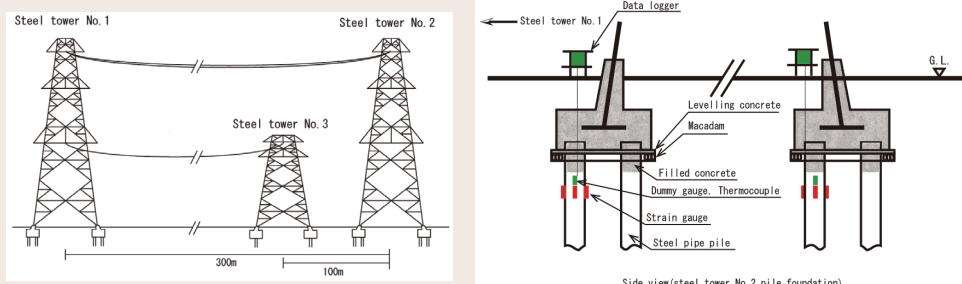


Fig. 3: Dynamic observation equipment of steel tower pile foundation

A seismometer above the foundation and strain gauges of the pile top were installed in the full-scale test facilities for snow-storm damage to overhead transmission lines at Kushiro-shi, Hokkaido (Installed in March 2014. Scheduled start of the dynamic observation is August 2014).

Improvement of Operation and Control Technologies to Diversify Fuel Types for Pulverized Coal-fired Power Plants

Background and Objective

The utilization of low grade coals is sought by pulverized coal-fired power plants in order to diversify fuel types. To reduce maintenance and inspection costs, and achieve environmental preservation, coal-fired power plants require countermeasures for sulfidation corrosion of boiler tubes and trace element control.

In this research, a guideline for the operating conditions of a mill and a burner, the blending method of coals, etc. is being established to use

low HGI coal*¹ (Low grindability coal) and low volatile coal (Low combustibility coal) in existing pulverized coal-fired power plants. In regards to countermeasures for sulfidation corrosion, an evaluation method of sulfidation conditions and a coating technology for the tube will be developed. Prediction models for the behavior of trace elements such as Hg, B, Se, and release control technologies in flue gas and waste water treatment processes are also under development.

Main results

1 Combustibility and grindability of low HGI coal and bituminous coal blend

As the blending ratio of low HGI coal mined in Australia to low volatile bituminous coal increased using a bunker blending method*², both emissions of NO_x and unburned carbon were able to be reduced since low HGI coal has a high combustibility rate and low nitrogen content (Fig. 1). However, the grinding power of a roller mill reached its upper limit as the blending ratio of low HGI coal increased in the normal operating condition of a particle separator in a roller mill (weight ratio of pulverized coal passing 200 mesh (75 μm) sieve; 70~80%). When coarse particles were emitted to reduce grinding power in a roller mill, both emissions of NO_x and unburned carbon

became greater than those under normal operating condition of particle separator.

Using the in-furnace blending method, in which low HGI coal was ground into coarse particles and bituminous coal was ground to normal particle size by different roller mills then fired by different burners, both emissions of NO_x and unburned carbon became approximately equivalent to the emissions in the bunker blending method under normal operating conditions of a particle separator (Fig. 2). This result indicates that the in-furnace blending method is effective for low HGI coal firing.

2 Development of a coating technology for preventing sulfidation corrosion of boiler tubes, and evaluation methods of sulfidation conditions

A coating technology to prevent sulfidation corrosion was applied to boiler tubes of an actual pulverized coal-fired plant. This method enabled approximately 100 m² coating within three days, and suggested that the method was a low cost and easy countermeasure for sulfidation (Fig. 3).

To upgrade the tool that evaluates the possibility of sulfidation corrosion on water wall tubes in a pulverized coal-fired boiler, a corrosion test was carried out under the transition range between sulfidation and oxidation (Fig. 4). The application range of the tool was extended by adding the test results.

3 Behavior elucidation and establishment of an emission control method for trace elements in coal-fired power generation plants

Recently, it was reported that selenium, which has a lower charge number than selenite, existed in FGD waste water, though the typical forms were considered to be selenite and selenate. The behavior of selenium in a conventional waste water treatment process was investigated through

a basic experiment using standard reagents and speciation of selenium in actual waste water samples. These investigations revealed that the selenium whose change members were less than tetravalent was easily removed in the conventional waste water treatment process.

*1 HGI (Hardgrove Grindability Index) is the evaluating factor for the grindability of coal. As HGI decreases, it becomes harder to grind. The HGI of bituminous coal utilized in Japanese power stations ranges from 40 to 70. The HGI of low HGI coal referred to in this study is lower than 40.

*2 Bunker blending method is when two types of coal, which are blended in a bunker before grinding in a roller mill, are fired at the same blending ratio for each burner of a boiler.

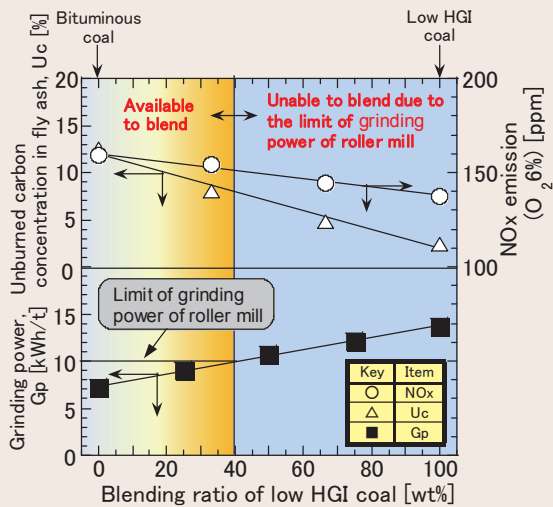


Fig. 1: Combustibility and grindability of low HGI coal at blending

As the blending ratio of low HGI coal to low volatile bituminous coal increased, both emissions of NOx and unburned carbon reduced as low HGI coal has a high fuel rate and low nitrogen content. However, the grinding capacity of the roller mill reached its limit due to the high blending ratio of low HGI coal. (In the case of this study, the limit of blending ratio of low HGI coal was approx. 40%.)

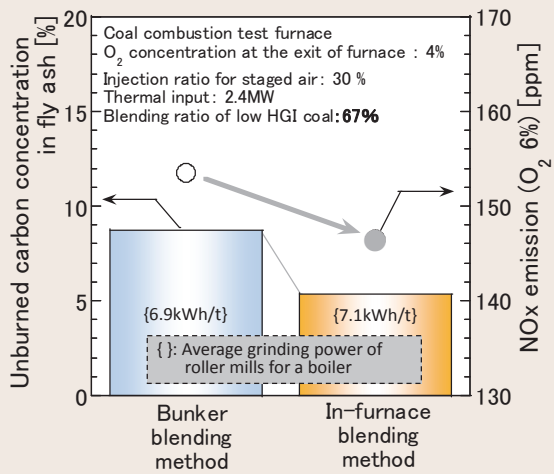


Fig. 2: Effect of low HGI coal blending method

Using the bunker blending method, when particles were made coarser to reduce the grinding force of the roller mill, the blending ratio of low HGI coal could be increased. However, both emissions of NOx and unburned carbon in fly ash were increased. Using the in-furnace blending method, in which low HGI coal was coarsely ground and bituminous coal was ground to ordinary particle size by their respective roller mills then fired in separate burners, both emissions of NOx and unburned carbon could be reduced.



Fig. 3: Application of CRIEPI-developed coating to an actual boiler

The coating consists of 4 layers, which were SiO₂, TiO₂, Al₂O₃, and TiO₂ from the substrate side, and its application required three days for an area of approximately 100 m². The total coating time of each layer was around 6 hours, and over 6 hours of drying time was required for each layer.

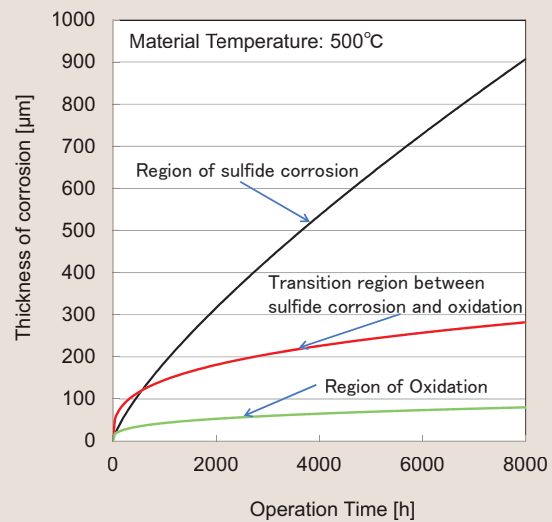


Fig. 4: Example of evaluated corrosion rate

The growth of a corrosion layer in the transition range between sulfidation and oxidation was investigated in a laboratory test. The thickness of a corrosion layer in a transition state was between that of oxidation and sulfidation.

Sophisticated Technology for Low-Grade Energy Resources

Background and Objective

Co-firing of biomass has been promoted as a measure to reduce CO₂ emissions in coal-fired power plants. However the co-firing rate requires improvement, due to the difficulty of pulverizing biomass compared to coal and the co-firing rate still remains too low at a mere few percent. At the same time, the use of low rank coal such as lignite has been proposed as an expansion strategy of fuel species for coal-fired power plants. Lignite

reserves are reasonably high in Asia, and it is a good target for coal-fired power plants, however poses the problem of being difficult to use due to its high moisture content, low heating value and high spontaneous ignitability. In this project, we aim to develop a carbonization technology for low-grade resources such as biomass and lignite to use in coal-fired power plants, and to establish an evaluation technology for low-grade resources.

Main results

1 Development of carbonization technology for woody biomass

1) Heat balance analysis for the carbonization process

Carbonization tests of cedar chips were carried out using CRIEPI's demonstration scale carbonization test facility, which had a throughput and maximum carbonization temperature of 4t/day and 650 degrees Celsius. The feed rate of cedar chips (40% moisture) was from 130 to 145 kg/h, and the carbonization temperature was between 340 and 400 degree Celsius. The fuel ratio*¹ of the carbonized cedar was between 0.19 and 0.91 (Table 1). Under all test conditions, auxiliary fuel accounts for around 20% of total heat input of the carbonization process. The heat loss of the carbonization process was as low as approximately 10% of total heat input, which is equivalent to a commercial plant, therefore, it will be possible to evaluate large-scale commercial carbonization

process using this test facility (Fig. 1).

2) Characterization of carbonized cedar and the carbonization process

In the carbonization process, the heat value ratio of carbonized cedar to raw cedar and the carbonization efficiency decreased with the increase in carbonization temperature, and these reduction rates increased as the carbonization temperature increased from 380 to 400 degree Celsius. Since the fuel ratio of carbonized cedar rapidly increased between 380 and 400 degree Celsius, it is believed that carbonization was accelerated in that temperature range (Fig. 2). By storing similar data for other biomass feedstock, it will be possible to predict the product properties of a commercial process by analyzing biomass feedstock.

2 Grindability estimation of coal used in coal-fired power plants containing a high percentage of carbonized wood

Assuming the use of carbonized wood at a high co-firing rate in coal-fired power plants, the grindability of coal containing a high percentage of carbonized wood was evaluated using a roller mill test facility. A raw cedar chip and three different carbonized cedar chips of 0.19, 0.25 and 0.58 in fuel ratio, were mixed with a coal, for grindability tests. These carbonized cedar chips were produced by the carbonization test facility described above. The mixing ratio of carbonized/

raw cedar with coal was set at 3-30% on a calorie basis. The grinding power increased as the mixing rate rose, but the increase in grinding power was significantly suppressed by carbonizing the cedar chips. The grinding power reduced with the increase in fuel ratio of the carbonized cedar chip. The carbonized cedar chip with a 0.58 fuel ratio and the coal demonstrated almost equal grindability (Fig. 3).

*1 The ratio of volatile matter and fixed carbon in the fuel increases with the progression of carbonization.

*2 One of the quality indicators of carbonized biomass, expressed as the product of heat value and production of carbonized biomass divided by the product of heat value and the feed rate of raw biomass.

*3 One of the performance indices of the carbonization process, expressed as the product of heat value and production of carbonized biomass divided by the sum of the product of heat value and feed rate of raw biomass and the product of heat value and feed rate of auxiliary fuel.

Table 1: Carbonization test conditions and fuel properties of raw / carbonized cedar

The conditions of the carbonization test and the industrial analysis data of raw cedar and carbonized cedar.

Run No.	Unit	Cedar	Fuel Ratio				
			Run1	Run2	Run3	Run4	Run5
Carbonization Temperature	°C	-	340	360	380	400	400
Feed Rate of Cedar	kg/h	-	146	128	134	146	129
Ash	% db	0.2	0.3	0.3	0.3	0.5	0.7
Volatile Matter	% db	85.7	83.8	82.1	81.3	63.1	52.1
Fixed Carbon	% db	14.1	15.9	17.6	18.4	36.4	47.2
Fuel Ratio	-	0.16	0.19	0.21	0.23	0.58	0.91
HHV	MJ/kg	20.6	20.7	21.2	21.6	25.7	28.6

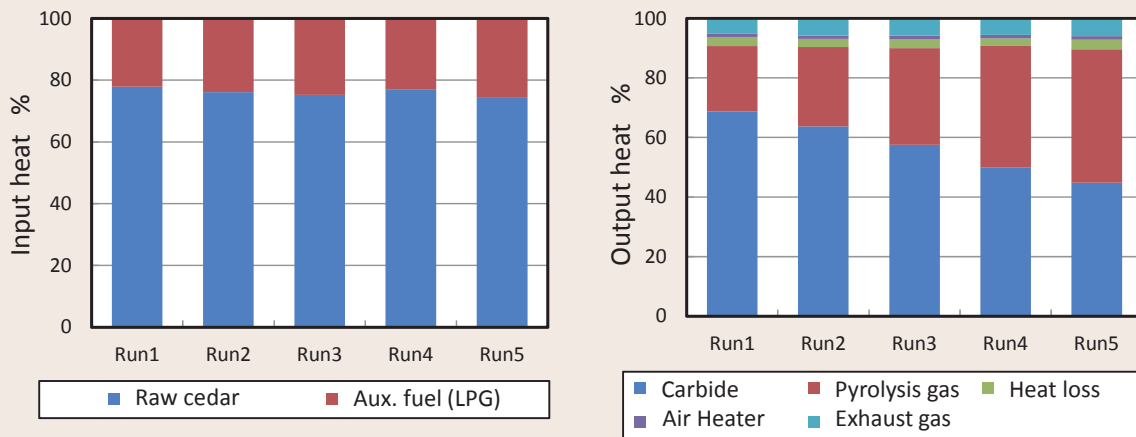


Fig. 1: Heat balance of the carbonization process (Left: Input heat, Right: Output heat)

The graphs show the input and output heats of the carbonization process obtained from a heat balance analysis of the carbonization test facility. The input heat is composed of heat generated by raw cedar and auxiliary fuel (LPG), while the output heat is composed of heat generated by carbonized cedar, pyrolysis gas, exhaust gas and loss from equipment. The information is used for optimization of carbonization conditions and design/operation of commercial carbonization plant.

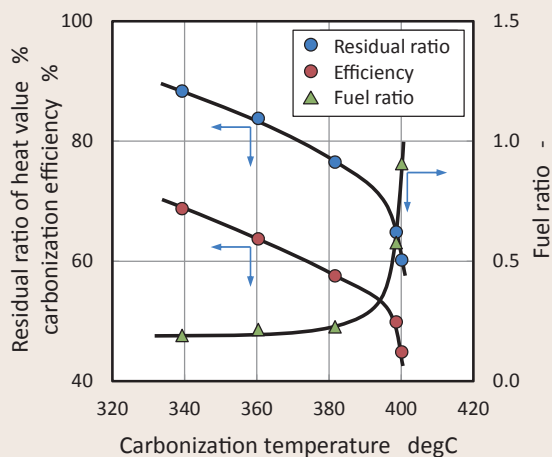


Fig. 2: Effect of carbonization temperature on the residual ratio of heat values in carbonized cedar and carbonization efficiency

The graph shows the relation of the carbonization temperature to the residual ratio of heat value^{*2} and the carbonization efficiency^{*3}. This data can be utilized for setting carbonization test conditions, optimizing test conditions and developing tools to predict the fuel properties of carbonized biomass.

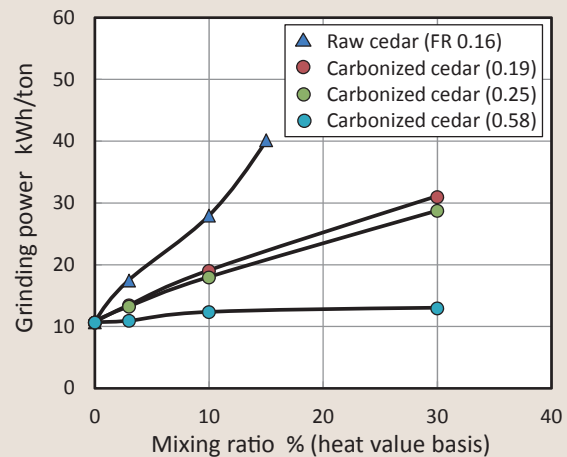


Fig. 3: Effect of mixing rate on grinding power

A grinding test of a coal and raw/carbonized cedar chips mixture was carried out using the roller mill test facility. It was difficult to grind the coal with 30% raw cedar chips. The grindability of carbonized cedar chips was greatly improved.

Assessment of System Security Assuming High Penetration of Photovoltaics

Background and Objective

As renewable energies spread, particularly photovoltaics (PV), it is important to ensure power system stability (rotor angle stability, frequency stability and voltage stability) following the occurrence of transmission system faults.

However, the effects of transmission system faults on power systems in the event of widespread PV penetration have not yet been fully investigated. It is important to clarify the effects and develop countermeasures to ensure power system stability in the future.

The purposes of this project are:

- (1) To evaluate the effects of power system faults on the transmission system
- (2) To conduct experiments and identify the characteristics of a Power Conditioning System (PCS) structured from an inverter of PV with anti-islanding protection
- (3) To establish numerical PV models for time-domain simulation
- (4) To develop countermeasures for ensuring power system stability in the future

Main results

1 Improved Convenience of PV Models for Simulation Analysis

Physical tests to identify the characteristics of PCS for residential PV in CRIEPI's Power System Simulator have shown that when the PCS is temporarily suspended after a transmission system disturbance, not only the control system of the inverter, but also the automatic islanding detection relay, is greatly affected.

Therefore, PV simulation models with an automatic islanding detection relay for the CPAT*¹ simulation analysis have been developed. In order to efficiently evaluate the effects of high PV penetration on system security, three typical PCS models for residential PV were combined into one as the standard model for CPAT (Table 1), to improve the convenience of CPAT users.

2 Experimental Extraction of Conditions for Generating Reactive Power Oscillation of the PCS by the Response of the Active Islanding Detection Method

In some tests using CRIEPI's Power System Simulator, periodic reactive power oscillation (period 0.1 second) has been observed. This oscillation is due to the response of the active islanding detection method of PCS*² for PV.

To investigate the conditions under which this phenomenon occurs, resistance loads and the PCS for PV are connected at the end of the test system (Fig. 1). Experiments are then carried out with the opening and closing of the resistance load as a system disturbance, while varying the capacity of

the PV and transmission line length of simulated 275 kV and 66 kV as parameters. The results show that this phenomenon is likely to occur under conditions in which the terminal voltage of the load is likely to fluctuate when the PV capacity is large*³ and the transmission line length is long (Fig. 2).

In the future, the detailed conditions under which this phenomenon occurs and the probability of occurrence in an actual power system will be studied.

3 Evaluation of the Fundamental Effects of Transmission System Faults on Power Systems with High PV Penetration and Wind Power Generation

Numerical simulations using CPAT were carried out for various full-scale power system models (Fig. 3) in order to evaluate the impact on the system stability in the case of high PV penetration and wind power generation (WP). The results show that the effects on the power system stability vary depending on the capacity and the position at which renewable energy power generation is

introduced, and also on load flow and system fault conditions. Because these influences are largely dependent on the characteristics of the individual power system, additional analysis on the standard power system model will be performed in order to summarize the effects on power system stability, including the relationship with the power system characteristics.

*1 CPAT (CRIEPI's Power system Analysis Tools) was developed by CRIEPI. In this study, a transient stability analysis tool of CPAT was used. CPAT is used by all 10 electric utilities in Japan.

*2 PCS for residential PV with a new islanding detection relay named AICOT (Anti-Islanding Control Technology) in CRIEPI's Power System Simulator

*3 The oscillation phenomenon occurs when the short-circuit capacity ratio (short-circuit capacity of the terminal to which the load is connected) is smaller than a certain value. The threshold is presumed to differ depending on the type and manufacturer of the PCS. It is also possible that factors other than short-circuit capacity ratio are involved in the phenomenon.

Table 1: Standard PCS model for residential PV in CPAT (3 kinds of automatic islanding detection relay are available)

Model #1	Active System: The AICOT(Anti-Islanding COntrol Technology) Passive System: System to detect Changing Rate of Frequency
Model #2	Active System: Frequency Shift System Passive System: System to detect Jumping Voltage Phase
Model #3	Active System: Variable Reactive Power System Passive System: System to detect Jumping Voltage Phase

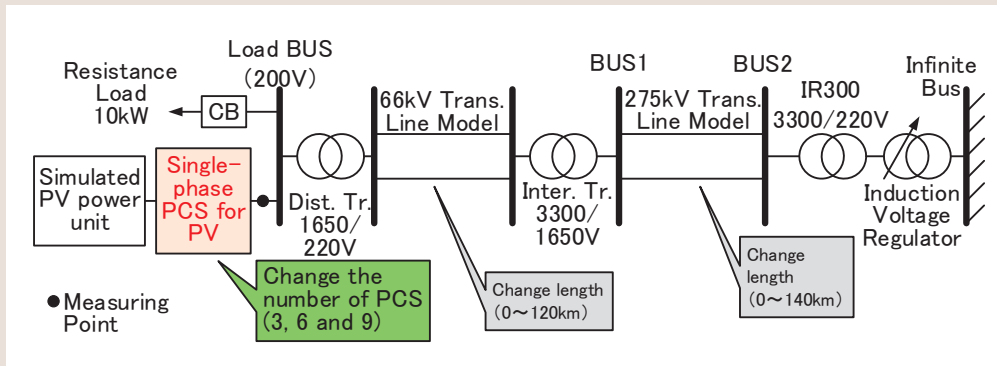
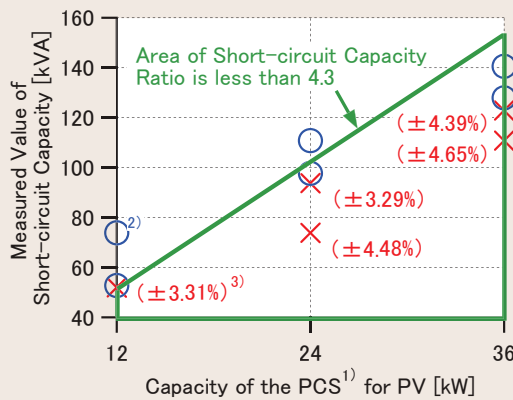


Fig. 1: Test system in CRIEPI's Power System Simulator (Experiments with the opening and closing of resistance load)



Notes:

- 1) PCS for PV: rated output 4 kW, ±1 kvar / 1 unit
- 2) X: Reactive power oscillation occurred.
O: No oscillation
- 3) Values in parentheses show the amplitude of the voltage of the load when each PCS unit outputs ±1 kvar.

Fig. 2: Test conditions under which reactive power oscillation occurred in CRIEPI's Power System Simulator

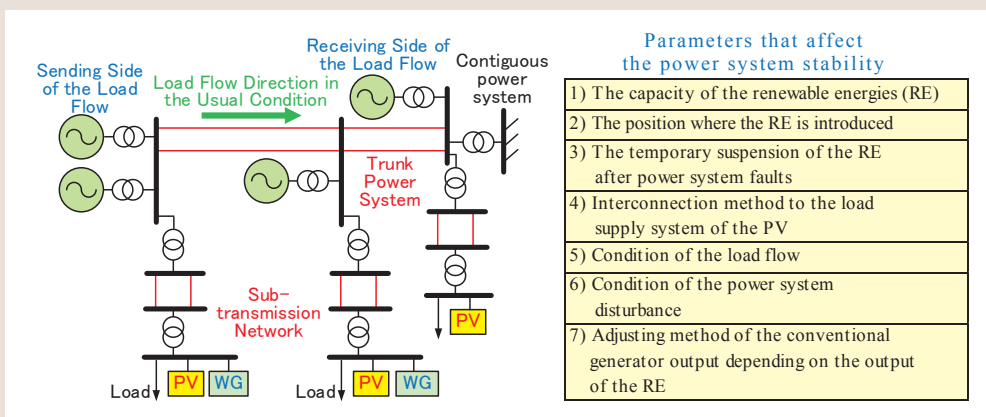


Fig. 3: Parameters that affect power system stability and image of a large-scale power system

Development of a Next-Generation Coordination System for Power Demand and Supply

Background and Objective

Expectations towards renewable energy sources (RES) such as photovoltaic (PV) power generation are intensifying and it is predicted they will penetrate the utility system in high volume. As such, it is necessary to develop techniques to achieve both effective use of RES and preservation of power quality, safety and stability

of utility systems at a low cost. The objective of our research are to establish basic techniques for distribution systems such as restraint of voltage rise, protective cooperation and so on, and to develop coordination system techniques for power demand and supply including a technique for the effective use of distributed power generation.

Main results

1 Development of an islanding prevention method in case of secondary transmission system faults

The establishment of a method to prevent islanding (Fig. 1) is necessary. Islanding may occur on a wide scale in the case of upper secondary transmission system (66kV) faults upon high PV penetration. Islanding detection characteristics have been clarified through the experiments and simulation analysis using a typical distribution system model in 2012 (R12020). In 2013, more detailed characteristics were clarified through experiments and simulation analysis* assuming several operation forms of distribution systems (system configuration, operation method in fault, grounding method etc). These included ungrounded distribution system with distribution towers as well as different locations and opening times of circuit breakers at fault

occurrence. The results led to the following findings. Islanding detection time tends to decrease more for ungrounded distribution systems compared with resistance grounded system and increase when the faults are cleared by operating ground over voltage relay (OVG, B in Fig. 1) at the same time as a circuit breaker (A in Fig. 1) of a transmission line is opened. The opening time of the circuit breaker of transmission line has little influence on the islanding detection time after the breaker opened (Table 1) (R13025). Based on these results, we plan to investigate facility and operation forms of the utility and measures in the facility/operation for preventing islanding responding to penetration of distributed power generation.

2 Development of 3-phase imbalance correction method for distribution lines

Voltage management of high voltage distribution lines may become difficult due to the increase of 3-phase imbalance by penetration of large capacity single-phase appliances such as heat pump type water heaters in addition to PV systems. A voltage imbalance correction method that controls each phase voltage independently using STATCOM is proposed, and its effectiveness has been validated

through simulation analysis. The results show that the proposed method suppresses the increase of voltage imbalance caused by increased penetration of PV (Fig. 2(a)), and decreases the number of locations where the voltage exceeds the regulated amount as well as shortens the duration of voltage deviation with the penetration ratio above 40% (Fig. 2(b)) (R13024).

3 Development of a new reactive power control method according to the change rate of PV output

When the volume of PV systems installed in a distribution system increases, the required capacity of fast-response and high-cost voltage control equipment (SVC) may increase in order to suppress voltage fluctuation. To reduce the required capacity of SVC by supplementing SVR operation, a reactive power control method of power conditioning subsystem (PCS) responding to the change rate of PV output was proposed (R12012). Because the proposed method is expected to supplement Load

Ratio control Transformer (LRT), the effectiveness is evaluated by simulation analyses. Results indicate that the proposed method is able to complement LRT operation, and the required capacity of SVC is further reduced by supplementing both SVR and LRT (Fig. 3) (R13019). Meanwhile, the constant power factor control is also effective to reduce SVC capacity, but the proposed method has the advantages of smaller distribution line loss compared to that of the constant power factor control.

* Experiments were conducted at Akagi Testing Center using ADAPS (Autonomous Demand Area Power System) Demonstration Test Facility. Simulation analysis used instantaneous value analysis program called Xtap developed by CRIEPI.

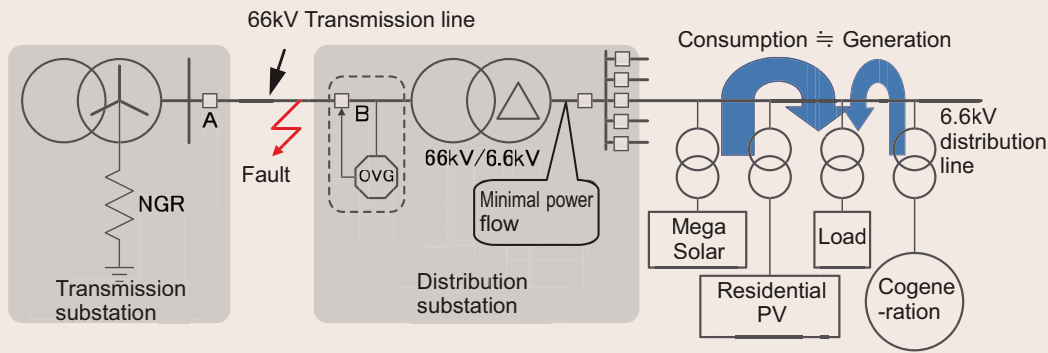


Fig. 1: Condition of the power system below the transmission transformer at islanding

Islanding may occur across a wide area including several 6.6 kV distribution lines when the electrical load and generated power of distributed generators are balanced after opening the circuit breaker at A, or simultaneously opening both at A and B after a 66 kV transmission line fault has occurred.

Table 1: Influence of differing system configurations and operations on the fault condition to islanding detection time (Simulation results)

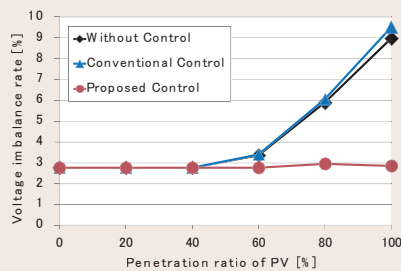
Results with a single-line grounding fault in a 22 kV system where a synchronous generator (2MW) and PCS (600kW, equipping new type active islanding detection function) for PV use are parallel operated. Islanding detection time tends to increase when the faults are cleared at the same time as a circuit breaker of transmission line is opened regardless of the grounding method, and is not influenced by the opening time of a circuit breaker in the transmission line from fault occurrence. Furthermore, islanding can be swiftly detected in the case of an ungrounded system when the faults remain.

(a) Resistance grounded system

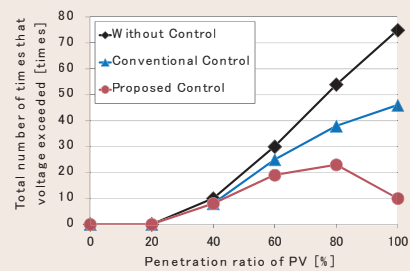
Neutral grounding method: 200A grounding resistance		Opening time of transmission line's circuit breaker [sec]		
		0.5	1.0	2.0
Islanding duration [sec]	Case of fault uncleared	0.856	0.856	0.856
	Case of fault cleared (Opening breaker at A and B simultaneously)	more than 3	more than 3	more than 3

(b) Ungrounded system

Neutral grounding method: Ungrounded (distribution tower)		Opening time of transmission line's circuit breaker [sec]		
		0.5	1.0	2.0
Islanding duration [sec]	Case of fault remained	0.327	0.326	0.327
	Case of fault cleared (Opening breaker at A and B simultaneously)	more than 3	more than 3	more than 3



(a) Voltage imbalance rate

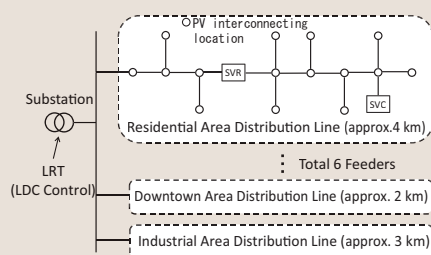


(b) Daily voltage exceeding times*2

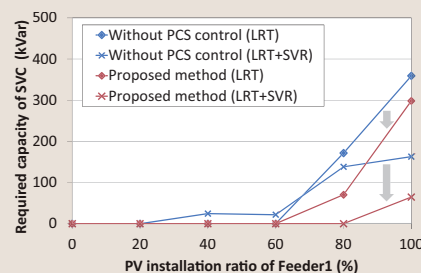
Fig. 2: Comparison between conventional and proposed method with each PV penetration ratio*1

*1 PV penetration ratio = Total capacity of installed PV/distribution line capacity.

*2 $n_1 + n_2 + \dots + n_i + \dots + n_{24}$, where n_i is the number of locations where distribution line voltage exceeds upper limit in 1 hour of i hour



(a) Distribution system model for simulation
A distribution bunk model consists of 6 feeders (residential area, downtown area, industrial area). PV systems are installed in all feeders.



(b) Effect of SVC required capacity reduction (complementing LRT and SVR)
Shows relationships between required capacity of SVC and PV installation ratio of a residential area distribution feeder.

Fig. 3: Effect of the proposed method on SVC capacity reduction

Next-generation Communications Network Systems

Background and Objective

Utility communication network systems have already been satisfactorily implemented for the automated generation and delivery of power, however these are yet to be developed for customer communications including smart metering, power asset maintenance and diagnosis. In addition, communications for power system protection are still proprietary and legacy (not IP-based).

This project deals with the integration of fundamental technologies developed in the previous project, along with the development of design methods and tools for demand area secure communications network interconnecting customers and distributed energy resources, a sensor network for power asset condition monitoring, and IP-based wide-area and high-speed control networks.

Main results

1 Development of network design assisting technologies for the demand area wireless multi-hop network

We developed a tool which estimates radio propagation losses to assist concentrator allocation design for multi-hop wireless smart meter networks taking into account the type of area and impact on the surrounding buildings (Fig. 1) (R13014). We also developed a propagation loss estimation method for smart meters which are placed in the pipeshafts of apartment buildings. For the estimation, experimental

results of radio wave propagation characteristics and electric field analysis software are used (R13006). These results can be used for effective design of a wireless multi-hop network and to assist in determining whether wireless multi-hop communication can be used for apartment buildings or not.

2 Construction of a prototype sensor network for facility maintenance in substations

In the sensor network system that we are developing for facility maintenance, easy and speedy installation of sensors is important for improving efficiency of maintenance work. We have constructed a prototype of the sensor network system for facility maintenance that is equipped with the plug-and-play (PnP) function and the wireless sensor network as elemental technologies. We have also confirmed a series of operations from starting up the sensor to collecting the data on the prototype (Fig. 2) (R13020).

As an elemental technique for stabilizing data collection with a wireless sensor network, we have proposed a method to estimate the cause of data loss occurrence (R13011). Additionally, as an elemental technique for associating a sensor with equipment measured by it, we have proposed a location estimation method of wireless nodes by using sound sensors and broadcasting sampling synchronization data (R13005).

3 Verification of a wide area monitoring, protection and control (WAMPAC) network using power system simulator

A WAMPAC network system associated with applications of wide area current differential protection and load shedding stabilizing control was integrally constructed, employing wide area Ethernet and time synchronization as well as functionally modular control devices that had been individually developed previously. The appropriate operations and effectiveness of the network system were verified using CRIEPI's power system simulator (Fig. 3) (R13012).

Time synchronization to simultaneously sample voltages and currents is required for a WAMPAC system with a large scale communication network consisting of subnetworks. We developed an inter-subnetwork time synchronization scheme and evaluated the accuracy to be less than tens of microseconds* even with network failures to obtain a prospect of large-scale and highly-reliable time synchronized networks (R13023).

* Accuracy of time synchronization for sampling is required to be less than 100 microseconds.

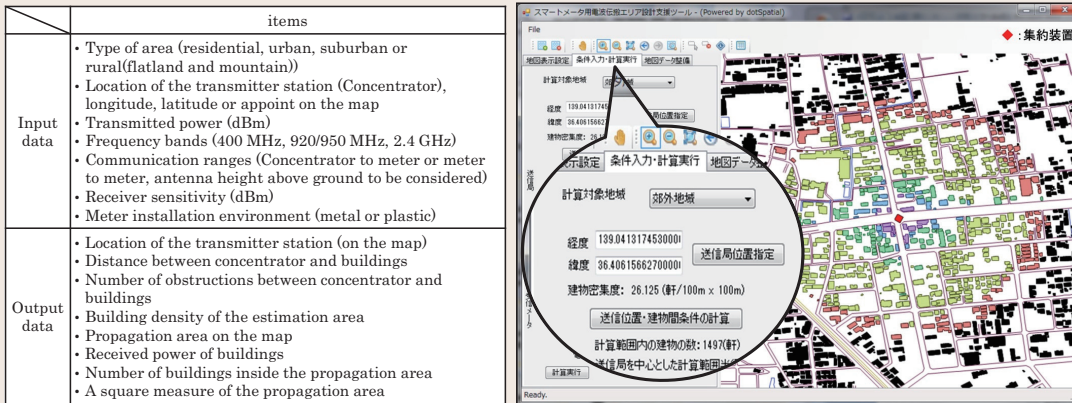


Fig. 1: Input/output data and an example of the display of the wireless multi-hop network design assisting tool

By inputting the type of area and other parameters, a color-coded coverage area is displayed on the area map. The receiving power level of each building and the condition of radio wave shielding around the building are evaluated and displayed also.

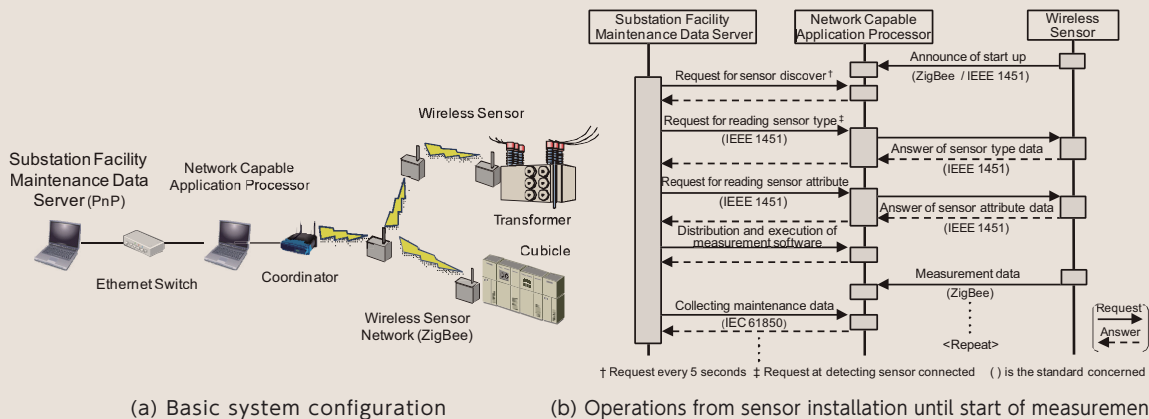


Fig. 2: Basic configuration and operations of the facility maintenance sensor network

A series of functions from sensor start-up until data collection is performed according to the standardized method for sensor specification acquisition and data transmission as well as the PnP function for distributing measurement software.

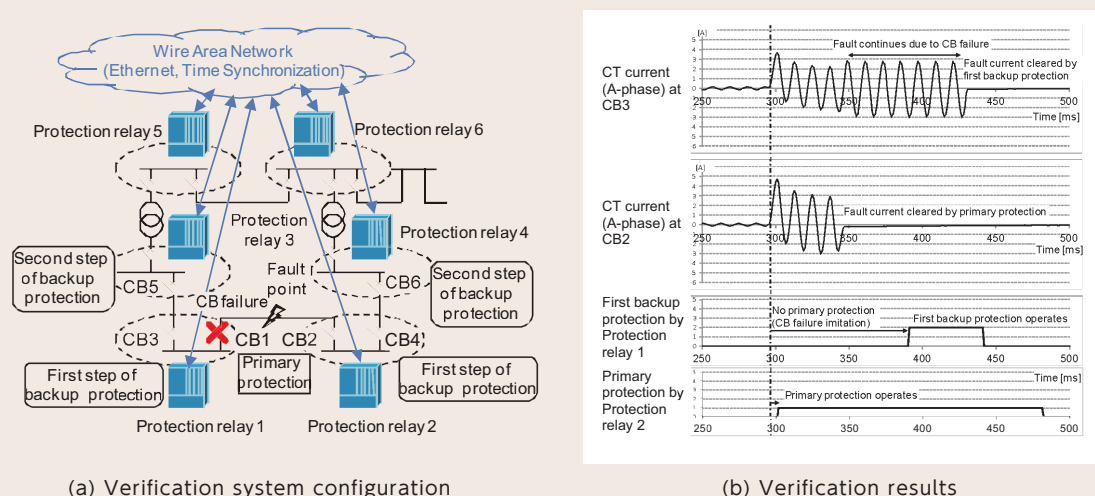


Fig. 3: Performance verification of wide area current differential protection using power system simulator

Each control device, or protection relay, is connected to others via an Ethernet-type wide-area communication network equipped with a time synchronization scheme to clear a fault (primary protection) by processing currents simultaneously sampled for determining the faulty section. When the primary protection fails to operate due to CB (CB1, CB2, etc.) failures or similar, backup protections extend the protection zones with step 1 and step 2 to clear the faulty zone.

Feasibility of Demand Response Suitable for Japan

Background and Objective

Recently, various attempts to utilize Demand Response (DR), such as encouraging peak shaving or load shift of electricity demand by electricity rate, have commenced as a form of experimental critical peak price by electric utilities or demonstration projects of smart communities. However, knowledge of participation rate for DR program, the amount of load shaving, or the degree of customers' response to rate change has

not been sufficiently accumulated.

In this project, we assess the feasibility of DR as a new application for securing grid stability as well as peak shaving from a viewpoint of acceptability and cost benefit. We also supply useful information for electric utilities such as the possible variation in rates or service and global optimization of energy utilization including renewable energy.

Main results

1 Development of a support tool for detecting workers active in DR actions

A tool for obtaining information on confirmation of DR notices to workers in office buildings has been developed. In order to verify the effectiveness of this tool, we conducted an experiment in an actual small office building with around 30 workers (Fig. 1). In the experiment, confirmation time was measured

and interview surveys were executed for 3 workers who confirmed DR notice. The experiment result demonstrates that confirmation behavior of workers observed by this tool has a consistency with concern about DR actions (Fig. 2) (Y13016).

2 A study on possibility of fast demand response in Japanese power systems

High penetration of intermittent renewable energy could require enhancements of power balancing capability in the development and operation of Japanese power systems. This study examined the possibility of fast DR as a supplier of ancillary services mitigating such grid balancing challenges and summarized the merits and demerits of fast DR. The merits are enhancements of power balancing capability and creation of cost-reduction opportunity of ancillary services. The demerits are influences on productivity in the customers' production process when a DR event is called. Uncertainty of power balancing capability from fast DR resources is also

an issue. The study also explored the possibility of implementation of fast DR for four industrial and commercial segments and showed that waterworks, sewerage works and refrigerated warehouses could be potential DR segments due to having time-unvarying electricity demand all day and night throughout the year, as well as having load shifting experiences. Air conditioning of buildings might also be a potential DR segment due to using a large amount of electricity, though unlike the above three segments, this varies hourly, daily and seasonally (Table 1) (Y13030).

3 Issues in cost-benefit analyses of smart metering in Europe

We investigated methodological issues in the cost-benefit analysis of smart metering in Europe and evaluated the results. Many European countries indicate that the net benefit is positive (Table 2). It is important to recognize, however, that these analyses often look at the benefit to society at large,

and that the impact of uncertainty in the benefit of energy savings is particularly large. There may be some non-monetary benefits that are only assessed qualitatively, though such benefits are considered to be small at the moment (Y13022).

4 Issues of estimating costs and benefits of Smart Grid projects in Japan based on the analysis of the U.S. and Europe

Cost-benefit analysis is important to the development of Smart Grid (SG) projects. We explored the methodologies of cost-benefit analysis that made progress in the U.S. and Europe. We found that the basic framework of the approach proposed by the Electric Power Research Institute (EPRI) is applicable to a great variety of SG projects. The European Commission (EC) established a guideline for conducting analysis in Europe which

is mainly composed of EPRI's approach. However, the EC modified the approach to cater specifically to European standards. Furthermore, the EC demonstrated their guideline on an actual SG project. Based on our assessment, we found some needs for modification of the EPRI's approach, for example, appropriately formulating the monetary benefits in our SG project, if it were to be applied in Japan (Y13019).

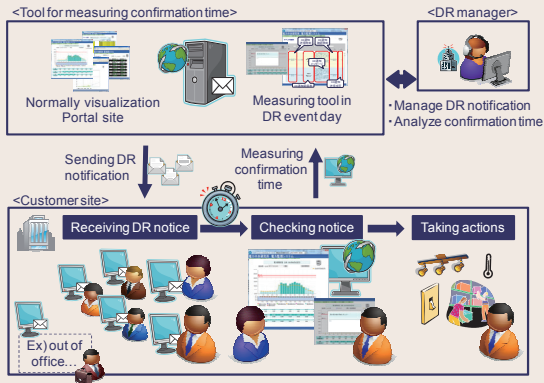
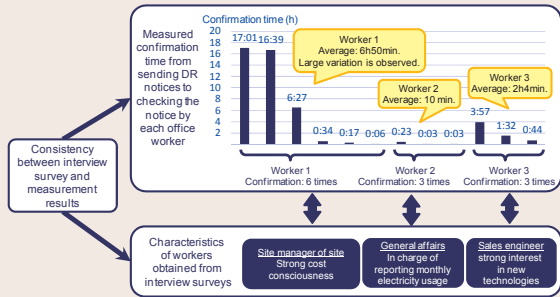


Fig. 1: Conceptual diagram of developed tool for detecting workers active in DR actions



- During this experiment, 9 DR events are issued.
- 6 other workers did not confirm the DR notice.

Fig. 2: Confirmation time from sending to viewing DR notices

Table 1: Possibility of fast DR for four potential and commercial customers

Waterworks, sewerage works and refrigerated warehouses each have an annual averaged load demand of approx. 300 MW in the supply area of Tohoku and Tokyo electric power companies, while air conditioning in buildings has a time-varying load demand, e.g. 7900 MW on summer weekdays and 1600 MW on spring and autumn weekends.

		Water work	Sewerage work	Refrigerated warehouse	Air conditioning in buildings
Time period for fast DR	Season	All year	All year	All year	Summer and winter
	Day	Everyday	Days when amount of sewerage is small	Everyday	Everyday, though weekday has a big DR potential
	Hour	24 hours	24 hours	24 hours	Business hours
Direction of demand change by Fast DR		Demand reduction and creation	Demand reduction only	Demand reduction and creation	Demand reduction and creation
Fast DR techniques		Control of pumps for water supply and delivery	Shut-off of pumps for lifting sewerage, Time shift of sewerage treatment	Control of refrigerators	Control of air conditioners and heat production sources

Table 2: Status of cost-benefit analysis and roll-out of smart meters in Europe

In Germany, a cost-benefit analysis indicated that smart meter roll-out is not cost-effective, even considering customer benefits. In the UK, an analysis suggested that although the benefit from smart meters for distribution network operator alone is not enough to justify the investment, the societal benefit of smart meters outweighs the cost.

Cost benefit analysis		Status of roll-out		Country	
Yes / No	Net benefit	Roll-out decision	Status		
Yes	Positive	Yes	Progress	Austria, Denmark, Finland, etc. (4 countries)	
			Preparation	France, UK, the Netherlands, Norway, etc. (8 countries)	
	Negative	No	Limited roll-out	Preparation	Germany
			Mandate monthly reading*	Complete	Sweden
			Complete	Italy	
No	(N.A.)	Yes	Progress	Spain	

* No formal decision to roll-out smart meters but monthly meter reading requires actual smart meters to be installed.

Table 3: Main results of cost-benefit analysis for Smart Grid projects in the U.S. and Europe

	Findings	Suggestions
Conditions in the U.S. and Europe	<ul style="list-style-type: none"> ● Clarified the concept, cost - benefit, and the methodological approach by EPRI ● Adopted EPRI's approach as a guideline for conducting analysis in Europe by EC ● Based on EPRI's approach, applied the approach to an actual SG project, InovGrid in Portugal, and verified by EC * 	<ul style="list-style-type: none"> → Acquisition of the detailed cost-effectiveness in various SG projects → EPRI's approach spreading to countries other than the U.S. → Applicability of EPRI's approach to actual SG projects
Development in Japan	<ul style="list-style-type: none"> ● There is not much difference in SG concepts between countries ● There are differences in the asset formation, operation and the technology between countries ● The ideas of Smart Community/City are similar to that of SG 	<ul style="list-style-type: none"> → Applicability of the idea of cost-benefits analysis and the framework based on EPRI's approach to SG projects in Japan → The necessity for improvement of the details of EPRI's approach based on actual conditions in Japan → Application of EPRI's approach to the cost -benefit analysis in Smart Community/ City

* Selected as a case study suitable for Europe

Development and Evaluation of Advanced Heat Pumps

Background and Objective

Heat pumps are attracting attention in and outside Japan as an effective technology to promote energy conservation and reduce CO₂ emissions. Much research and development is carried out to improve efficiency, to use low-GWP (global warming potential) refrigerants, and to expand applications to a wide variety of thermal demand.

In this project, we aim to develop and evaluate highly efficient, compact, and low-priced heat pumps using low-GWP refrigerants for residential hot water supply, room heating, industrial process heating and so on. We contribute to the launching and popularization of heat pumps attractive to end users.

Main results

1 Commencing full-scale operation of a New Heat Pump Test Facility

We have designed, manufactured and installed a new unique test facility for the development and evaluation of heat pumps in industrial and commercial applications such as a steam generating heat pumps in sterilizing processes and hot air generating heat pumps in drying processes. Full-scale operation of this facility commenced in the second half of FY2013 (Fig. 1).

Making use of this facility, we aim to obtain data on efficiency and heating capacity under various operating conditions necessary for end users, to construct testing and evaluating methods, to extend our knowledge of generation and utilization of steam and so on, and to strengthen relationships with end users, manufacturers and so on.

2 Evaluation of an industrial steam generating heat pump

With our New Heat Pump Test Facility, we are testing for the industrial steam generating heat pump, SGH165*¹, to evaluate efficiency and heating capacity under various operating conditions whose

parameters are heat source water temperature equivalent to drain temperature in factories, steam temperature and so on (Fig. 2).

3 Evaluation of a large capacity commercial heating system

With our New Heat Pump Test Facility, we are also testing for the commercial heating system which is a combination of a heating tower*² and a water source heat pump chiller, to evaluate

characteristics of frosting*³ and performance of defrosting*³ under various operating conditions which have parameters such as air temperature and air humidity (Fig. 3).

*1 SGH is an abbreviation of Steam Glow Heat pump and applicable to industrial heating processes such as sterilization, concentration, drying, distillation and so on. There are two SGHs, one is SGH120 generating 120°C steam and the other is SGH165 generating 165°C steam, by recovering waste heat from factory drainage.

*2 A heating tower is a heat exchanging system in which brine, or antifreeze solution, absorbs heat from cold outside air. A water source heat pump chiller can generate hot water for room heating by use of an air source heat in combination with a heating tower.

*3 Frosting means freezing of water contained in cold outside air on the surface of a heat exchanger. As frost becomes a thermal resistance and an obstruction of air flow in a heat exchanger, defrosting, or the melting frost, is needed for the operation of a heating tower and an air source heat pump.

【Specification of Tested Heat Pumps】

Industrial Hot Water Generating : max. 600kW
 Industrial Steam Generating : max. 600kW
 Industrial Hot Air Generating : max. 200kW
 Turbo Chiller : max. 2,100kW
 Air Source Chiller : max. 350kW

【Conditions of Temperature and Humidity】

Heat Source/Sink Air : -20~50°C, 30~90%
 Heat Source/Chilled Water : 10~90°C
 Heated/Cooling Water : 10~90°C

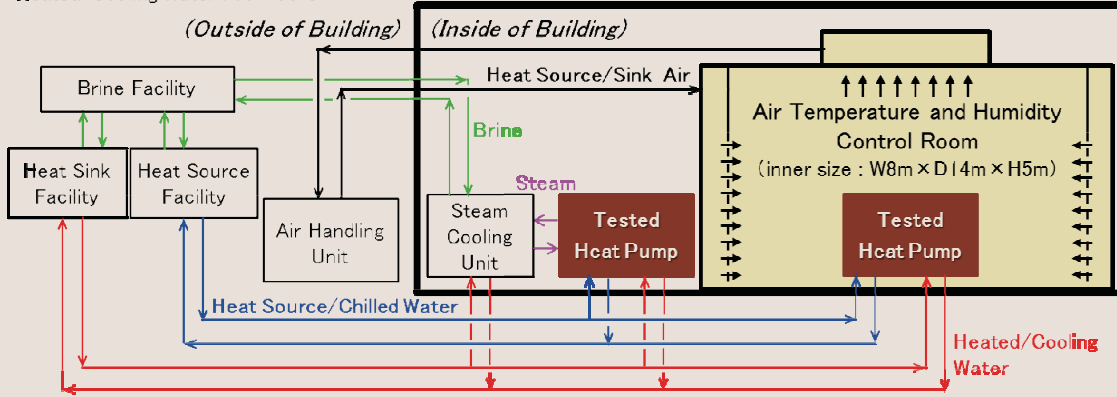


Fig. 1: New test facility for development and evaluation of heat pumps in industrial and commercial use

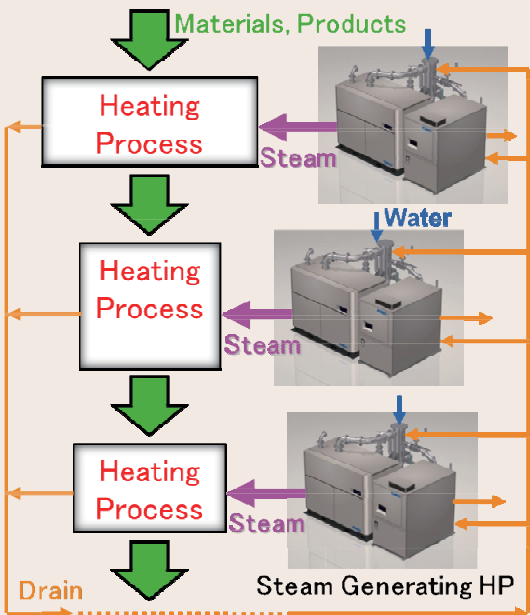


Fig. 2: Industrial steam generating heat pump

Steam condenses and turns into drainage after being used in various heating processes in factories. Efficient use of energy is possible by recovering waste heat of drainage. The higher the temperature of drainage, the higher the efficiency of steam generating heat pumps.

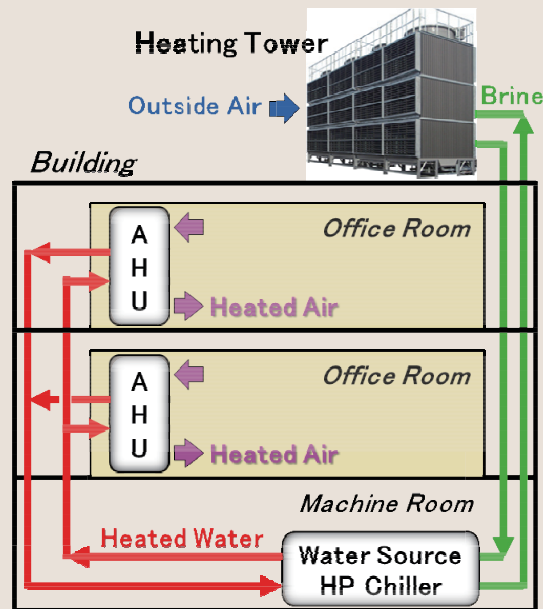


Fig. 3: Heating Tower

In a heating tower, brine, or antifreeze solution, absorbs heat from cold outside air. A water source heat pump chiller absorbs heat from brine and generates heated water. In an air handling unit, heated water releases heat in indoor air to heat a room.

Establishment of Evaluation Technologies for High Performance Secondary Batteries

Background and Objective

Secondary batteries are expected to be utilized not only for load leveling energy storage, but also for stabilization of electric power grid systems connected with renewable power sources such as a photovoltaic and wind power generators. It is thus important to establish the technologies contributing to exact evaluation of their remaining life time and to keep improving the safety technologies for their long-period

operations. We will elucidate the degradation mechanism of lithium-ion batteries (LIB), which have excellent energy density and energy efficiency, as the proper understanding of the degradation mechanism enables exact life-time evaluation. We will also establish comprehensive analysis methods for LIB in order to realize longer life and improve safety.

Main results

1 Elucidating the degradation mechanism of LIB after charge-discharge cycling test

For elucidation of the degradation mechanism, it is important to measure the potential of cathode and anode individually on an operating LIB. The lithium manganese oxide-based cathode and the graphite-based anode were first extracted from a commercially available LIB cell with faded capacity after a long cycling test. Both electrodes were then reassembled into two coin-type half cells with lithium metal as a reference (counter) electrode (Fig. 1), and these two cells were electrically connected at the lithium-metal reference electrodes, which can reproduce the battery performance of the original cell. Next, the test cell was charged and discharged while monitoring the potential

of not only the cathode and the anode, but also the reference electrode. From the analysis, it was revealed that the capacity fading occurred mostly due to less overlapping of individual operation regions (narrowing) for cathode- and anode-side half cells. It was also found that, in addition to the narrowing, the decrease of the reversible capacity caused by inactivation of the active material* at the cathode gives secondary contribution to the capacity degradation of the cell (Fig. 2) (Q13404). We will confirm if this degradation mechanism is applicable to other LIB with different cathode (anode) materials, and propose new materials that realize a prolonged cycle-life.

2 Development of a method to identify the material responsible for the capacity fading in combined cathodes

Certain LIBs use a combination of two active materials as a cathode in order to enhance the performance of capacity and life-time. For proper understanding of the effect of combining on life-time enhancement, it is important to know the individual capacity of each active material in a combined cathode. Through the detailed analysis of capacity-vs-voltage characteristics, we have found that several peaks appear in the differential capacity-vs-voltage curves. Each of them can be assigned to the response from one of the activation

materials, and we can estimate the capacity of each cathode materials by counting the area below each peak (Fig. 3). The result indicates that the mass ratio of the two cathode materials can be estimated simply as the total capacity should be the sum of the capacity attributing to each cathode material. This allows identification of the cathode material mainly contributing to capacity fading^[1]. We will use this method to verify the origin of long-life LIBs with a combination of various cathode materials.

3 Analysis of internal resistance in solid-electrolytes LIBs

An ongoing effort to improve the safety of batteries is required in order to utilize them as an energy storage system connected with power grids. Solid-polymer-electrolytes (SPE) are one of the promising electrolytes for the realization of safer batteries, with more potential than organic solvents normally used in LIB. We constructed the same type of all solid LIBs consisting of a $\text{LiNi}_{1/3}\text{Mn}_{1/3}\text{Co}_{1/3}\text{O}_2$ cathode and a graphite anode as shown in Fig. 1, and

performed AC impedance measurements during a long-period charge-discharge cycling test. From the result, it was revealed that the main reason of the increase of internal impedance was the increase of the interfacial resistance at the cathode-electrolyte interface (Fig. 4), which indicates the importance of externally controlling the interface condition for suppressing capacity fading^[2].

* The materials which take charge-discharge reaction in a battery

[1] T. Kobayashi et al., J. Power Sources, 245, 1-6, 2014

[2] K. Shono et al., J. Power Sources, 247, 1026-1032, 2014.

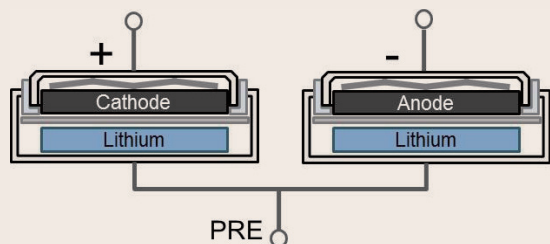


Fig. 1: Simple cell structure within the pseudo reference electrode for measurement of each electrode potential

Instead of special cell construction needed to install reference electrode between the cathode and anode, normal coin-type cell construction is now available by using lithium metal as the pseudo reference electrode (PRE). We disassembled the battery and reconstructed two coin-type cells with a cathode and anode in a glove-box filled with argon gas, and we confirmed cell capacity did not change before and after the disassembly.

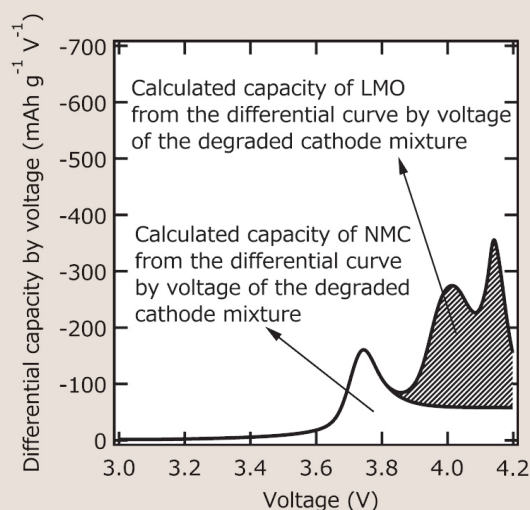


Fig. 3: Evaluation method of individual cathode material in the mixture cathode

In many cases, manganese oxide is used with other cathode materials with different composition. We estimated the capacity of a LiMn_2O_4 [LMO] and a $\text{LiNi}_{1/3}\text{Mn}_{1/3}\text{Co}_{1/3}\text{O}_2$ [NMC] in the cathode mixture, by analysis of the voltage derivative curve of the cathode capacity. We separated the area of the derivative curve based on the characteristics of materials as shown in the figure, which shows the capacity of each cathode material.

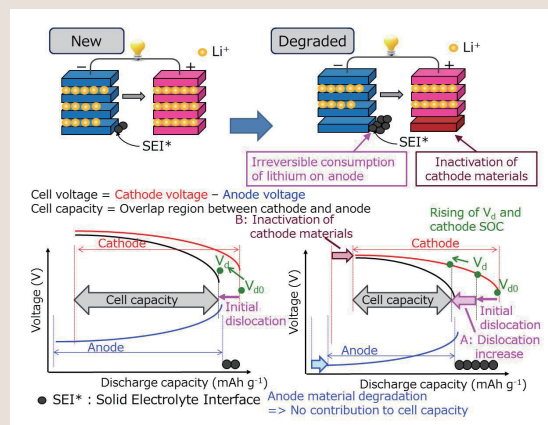


Fig. 2: Capacity fading mechanism evaluated by disassembly and reassembly

A capacity of lithium-ion battery is determined by the size of overlap in the cathode and anode capacity operation area. In a new cell, it is well known that the initial charge-discharge makes film layer on the anode surface by consumption of lithium (• in the figure). We clarified that capacity fading was due to continuous consumption of lithium leading to increasing dislocation of cathode and anode operation regions (A in the figure), and deactivation of the cathode active material (B in the figure) by analysis of discharge end cathode voltage, V_d , and SOC rising.

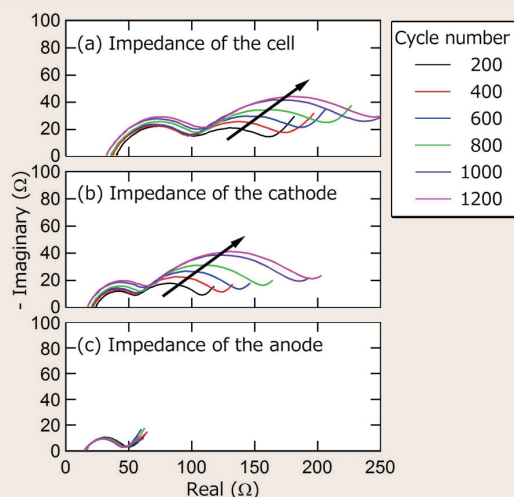


Fig. 4: Analysis of internal impedance of an all-solid lithium-ion battery during long-period operation

We studied the change in internal resistance of a lithium-ion battery consisting of all-solid electrolytes during long charge-discharge operation, using two coin-type cells with the pseudo reference electrode as shown in Fig. 1 by FRA^{*1}. The results showed that the increase of cell impedance (a) is mainly due to the impedance at the interface between the cathode and the electrolyte (b). However, there are almost no changes in the impedance of the interface between the anode and the electrolyte (c).

*1: Frequency Response Analyzer is used to measure AC current response vs. voltage at various frequencies. The impedance data were plotted to the axis with the real number component as x-coordinates and the imaginary number component as y-coordinates.

Socio-Economic Research Center

Brief Overview

Integrating academic expertise in economics, risk management, legal studies, energy system analyses, and environmental sciences, the Socio-Economic Research Center develops viable options for sound

management of electric utilities and energy/environmental policies in an effort to tackle the challenges of the industry.

Achievements by Research Theme

Utility Management and Policy

Aiming at revealing desirable institutional designs for electric utility industry beyond the ongoing utility reforms, the team attempts to develop analytic methodologies and presents implications in terms of management strategies, future growth opportunities as well as resources required for those changes.

■ After the liberalization of electricity industry in Europe, considerable number of energy companies have established a trading division or subsidiary (referred to as “TRD”). Since such organizational structures do not exist until now in traditional electric utilities in Japan, we figured out actual roles and aims of existing TRDs through the interview survey to TRDs, and thereby examined conditions for effectively functioning of TRD if Japanese energy

companies apply it (Fig. 1). (Y13004).

■ Through a review of continuous social surveys on energy and environmental issues conducted in Japan from 1988 to 2013, we revealed trends of public opinion, such as awareness of the safety and necessity of nuclear power had increased, due to the growing interest in global warming over 10 years from around 2000, which then reversed suddenly as the Fukushima Daiichi nuclear disaster occur.

Economic and Social Systems

The team focuses on obtaining a clear understanding of how government actions affect Japan's economy, especially energy and electricity demand, by collecting and analyzing information on changes in policies, economic trends and energy markets.

■ We analyzed the impact of North American energy demand and supply changes in 2020, immediately after commencing LNG export from North America. Contrary to the widely prevalent expectation that the export will lower Japan's average import price of LNG by at least 10%, the result showed that the impact on price is less than half of that expected, in the case that the energy conservation in the US does not advance significantly or their natural gas production stagnates. (Y13023)

■ We forecasted Japan's economy and electricity demand using CRIEPI's short-run macro-econometric model (CRIEPI-SMMQ). According

to the latest forecast, real GDP growth in fiscal 2014 will slow to +0.6% mainly due to sluggish demand after the consumption tax hike. Based on the above economic condition, the growth of electricity demand is forecasted to be +0.3% in 2014. (Y13001) In addition, using our input-output models, we analyzed the impact of a 10% increase in oil prices on production activities by industry (Fig. 2). The result shows that relatively large negative impact occurs in energy-intensive industries such as petroleum products (producer price: +5.5%, production: -2.4%), and non-ferrous metal refineries (producer price: +4.0%, production: -1.9%). (Y13027)

Energy Technology Assessment

While rebuilding a new set of methodology of energy technology assessment in the new era after the Great East-Japan Earthquake, the team strives to support reliable electricity supply in a sustainable manner, with a special emphasis on nuclear power at this time.

■ In order to clarify practical actions to be taken by nuclear operators as well as regulatory authority based on the guidance by International Atomic Energy Agency (IAEA) relating to ‘Nuclear Security Culture’, we showed concrete images of nuclear

security measures which should be taken in Japan through a thorough review of the implementing guide of Nuclear Security Culture published by IAEA, supplemented with an analysis of security threats that actually revealed recently. (Y13002).

**Achievements
by Research
Theme**

■ Surveying the case of investigation framework by Nuclear Regulation Authority (NRA) on the shatter zones at the Tsuruga Power Station, we pointed out the procedural inadequacy such as deficiency to effectively reflect associated scientific knowledge to evolve (Fig. 3). Through analyzing such regulatory problems, we proposed regulatory reformations

including; a) converting internal consultative experts committees appointed by the NRA into a statutory council or a special purpose committee under the act, and b) substantializing institutional separation of risk assessment from risk management in NRA. (Y13024).

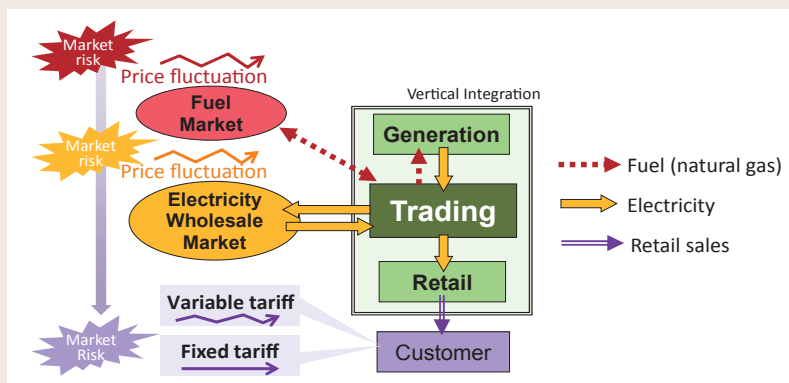


Fig. 1: A TRD model of notable energy Companies in Europe

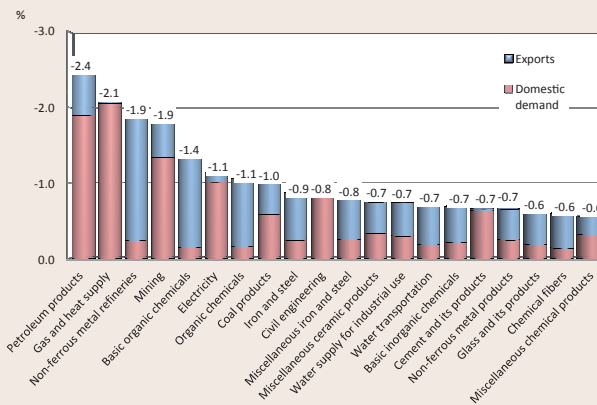


Fig. 2: Influence of soaring fuel prices on production activities by industry -- Top 20 industries

Using our input-output models, we estimated an influence on production in the case of a 10% increase in crude oil price and 7% increase in LNG price. The vertical axis shows the rate at which production would decrease, and the details of the bar chart indicate the contribution. Relatively large negative impact is observed in energy-intensive industries, e.g. petroleum products (-2.4%), gas and heat supply (-2.1%) and non-ferrous metal refineries (-1.9%).

Regulatory Problems that the Shatter Zones at the Tsuruga Power Station Issue presents	Background Factor	Approach to Regulatory Solutions	Contents of Regulatory Solutions
Deficiency to effectively reflect associated scientific knowledge to evolve	Lack of regulatory procedures and legal framework for the investigation that contains scientific uncertainty	Enforcing and improvement of accountability and self-regulation in the NRA, through regulatory controlling for administrative discretion	Reform internal consultative experts committees appointed by the NRA, which are exercising decisive influences on administrative disposition while without any statutory basis, into a statutory council or a special purpose committee under the Act.
Insufficient institutional independence of risk assessment from risk management in the NRA			Substantialize institutional separation of risk assessment from risk management in NRA by statutory measures.
Legal difficulty in conducting administrative dispute to enforce administrative remedies			Make procedures and rules concerning experts' deliberative judgments into administrative by laws to the extent necessary to secure accountability and self-regulation in the NRA.

Fig. 3: Regulatory Problems that the Shatter Zones at the Tsuruga Power Station Issue presents and Regulatory Solutions

System Engineering Research Laboratory

Brief Overview

The System Engineering Research Laboratory (SERL) conducts research on the planning, operation, control of, as well as analysis methods for, electric power transmission, distribution systems, and information/communication systems, in order to facilitate the

secure supply of electricity generated by large-scale and distributed power sources. The laboratory also pursues research on development, testing, and assessment of customer service technologies to achieve more efficient use of electricity.

Achievements by Research Theme

Electric Power Systems

We develop the fundamental techniques of transmission system analysis and evaluations, control and protection for economic and stable operation of the system. Also, using these fundamental techniques, solutions for recent technical issues surrounding the increase in renewable energy introduction, wide-area interconnection and so on are developed.

- To deal with aging transmission equipment, a coordination method of individually determined maintenance/replacement plans is necessary, to make a consistent and efficient plan for the whole system. Therefore, a method to adjust maintenance/replacement plans was developed, which minimizes an objective function composed of five factors concerning difference from initial plans, cost and outage risk (Fig. 1) (R13021).
- Modular multilevel converter (MMC) is a new type of converter and its introduction will continue to spread due to its superior characteristics. However, the calculation cost of simulation for MMC is expensive as the MMC arm has hundreds of cells.

We developed a novel MMC model on which all cells to a voltage source and resistor. The developed model can calculate at a speed of 15.2 times faster than a detailed model in a test circuit (R13027).

- A novel high voltage dc transmission system applying dc boost converters has been studied in our laboratory. A control method has been developed for the system to realize its continuous operation under grid faults. A series of simulation results demonstrate its effectiveness under the grid faults. It is applicable for large scale offshore wind power generations to deliver the power over long distance submarine cable (R13017).

Customer Systems

We develop elemental techniques and tools to support promotion of energy savings by customers. To maintain and enhance power quality of distribution lines, we also develop elemental techniques for supporting estimation and measurement of harmonics generated by customers.

- The ventilation design for commercial kitchens based on the conventional ventilation design standard does not take into account the tendency of cooking appliances to generate heat and moisture. Therefore, the conventional ventilation rate of exhaust hoods for multiple cooking appliances must be excessive. We elucidated ventilation requirements of exhaust hoods for multiple cooking appliances by conducting experiments. The ventilation requirements for multiple cooking appliances are lower than the sum of the individual ventilation rates of exhaust hoods for each cooking appliance, and they are also lower than ventilation requirements based on the conventional ventilation standards (R13015).
- In regards to supporting promotion of energy saving, we developed a heat source characteristic model for room air conditioners up until 2012 by which the electric power consumption during heating and

cooling can be estimated. In 2013, we improved the model so that the electric power consumption and heat load under unsteady states can be calculated. Validity of the new model was evaluated by conducting experiments (R13016).

- Thus far, we made clear that the fifth harmonic current (amplitude and phase angle) could be classified two groups of the middle voltage three phase load group and the other group. Applying the characteristics, a method to estimate fifth harmonic current of each customer in the distribution line was devised. The method is applicable even if measurement condition were limiting, such as only one measurement place in a distribution substation feeder. The results of numerical experiments using a seven node distribution network model indicated that proper estimation could be obtained by the method (R13004) (R13028).

Communications Systems

In order to secure high reliability of communications networks for power utilities required for operations and control of power systems, we develop disaster tolerance improvement technologies for communication systems, construction technologies for communication systems to assist restoration at damaged power systems and security technologies for SCADA systems.

Achievements by Research Theme

■ In microwave radio communication systems, lightning surge current through waveguide can damage communication equipment. To reduce this problem we have proposed utilization of optical fibers as an alternative to waveguide. We confirmed the communication characteristics of radio signal in receiving systems worked by optical fiber power supply. We also evaluated the total communication quality by connecting radio transmitting and receiving systems and confirmed that communication quality was satisfactory. Additionally, output power of radio transmitter was prospected to be close to feasible level by improving output efficiency (R13008). In the future, we will improve the output enhancement method for practical use.

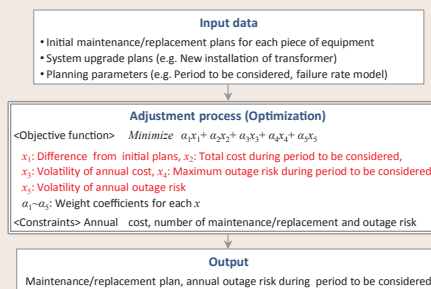
Mathematical Informatics

To achieve accurate diagnosis during maintenance and inspection of electric power equipment, we develop diagnosis methods based on high performance machine learning and image processing techniques. We also develop optimization methods for complex large-scale systems.

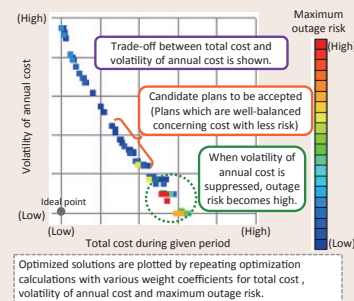
■ To address the issues associated with high penetration of renewable energy sources, such as output fluctuation and surplus power, we proposed a basic framework for a tool to simulate demand and supply operations of power generation units and power storage facilities under the uncertainty of renewable energy sources. As the first step of

■ To make a design guidance of long distance multi-hop wireless LAN for rapid construction of temporary communication channels upon occurrence of a disaster, we estimated characteristics of multi-hop and communication in long span and low height above ground that is supposedly used at a disaster area. As a result, transmission loss estimation in situ is prospected by the type of obstruction (building, forest, steel tower, etc.) and the area of obstruction on the transmission path. Moreover, by measuring multi-hop communication characteristics at varying distances of a section, we confirmed that the total throughput is dependent on that of the longer section (R13009).

simulator development, for photovoltaic power output with no uncertainty, we developed a prototype of the planning module which generates the demand and supply operation plan for one month efficiently, passing data to a daily plan from a monthly plan (R13013).



(a) Flow chart of proposed method



(b) Example of calculation results

Fig 1: Adjustment of maintenance/replacement plans based on multi-evaluation

Weighted combination of the factors is used as the objective function in the adjustment process, and by applying adequate weights, a plan which is consistent with planner's policy can be obtained. Calculations with various weight coefficients will show relation among factors such as trade-off and significantly help to develop a more efficient and accountable plan.

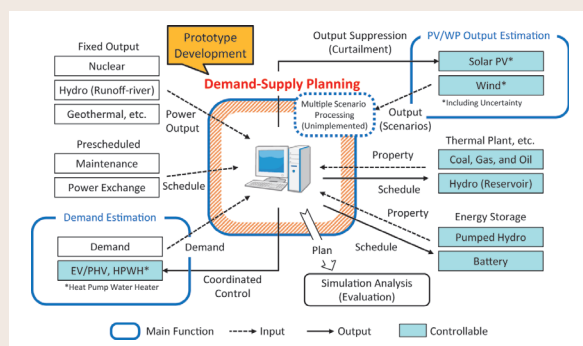


Fig. 2: A basic framework for a demand and supply operation simulator

The planning module, which is the main function of the simulation tool, can generate a demand and supply operation plan in a realistic time by omitting some constraints or simplifying a fuel cost function according to a planning period or desired accuracy.

Nuclear Technology Research Laboratory

Brief Overview

The Nuclear Technology Research Laboratory aims at positively contributing to the solving/alleviation of energy and global environmental problems by means of developing nuclear technologies, including base technologies to support the safety and stable

operation of LWRs as well as the recovery from the Fukushima Daiichi nuclear power plant accident, so that the use of nuclear energy may be accepted by society in a positive manner.

Achievements by Research Theme

Nuclear Reactor Systems Safety

Technologies to maintain and improve the reliability of reactor safety systems, along with the technologies of accident prevention and mitigation at severe accidents have become important to the enhancement of light water reactor safety. We aim to develop those fundamental technologies in connection with the field of thermal-hydraulics and risk assessment.

- As a collaborative study with USNRC, we have been enhancing the nuclear system analysis code, TRACE, which is developed by USNRC and used for worldwide regulatory research. The TRACE code was validated against our experiments which simulated transient events with a reduction in power and coolant flow, and was found to be capable of reproducing the flow redistribution between channels with different powers. The results conclude that TRACE code can reproduce transient events at a sufficiently high accuracy.
- To clarify the cooling characteristics of fuel rods during a water level decrease in reactor vessels, a boil-off experiment using a simulated fuel rod bundle was conducted (Fig. 1). Our experiments clarified the effect of flow rate, thermal bundle power and water temperature on the flow dynamics (void fraction, bubble velocity, bubble diameter, etc.) and fuel rod temperature under atmospheric pressure condition, making the accurate evaluation of time required for fuel rod damage possible*1.
- Installation of a filtered containment venting system (FCVS) is required for severe accident

countermeasures. For the FCVS operation, understanding of its performance in various accident situations and building a database on the decontamination factor under various conditions is necessary. For this purpose, aerosol test, iodine (I₂) test and organic iodine (CH₃I) test was performed under atmospheric pressure using a quasi-full-scale test facility. Moreover, a quasi-full-scale test facility which can test in high temperature and pressure condition was constructed (Fig. 2)*1.

- For use in probabilistic risk assessments (PRAs) of Japanese nuclear power plants (NPPs), a common cause failure (CCF) database containing the analysis results of CCFs of domestic NPPs has been developed in the NUCIA system in JANSI. CCF is one of the dominant risk sources in NPPs. Moreover, candidate solutions have been proposed for the technical problem that a portion of the Monte Carlo calculations for failure rate estimation of components with rare failures are not sufficiently converged; a problem revealed in the application of JANSI generic failure rates to the PRA in domestic NPPs.

Nuclear Fuel and Reactor Core

Research aiming for enhancement of light water reactor safety has been conducted to obtain an understanding of cladding degradation mechanisms, clarification of chemical properties, thermal performance and mechanical behavior of nuclear fuel in accidental conditions, and upgrading computer tools for reactor core burnup performance analysis. Evaluation of molten fuel characteristics and development of subcriticality measurement methodology for fuel debris have also been promoted for contributing to decommissioning of Fukushima-Daiichi nuclear power plant.

- For securely maintaining subcriticality of a degraded reactor core during a severe accident, the concept of "accident-tolerant control rod"*2 was proposed, which would be intact before fuel meltdown, coexist with fuel material after fuel meltdown, and be operational in a similar manner to conventional control rods during normal reactor condition. The candidates of appropriate neutron absorber materials and the fundamental structures of accident-tolerant control rod were obtained as a result of reactor

performance analyses and material tests. (L13005)

- Toward the preparation for fuel debris removal in Fukushima-Daiichi nuclear power plant, an ultra-high temperature furnace for manufacturing simulant fuel debris was upgraded so as to attain a temperature higher than 2700 degree-C, which is necessary to melt fuel. This furnace was successfully used to fabricate zirconia-calcia mixed oxide melt (ZrO₂ - CaO) having the melting point near to that of the fuel debris.*3

Nuclear Fuel Cycle

For the early commencement of commercial operation at Rokkasho reprocessing plant, we conduct experiments

Achievements by Research Theme

necessary for the new safety regulation standard. Also, the development of contaminated water treatment technology is carried out for preventing the spreading of radioactive contamination in the case of a severe nuclear accident. Applying the pyrochemical technology, "debris" fuel is estimated in order to develop a treatment method for the damaged fuel generated in a core meltdown accident. In this way, CRIEPI can maintain the technical level of pyrochemical process.

■ It was necessary to study the radiation elements release behavior during dry out of the high level liquid waste concentrated solution (HLLW) in the event of a severe accident at a reprocessing plant. Release rates of Ru element, which is major elements for radioactive risk, were measured using actual HLLW. Also the Ru release rate from the residue (Mo, Ru, Rh, Pd and Te metallic particles remaining in the fuel dissolution process) was estimated under the high temperature condition during a severe accident. Results obtained in the experiment using the simulated residue showed that very little Ru was

released.

■ Electrochemical properties of simulated debris in molten salt were estimated and the reduction behavior of the debris was also studied in order to develop a pyrochemical technology which can be applied to the debris fuel generated during a core meltdown accident. Additionally, the reduction tests using actual debris generated in an TMI accident were carried out. Sufficient data were obtained to evaluate the applicability of pyrochemical technology to the debris fuel treatment.

Human Factors

In order to contribute to building an organization that exhibits good performance without any human error during both normal operation and emergencies, we will develop measures toward preventing human error and fostering a safety culture by bringing out the features of individuals, teams, and organizations.

■ In order to promote embedding and observance of safety behaviors which are essential regardless of normal operation and emergencies, we clarified work conditions (work characteristics and structures such as being put under time constraint and troublesome tasks) that affect the psychological process of safety

behaviors*4 by literature review and subjective experiments. It is expected that introducing safety rules in consideration of the effects of these conditions will promote self-active safety behaviors by workers. (L13001, L13004)

*1 Part of this research was conducted as the Infrastructure Development Project for Enhancement of Safety Measures at Nuclear Power Plants sponsored by the Ministry of Economy, Trade and Industry.

*2 Accident-tolerant control rod is included in the framework of the Civil Nuclear Energy R&D WG between the Japanese and US governments.

*3 entrusted by Japan Atomic Energy Agency.

*4 A process that a worker decides to perform a safety behavior through "a subjective assessment of hazard", "a supposition of the positive result of the behavior (ability to avoid risk, feeling of satisfaction)", and "a supposition of the negative result of the behavior (decrease in work efficiency, increase in workload)". (I.e. safety behavior that is supposed to avoid high risk and to be low workload will be performed even if the hazard is invisible.)

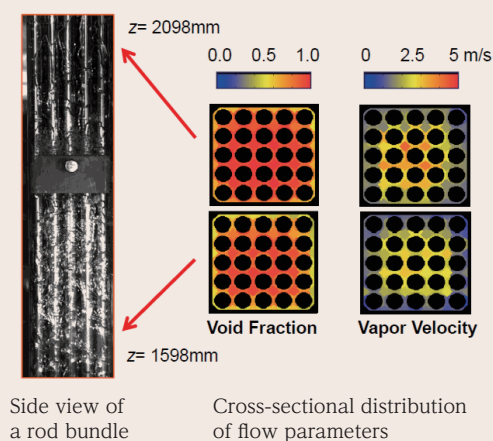


Fig. 1: Visualization of boiling two-phase flow in 5x5 rod bundle (inlet flow rate 0.3m/s, inlet subcooling 1 K, thermal bundle power 37.5 kW)

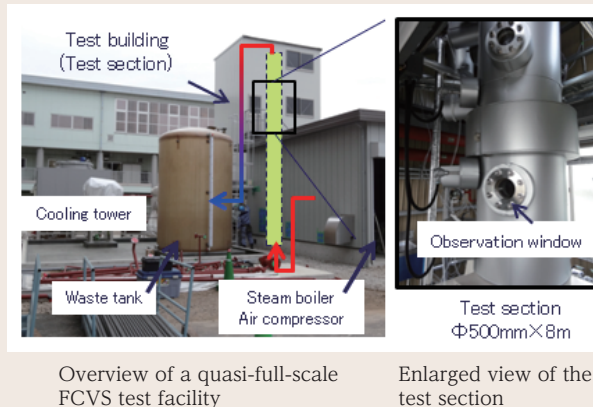


Fig. 2: Quasi-full-scale FCVS test facility. Specifications: test section (inner-diameter: 500 mm, height: 8 m, design pressure: 1.6 MPa), steam boiler (mass flow: 800 kg/h, pressure: 0.8 MPa), air compressor (flow rate: 4.0 m³/min).

Civil Engineering Research Laboratory

Brief Overview

The Civil Engineering Research Laboratory extensively promotes studies regarding geology and geotechnical engineering, earthquake engineering, structural engineering, and fluid dynamics, which are essential for maintenance work and natural

disaster mitigation at electric power civil engineering facilities, as well as for back-end management in nuclear fuel cycle and underground energy utilization technologies.

Achievements by Research Theme

Geosphere Science

To solve issues associated with the siting and construction of electric power facilities and maintenance and asset management of aging facilities, we quantify evaluation methods for earthquake faults, estimation methods for explosive magnitude of volcanic eruptions, assessment methods for the stability of underground facilities, and methodology for groundwater solute transport modeling.

■ To develop a new method for evaluation of fault activity relating to those faults without sedimentary covers, we examined the spatial distribution of various types of microfractures within the damage zone surrounding a Quaternary-active fault which is located east of the epicenter of the 1943 Tottori earthquake, and compared them with previously reported results for a Quaternary-inactive fault. We showed that the Quaternary-active fault has a damage zone characterized by a fracture density that decays exponentially with distance from the fault for open microfractures that represent an opening between opposing fracture walls and lack cementation. Here, we developed a new approach in which we examine the history of fault activity based on whether or not open microfracture density

increases with proximity to the fault.

■ To characterize upward movement phenomenon of carbon dioxide (CO₂) for geologic storage of CO₂, a conceptual diagram of upward gas migration in shallow ground and a hydrogeological structure model coupled two phase flow model of groundwater and gas were constructed using results of surveys and tests performed at natural gas emission parts along the fault and its fractured zone. A numerical simulation of the natural gas upward movement in the ground was conducted by using the abovementioned models and results showed that consideration of capillary pressure, initial saturation of underground gas, fault fracture zone, and trap structure caused by fault displacement could reproduce the behavior of the upward movement.

Earthquake Engineering

We aim to establish proper countermeasures to control risks associated with natural disasters, mainly earthquakes, for electric power facilities and equipment. We also develop low-cost solutions for the maintenance of electric power facilities.

■ We conducted a geophysical exploration at K-NET Minatomachi station (HKD020) where a large acceleration record was obtained during the 2004 Rumoi earthquake (M6.1). The results of this exploration showed that the depth of the basement rock, which is corresponding to the base stratum where the standard seismic motion is formulated for the design of nuclear power plants, is deeper than that derived from previous investigations. We also estimated the basement earthquake motion using the new subsurface model and dynamic property of soils (Fig. 1). (N13007) This result was utilized as a reference of the “seismic motion formulated without a hypocenter” in the Review Meeting on Conformity to

the New Regulatory Requirements for Nuclear Power Plants by Nuclear Regulation Authority, Japan.

■ We developed a high-precision borehole inclinometer using FBG optical sensors to investigate the mechanisms of slope behavior around dam reservoirs and foundations of transmission towers. The new inclinometer detected a very slow slope-movement of a few mm a year, which cannot be detected by the conventional methods. It was revealed through a detailed investigation by boring that the concentrated displacement in the ground detected by the device corresponded to the preliminary step toward a primary slip of the slope. (N13006)

Structural Engineering

To secure the safety and reliability of steel and concrete structures as well as extend their lifespans, we develop structural performance evaluation methods considering natural hazards such as earthquakes, wind, heavy snow, along with aged deterioration caused by environmental actions such as chloride-induced deterioration, frost damage and temperature changes.

■ We established “Seismic Analysis and Performance Evaluation Manuals” for concrete gravity dams and spillway gates, and described a framework of seismic

performance evaluation using Finite Element Method Analysis, characteristics of evaluation, analysis models and examples. These manuals are practical

Achievements by Research Theme

guidebooks covered with various techniques for performance evaluation, equivalent to “Guideline for the Seismic Performance Evaluation of Dams against Large Earthquakes (draft)” published in March 2005 by the Ministry of Land, Infrastructure and Transport, and are expected to be used in soundness evaluation of large-scale earthquakes. (N21) (N22)

- We developed an estimation method of chloride ion effective diffusion coefficient in concrete using

Fluid Dynamics

In order to evaluate the impact of volcanic eruption and fires on the safety of nuclear power plants and also to improve construction, operation, maintenance, and natural disaster mitigation technologies for hydro, solar and wind power plants, we strive to develop basic evaluation technologies of hydraulic and atmospheric fluid flows relevant to such facilities.

- In order to find a rational design basis for wind force acting on electricity distribution facilities, wind tunnel experiments were conducted for a scaled-model of airy residential area where 2-story houses are regularly arranged with 25% plane area density. The results clarified the extent of location where wind force is at least halved and C-class wind load is applicable. The scientific data will be utilized to evaluate applicability of C-class wind load to actual

volume resistivity which is an important physical property in order to assess the chloride induced deterioration of reinforced concrete structures. Volume resistivity is easily measurable for in-situ, thus this method is expected to be utilized for an efficient implementation of the inspections and investigations of reinforced concrete structures located in seaside areas, such as thermal power plants. (N13002)

distribution facilities. (V13016)

- Numerical simulations were conducted for wind around photovoltaic (PV) panels arranged in array to identify panel location where wind force on each panel decreases by more than 50% in comparison with that of single PV panel. The results can be used to design panel support structures based on a reasonable wind force condition, leading to reduction of the construction expenditures. (N13012)

Underground Energy Utilization Technologies

We aim to develop exploration and evaluation technologies for utilizing underground space and developing underground energy such as CO₂ geological storage, large scale electric power storage and geothermal power generation.

- To support electric power utilities to address future introduction of regulations about applying CCS to coal-fired power plants in Japan, we investigated trends in technical developments and policies related to CCS in countries around the world. In Europe, collaboration between enterprises with large CO₂ emissions is progressing, while progress

of CCS deployment is falling short of governmental expectations due to economic recession. On the other hand, under the U.S. governmental visions related to retaining energy security by developing energy sources in the country, CO₂ captured from CCS-equipped plants is being utilized to EOR (Enhanced Oil Recovery).

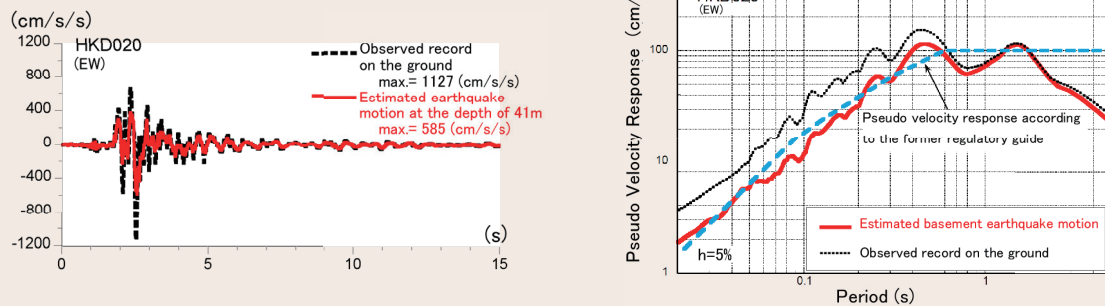


Fig. 1: Comparisons of the observed record during the 2004 Rumoi earthquake and the estimated basement earthquake motion

An earthquake ground motion with a peak ground acceleration of 1127 cm/s/s was recorded at K-NET Minatomachi station (HKD020). The results of geophysical exploration showed that the depth of the basement rock top was GL-41m, which is deeper than the depth derived from previous investigations. We estimated the peak acceleration of the basement earthquake motion to be 585 cm/s/s through equivalent linear analysis considering the non-linear soil response of the surface layer with a thickness of 6 m (left). It is revealed that the pseudo velocity spectrum of the estimated basement earthquake motion was almost the same level as that of the “earthquake ground motion without the site specific epicenter” by the former regulatory guide of the Nuclear Safety Commission of Japan.

Environmental Science Research Laboratory

Brief Overview

The Environmental Science Research Laboratory has promoted basic research on atmospheric, river, coastal and marine environments as well as biology, chemistry, and biotechnology, for the construction

and stable operation of electric power facilities, establishment of a low-carbon society, and reduction of various environmental risks associated with the electric power industry.

Achievements by Research Theme

Atmospheric and Marine Environment

Research objectives are to develop technologies for predicting and assessing atmospheric and marine environments in order to deal with problems, such as air pollution associated with thermal, geothermal, and nuclear power plants and the marine dispersion of radioactive materials.

■ A wind tunnel experimental technique that can reproduce a stable thermally stratified boundary layer was developed to clarify the effects of surrounding buildings and atmospheric stability on the gas dispersion from power plants. An experiment on gas discharged from the vicinity of a reactor building using the developed technique clarified that the effect of atmospheric stability on gas

concentration at the ground surface is small.

■ A model that reproduces the formation of the low-temperature, low-salinity North Pacific Intermediate Water was developed to assess the marine dispersion of radioactive materials. This model enables the accurate assessment of the vertical movement of radioactive materials and thus the accurate simulation of their dispersion in surface layers (V13009).

River and Coastal Environment

Research objectives are to develop technologies for monitoring, predicting, and assessing hydrospheric environments in order to solve related environmental problems. Hydrospheric environments include rivers and reservoirs affected by hydroelectric plants, as well as environments near coastal power plants, such as thermal and nuclear power plants.

■ A ground 3D laser scanner, photogrammetry technique, and a drone helicopter were combined into a tool for the comprehensive assessment of river environments that can be used for updating water rights and supporting sediment throwing in hydropower dams. This research provides insight into the development of a method for visualizing the complicated river-channel topography of mountain streams.

■ The operation of a PC simulation program was developed for a quick estimation of the dispersion area of submerged thermal discharges from coastal power plants. A graphical user interface (GUI) was applied to help users set conditions for a simple model simulation and display its results. A manual for the simulation program was also prepared to encourage relevant electric utilities.

Biological Environment

Research objectives are to develop technologies to address problems related to biofouling and jellyfish, as well as to prevent accidents at power facilities caused by birds and animals, and thus contribute to realizing a stable power supply and rationalization of maintenance. The effects of commercial and intermediate-frequency electromagnetic fields on health were also examined to promote general public understanding.

■ An automated jellyfish monitoring system was developed to ultrasonically quantitatively evaluate jellyfish patches arriving at coastal power plants. The system can detect jellyfish patches to depths of up to 50 m. Efficient operation of countermeasure equipment such as rotary screens can be expected by installing the system in the coastal area in front of power plants.

■ Due to the lack of relevant biological studies to date,

the possible health risks of 20 kHz, intermediate frequency, magnetic field generated from home appliances were investigated. Exposure to a 20 kHz magnetic field exerted no changes in the hematology and histopathology of rats. Together with previous rat studies on 60 kHz magnetic fields, the obtained results did not indicate toxicity of the intermediate frequency magnetic fields under experimental conditions examined (V13010).

Bioengineering

Research objectives are to develop technologies related to the economic treatment of transformers contaminated with trace polychlorinated biphenyl (PCB) and the advanced utilization of unused carbon resources, as well as energy-saving technologies for customers in the agricultural sector.

■ The circulative and energizing cleaning techniques,

both under development, were attested as

decontamination techniques for PCB-contaminated transformers by the Ministry of Environment (Government of Japan). Guidelines on circulative cleaning techniques were published by the Ministry leading to the realization of guideline-based decontamination facilities for contaminated transformers.

- The use of Jatropha oil in diesel engines for power generation is being examined. A mixture of Jatropha and diesel oil less than 1:4 exhibited engine suitability (in terms of fuel consumption and exhaust

gas properties, for example) comparable to that of light oil (V13011).

- The power-generating potential of biogas produced by methane fermentation was assessed on the basis of the amount of high-water-content waste biomass such as sewage and sludge from livestock generated in Japan. Sites that can generate power exceeding 1,000 kW (above which power generation is possible on a commercial scale) were estimated to be approx. 60 sewage treatment facilities and approx. 130 animal excrement treatment facilities (V13012).

Environmental Chemistry

Research objectives are to develop technologies for the effective use of coal fly ash and desulfurization gypsum generated at power plants, as well as cost-effective technologies for the management and treatment of trace elements in wastewater from power plants, in order to support the high-performance and stable operation of coal-fired power plants.

- A method for quickly assessing the elution of fluorine was developed to streamline the quality control of desulfurization gypsum. In this method, a wet ball mill is used, which greatly shortens the elution process that previously required a considerable amount of time through optimization of operations (V13014, V13015).
- An X-ray fluorescence analysis of simultaneously quantifying the Se, As, and Cr concentrations in coal

fly ash in 1 h was developed to promote the effective utilization of coal fly ash. Compared with the conventional wet analysis method, the developed method requires neither complicated pretreatment nor advanced analytical expertise and can reduce the measurement time to 1/15. Hence, it is effective for the onsite quality control of coal fly ash in power plants (Fig. 1) (V13023).

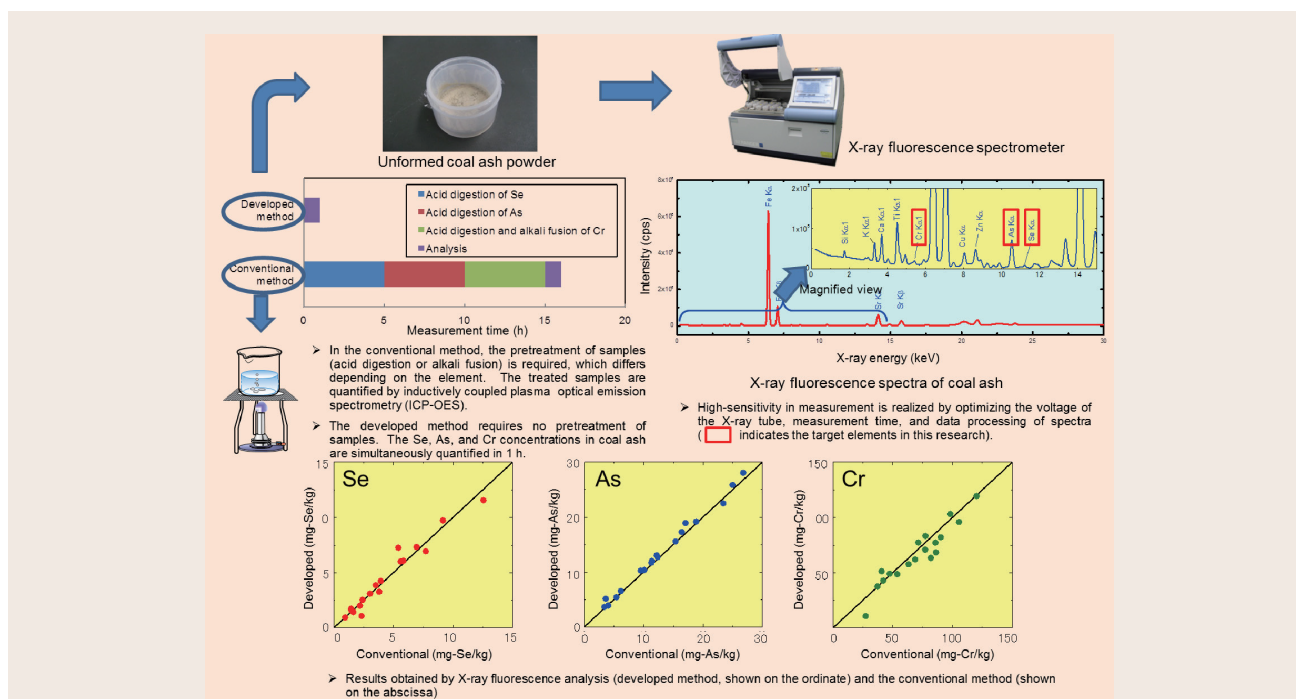


Fig. 1: Simple and rapid quantification of Se, As, and Cr concentrations in coal ash

The accuracy of the developed method was examined using 18 types of ash obtained from existing power plants. Results obtained by this method were practically equal to those obtained by the conventional wet analysis method. In this method, the effect of interfering components is minimized by data processing of spectra and the measurement time is optimized, thus achieving a simple and rapid analysis. The method can be used for the onsite quality control and selection of coal ash in power plants.

Electric Power Engineering Research Laboratory

Brief Overview

The Electric Power Engineering Research Laboratory is engaged in the advancement of fundamental technologies, including electrical insulation, high voltage technology, lightning protection, electromagnetic environment and high current

technology for power transmission and distribution equipment. It is also developing next-generation power equipment and XTAP (eXpandable Transient Analysis Program), simulation and application of arc, application of power electronics and lasers.

Achievements by Research Theme

High-voltage and Insulation

We aim to clarify the deterioration mechanism of solid electrical insulation materials used in aged electrical equipment, advance external insulating technology for transmission lines, improve the accuracy of high voltage measurements and evaluate new insulation materials for next-generation power transmission and distribution equipment.

■ The deterioration of O-rings used for sealing gas insulated equipment influences equipment life. We proposed an estimation method for compression set*¹ based on a visco-elastic model in order to construct the deterioration evaluation method for O-rings. Using this method, the compression set is predicted by obtaining the physical characteristics of visco-

elastic model and usage environment conditions (Fig. 1)*² (H13013).

■ Measurement uncertainties of Japanese national-standard-class measuring system*³ for switching impulse high voltage have been evaluated and it was found that they are of a minimal level compared with those of leading countries (H13003).

Lightning and Electromagnetic Environment

We aim to develop technologies for the lightning protection design and the insulation coordination that are applicable to the demand and supply system of electricity and energy in an information-communications technology (ICT) society, as well as to establish the technologies for the assessment of electromagnetic compatibility (EMC) and electromagnetic environment in power systems and consumer equipment.

■ To improve the prediction precision of outage rate for multiphase faults on 77 to 154 kV transmission lines caused by lightning, the flashover phenomenon in two arcing horns*⁴ arranged in parallel was experimentally investigated in terms of flashover characteristics -

the 50% flashover voltage and the leader developing process. Based on the experimental results, the probability of the simultaneous generation of flashover was clarified to have a proportional relation with the peak value of applied voltage (H13008).

Applied High Energy Physics

We aim to develop numerical analysis methods of pressure rise and propagation characteristics to complement the internal arc testing of electric power equipment, as well as to develop innovative measurement technologies using laser and optical technologies and to work on their application toward the diagnosis of power delivery apparatuses. We also develop plasma melting technology to reduce the volume of radioactive waste for disposal.

■ Some openings and wire meshes are installed in electrical equipment such as switchgears to control the pressure rise due to fault arcs in equipment. In order to estimate the pressure rise and propagation in the equipment by numerical analysis, a simple calculation model was developed in which wire meshes were considered a medium of pressure loss and heat sink / conductor. 3D pressure rises in switchgear with wire meshes were calculated using this model. Results showed that calculated pressure developments were in good agreement with experimental results (Fig. 2). This indicates that the calculation method and the model for the

effects of the wire meshes are well suited for the understanding of the experimental results (H13011).

■ Terahertz waves are effective for measuring the thickness of the topcoat of thermal barrier coating applied to high temperature components in gas turbine thermal power generation, which is usually about 300 micrometers. Measurement accuracy was improved by taking the effects of the surface roughness into account. The measurement method was applied to a real component (gas turbine blade), and the measurement result agreed with the microscopic observation result of the cross section of the blade to within 6%. This confirmed the validity of the method^[1].

Electric Power Application

We aim to develop analysis methods for electric power quality and technologies to achieve design and management of rational electric power systems connected to power electric equipment through the development of cooperating technologies with customers for improving electric power quality.

■ A technique of processing an internal state update in parallel was developed for the improvement in calculation speed of electromagnetic transient simulations programs (XTAP). Moreover, to speed up computation time, a method to reduce computational demand of a remote power system

located far from the source of a simulated transient event was developed (H13005) (H13010).

■ In the distribution system, in order to simplify dynamic voltage analysis, the analysis model for XTAP of a distribution substation and a step voltage regulator was developed (H13007).

High Current Technology

To estimate the performance of electric equipment upon a short-circuit fault, we aim to improve short-circuit test techniques and establish measuring techniques for power frequency current.

■ We developed a simulation code relating to the breaking characteristics of strands of ACSR used in transmission lines by fault current AC arc. The

calculation results were in good agreement with the experiment results obtained by AC arc tests (H13001).

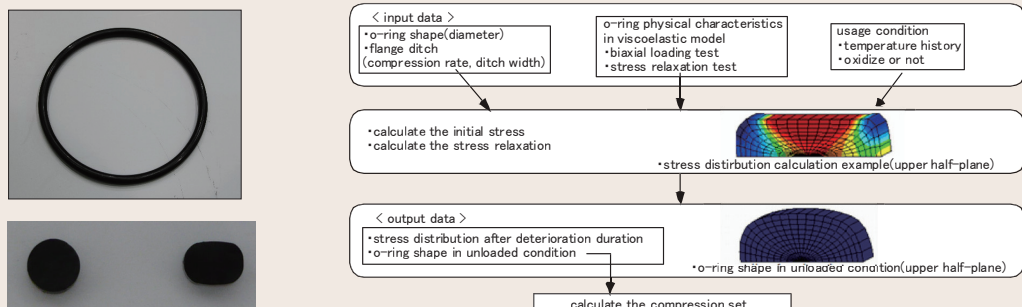
[1] T. Fukuchi et al., IEEJ Trans. FM, Vol. 133, No. 7, pp. 395-401 (2013)

*1 An index of remaining permanent deformation when compression force of an o-ring is removed.

*2 Joint study between CRIEPI and Tsukuba University.

*3 The national standard class voltage divider is owned by Chiba Institute of Technology and the national standard class measuring system is operated under Japan High-voltage Impulse testing Laboratory Liaison (JHILL).

*4 Rods attached to the both ends of insulator string, which protect the insulator strings from the arc discharge following the flashover.



(a) New (left) and deteriorated (right) o-ring

(b) Calculation flow

Fig. 1: An example of an aged o-ring and the compression set prediction flow

Initial stress and stress relaxation are calculated by constructed method based on physical characteristics and diameter of o-ring and setting condition. The o-ring compression set of can be predicted based on stress distribution and shape of the o-ring in an unloaded state after an optional time.

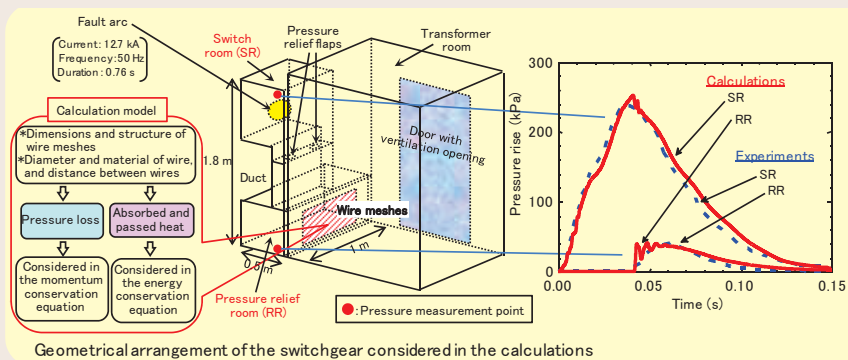


Fig. 2: Comparison between the experiment* and calculation of pressure rise due to fault arc in the switchgear

The calculation results of pressure developments due to fault arc in the switch room were in good agreement with the experimental ones, i.e. the pressure rise in the pressure relief room was suppressed by the opening of pressure relief flaps and the effect of the wire meshes.

*A. B. Wahle. "Untersuchungen zum Einsatz von Energieabsorbern in Ringkabelschaltanlagen im Störlichtbogenfall", Ph. D. dissertation RWTH Aachen University (2007).

Energy Engineering Research Laboratory

Brief Overview

The Energy Engineering Research Laboratory is aiming to achieve security, as well as construct power and energy supply and demand systems,

through the R&D of clean and high efficiency thermal power generation technologies and advanced heat utilization systems.

Achievements by Research Theme

High Efficiency Power Generation

To secure reliability and decrease the operation and maintenance costs of thermal power plants, the rationalization of maintenance and management for the boiler tube and the gas turbine hot gas path parts, as well as the evaluation technology of applicability of non-conventional liquid fuel to the thermal power plant are under development. In order to improve efficiency and reduce carbon emissions, we aim to support the smooth introduction of IGCC commercial plants and evaluate a next-generation coal-based thermal power plant system.

- Miniature sample creep tests and metal temperature analysis of actual boiler tubes have been performed to accumulate reference data for the reasonable judgment of the chemical cleaning interval. It was discovered that the chemical cleaning interval could be extended through forecasting the damaged condition of the boiler tube based on the actual operation data of the thermal power plant boiler.
- The nondestructive method that identifies the delamination of thermal barrier coating on hot gas path parts developed by CRIEPI was examined to find appropriate test conditions. The result of this examination revealed the reasonable test condition as a function of top coat thickness and consequently the method could identify the delamination of the actual parts clearly. (M13007).
- The operating data of Nakoso Unit 10, which was

an IGCC demonstration plant and has been in commercial operation since FY2013, were analyzed in order to predict the gasification performance of the candidate coal. We extended our knowledge about plant performance and suitability to investigate coal types for IGCC, and contributed to the stable commercial operation of the IGCC plant.

- Gasification tests using the 3t/d coal research gasifier and reaction analyses were conducted for investigating oxygen-CO₂ blown gasification characteristics in the high efficiency IGCC system with CO₂ capture which CRIEPI proposed as a future option for low-carbon emission technology. The result showed that the increase in CO₂ concentration in the gasifying agent contributed to improvement in carbon conversion efficiency (M13005).

Advanced Fuel Utilization

In order to diversify energy resources and improve the environmental friendliness of coal-fired power plants, the Energy Engineering Research Laboratory is developing combustion enhancement methods for low combustibility coal, evaluation methods and countermeasures for spontaneous ignition of solid fuels, trace element measurement methods, brown coal dewatering method and manufacturing methods for fly ash solidification material.

- For the spontaneous combustion of coal and biomass, we investigated recent accidents, preventing methods and monitoring methods. The results indicated that the spontaneous combustion during indoor fuel storage occurred more often than during outdoor fuel storage and the monitoring system using an odor sensor would be effective for use with indoor fuel storage, especially silo storage.
- For the effective use of coal fly ash (FA), we examined a manufacturing method that enables

mass-production of FA-shell solidification materials at low cost. We found that FA solidification material without addition of the cement for earthworks, could be produced using a method of concrete placement with vibration (M13304).

- The measurement method for gaseous boron in a combustion flue gas was tested for a simulated coal gasification gas. This result indicated that the method was applicable to a coal gasification gas.

Heat Pump and Thermal Storage

For developing high-efficiency heat pumps and expanding their application areas, we search and evaluate innovative technologies. To assist in proposing energy-saving solutions to customers, we develop simulation tools for analyzing energy consumption.

- Regarding the proposed frost-free heat pump, we

evaluated the potential of the practical system based

on experimental results of the solid desiccant coated heat exchanger. In cold climates, at -7°C and 80% relative humidity, the system could achieve 3.0 COP. It

could also achieve non-frost operation for more than 40 minutes which was the same as the defrost interval of the current air heat source heat pump system.

Energy Conversion Engineering

Basic technologies that relate to the evaluation of thermal efficiency and fuel cells, and environmental analysis, etc., will be developed to improve operability and thermal efficiency of the thermal power plants and geothermal power plants.

- An efficiency improvement of existing gas turbine combined cycle, GTCC, repowered in combination with state-of-the-art Solid Oxide Fuel Cells (SOFCs) was examined. The efficiency of a 1250°C class GTCC rose from 53% to 69% in low heating value, LHV, whereas the efficiency of a 1500°C class GTCC went up from 59% to 71% in LHV in response to an increase in capacity of SOFCs. (M13003)
- Transient voltage response of SOFC (Solid Oxide Fuel Cell) to instantaneous variation of load (up to 1 sec) was evaluated using several bench-scale cells to build a model representing voltage response. The

output control of the SOFC system based on this response would be effective measures to balance fluctuations in generation from renewable sources such as solar and wind power. (M13002)

- X-ray absorption fine structure (XAFS) was applied to the determination of chemical form of trace mercury in complex mixtures such as coal ash and sludge by using SPring-8. The result showed that there is a possibility to estimate the chemical form of mercury from slight structural changes in X-ray absorption edge. (M13004)

Innovative Numerical Simulation Technology

Comprehensive numerical simulation tool is being developed by integrating multi-scale and multi-physical numerical schemes and models in order to solve issues taking place in thermal power generation plants by accurately evaluating performance and optimizing the operating conditions of thermal equipment, such as pulverized coal combustion boilers, coal gasifiers, and gas turbines.

- The detailed flame structure where devolatilization from pulverized coal particles, soot and luminous flame formation were taking place was clarified using laser diagnostics. In order to predict such phenomena, a numerical method that enabled computation of large elementary reaction mechanism concerning tar polymerization and decomposition within a practical computational cost was developed.

- The chemical analysis of SCR catalyst showed that the deposition of ash particles on the catalyst surface was one of the major mechanisms suppressing DeNOx catalytic reactions in the DeNOx SCR system in a coal-fired power plant. A numerical estimation method of ash particle deposition on the catalyst surface was also developed to predict such phenomenon.

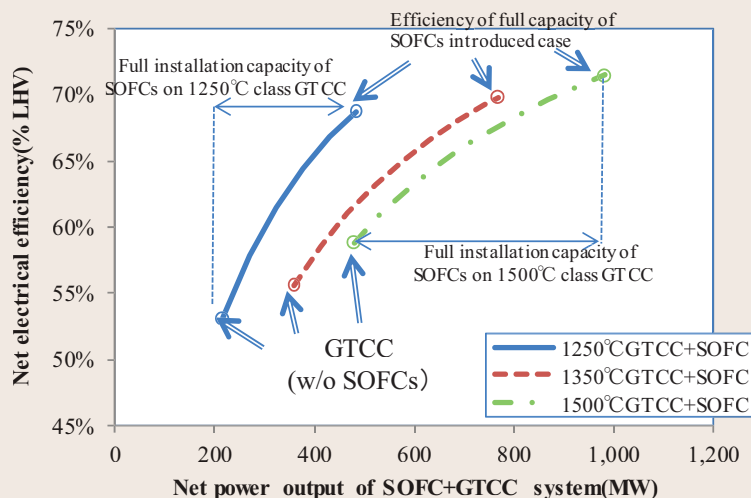


Fig. 1: Efficiency improvement of existing GTCC repowered by SOFCs

The maximum capacity of installed SOFCs is regulated by the air flow rate from the compressor of GTCC. The installable capacity of SOFCs is 250 MW while the corresponding efficiency improvement is 16% for 1250°C class GTCC case. For the 1500°C GTCC case, the installable capacity of SOFCs is 460 MW, while the corresponding efficiency improvement is 12%. Higher efficiency improvement by the installation of SOFCs is obtained in 1250°C class GTCC case.

Materials Science Research Laboratory

Brief Overview

The aim of the Materials Science Research Laboratory is to contribute to reliable electric power supply and creation of a low-carbon society through fundamental material research for field

applications to electric power plants, renewable energy utilization, and new materials development for energy conservation.

Achievements by Research Theme

Structural Materials

We will contribute to the reliable and stable operation of thermal and nuclear power plants through research activities such as fundamental data accumulation of high-temperature materials strength and corrosion behavior, development of lifetime evaluation methods for aged structural components and the development of non-destructive inspection technologies.

- The welded portions of 9Cr steel elbow pipe which had been used for a prolonged period of time in an actual plant were evaluated through a creep test, microstructure observation, and a hardness test. The results indicated that the intrados welded portion has a shorter residual life than the extrados welded portion (Fig. 1). Moreover, a correlation was observed between the voids, which represent creep damage, and the hardness of the welded portions^[1].
- Strain rate-dependency of rupture ductility (Fig. 2) and fatigue property were obtained on Alloy 617 candidate for an Advanced-Ultra Super Critical

(A-USC) thermal power plant as fundamental information required for creep-fatigue evaluation (Q13001).

- The technique for identifying areas of sulfidation on water-wall tube in coal-fired boiler estimated by analyzing the chemical composition of ash on the tube surface has been applied to some commercial boilers. The relationship between gas composition fluctuation in coal-fired boilers and sulfidation behavior of the water-wall tube was investigated, and some important data were acquired in order to improve the predicting method of sulfidation rate.

Materials for Energy Conversion and Storage

We will develop technologies to evaluate the field performance of photovoltaic (PV) systems to prepare for mass installation in the future. The application technologies of functional materials based on electrochemistry will also be studied for the effective use of renewable energy.

- A new type of weather classification based on solar irradiance variability was presented to facilitate low cost prediction of power yields of grid-connected PV systems. We have obtained prospects of the utilization of AMeDAS data through analyses of solar irradiance with the developed weather classification (Q13005).

- Electrochemical synthesis of ammonia in a molten salt system has been investigated as an attractive candidate for a carrier of hydrogen energy. The dissolution of the synthesized ammonia was observed in the presence of H⁻ ion produced by a side reaction on a hydrogen gas electrode, which led to the decrease in the conversion yield of ammonia (Q13004).

Advanced Functional Materials

We will develop new functional materials such as high-temperature superconductors and organic semiconductors by utilizing various sophisticated techniques of growing high-quality crystals and controlling their basic physical properties.

- We improved growth techniques of iron-chalcogenide superconductor thin films, and succeeded in raising superconducting critical temperature from 8 K to 12 K in FeSe, and from 14.2 K to 19 K in FeSe_{0.5}Te_{0.5} composition^[2]. These materials exhibited extremely high critical current density in a high-magnetic field, and are expected as one of the candidates of practical superconducting coated conductor materials.

- We developed new kinds of organic devices called light-emitting electrochemical cell, and succeeded in preparing three basic colors, red, green, and blue (RGB) that are indispensable for display applications (Fig. 3). These devices also exhibited a refreshing effect by current alternation, which is one of the key technologies for long-term stability (Patent 2013-145690, 2013-145691, 2013-14562).

High Performance SiC Semiconductor for Power Electronics

To realize next generation low-loss power conversion equipment, we will establish a high-quality silicon carbide (SiC) crystal growth technology which enables the fabrication of low-loss, high-voltage, SiC power devices able to handle large currents.

**Achievements
by Research
Theme**

■ We established a 6-inch diameter, fast, low-defect density SiC crystal growth (epitaxial growth) technique achieving a high growth rate of 50 $\mu\text{m}/\text{h}$ with high uniformity by conducting collaborative development with several companies^[3].

■ We succeeded in fabrication of ultra-thick, multi-layer SiC crystal wafers capable to be applied to very high voltage (>13 kV) SiC transistor devices and demonstrated the low-loss current conduction performance close to the SiC limit in prototype devices.

Materials Science Research Fundamentals

We will promote fundamental research for predicting material properties and evaluating localized stress states by a combination of computer simulations and advanced materials analysis methods aiming at a breakthrough in materials research.

■ The coarsening behavior of Cr_{23}C_6 precipitates in a high-temperature ferritic steel was investigated at an atomistic scale through molecular dynamics

computer simulations using a newly developed inter-atomic potential for Fe-Cr-C ternary alloys.

[1] S. Nagai et al., Proc. 7th Int. Conf. on Advances in Materials Technology for Fossil Power Plants, 609-701, 2013
 [2] F. Nabeshima et al., Appl. Phys. Lett., 103, 172602, 2013
 [3] H. Fujibayashi et al., Appl. Phys. Express, 7, 015502, 2014

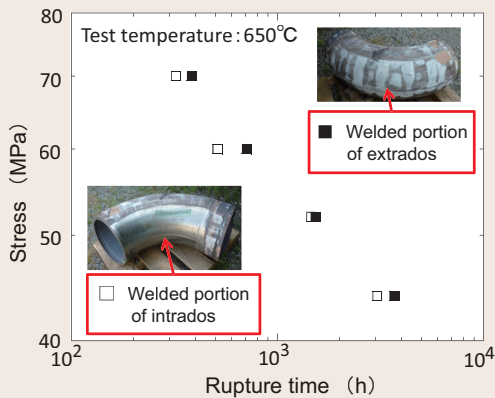


Fig. 1: Creep test results on a 9Cr steel elbow pipe used for long-tem

In the creep test on welded portions of an elbow pipe that had been used in an actual plant for a prolonged period, the creep rupture time was shorter in the extrados side of the elbow pipe.

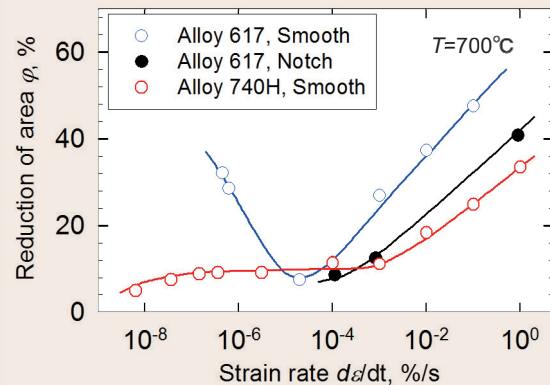


Fig. 2: Relation between strain rate and ductility (700°C)

Ductility significantly changes with strain rate in both materials but smooth specimens of Alloy 617 particularly showed unique behavior, showing the minimum ductility at an intermediate strain rate.

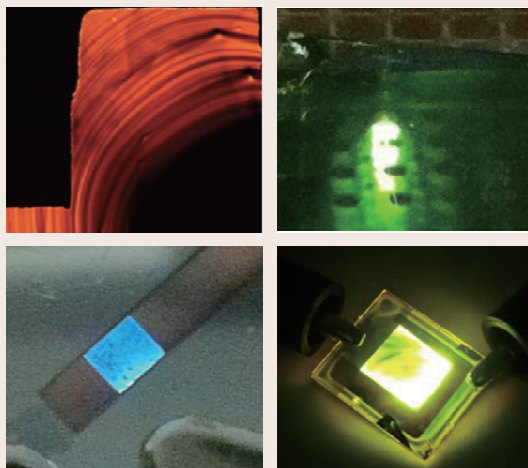


Fig. 3: Multi-colored light emission from Light-emitting Electrochemical Cell devices (red, green, blue, and yellow emission)

We will continue the technology development of these devices to realize new-types of energy-saving lighting device and displays.

3. Major New Research Facilities

Large-scale Tsunami Physical Simulator

Background

Safety reviews of nuclear power stations in accordance with the new regulatory requirements are being carried out by Nuclear Regulation Authority (NRA), Japan. Furthermore, periodic safety reviews for NPSs are also required after NPSs recommence their operations. The NRA requires these periodic safety reviews to include probabilistic risk assessment (PRA) for NPSs, and this involves assessing risks against not only design basis tsunamis but also beyond-design basis tsunamis. In order to appropriately perform

the risk assessment against beyond-design basis tsunamis, systematization of the evaluation and verification methods for fragility of structures and instruments against tsunami in inundation areas are needed. To carry out verification tests for the fragility of structures and instruments in NPSs against giant tsunamis, CRIEPI has installed a Large-scale Tsunami Physical Simulator, a large flume in which various kinds of tsunami inundation flows are generated faithfully on large-scale.

Outline

This facility is able to generate tsunami-inundation flow with a steep front, long-duration, high-speed and large-depth flow on a large scale. For example, the inundated tsunami with a depth of 5 meters observed at Kesennuma city on the 2011 Tohoku earthquake is reproduced on a 1/3-scale in the flume. This facility makes

verification experiments of fragility of the structures or instruments under site specific tsunami inundation flows possible. Using this facility, large-scale experiments for evaluations of tsunami hydrodynamic load, debris impact load, and damage mode of structures under tsunami-loading conditions.

Specifications

Size (test section): 20 m length, 4 m width, 2.5 m height (with a 1 m deep scouring pit).
Maximum velocity: 7 m/s
Maximum flow volume: 10 ton/s
Volume of water tank: 650 ton
Maximum depth of water tank: 6.5m



[Location and date of installation]

Abiko area / February, 2014



Photo 1: External view of the Large-scale Tsunami Physical Simulator

Full-scale Test Facilities for Snow-storm Damage to Overhead Transmission Lines (Abbreviated name: Kushiro Test Line)

Background

In order to reduce snow-related accidents which lead to wide-scale power outages, evaluation of the effects of countermeasures for wet snow accretion with strong wind and galloping on snow accreted multi-bundled conductors are important. For verification of the effectiveness of the measures and clarification of the physical

process of snow-storm damage, full-scale test facilities were constructed in the Otanosike area of Kushiro city, Hokkaido, where frequent snow accretion is assured with strong north-northeast winds when low pressure systems pass through the southeast shore of eastern Hokkaido in winter.

Outline

The facilities consist of two main towers to support four and two-bundled conductors, and another smaller tower to support single conductors. Ongoing remote observation is performed using various meteorological instruments and network cameras placed at the towers and on

an observation pole, which enable the observers to monitor and record data successively at our own laboratory. Moreover, DC voltage is applied to two of the single conductor lines to evaluate influence of the heat generation of the conductors by flowing current to snow accretion.

Specifications

[Tower design condition]

Upper arm (400 m in span, 40 m in height): four-bundled conductors $\times 2$ lines, ACSR810 mm² conductor or less

Middle arm (400 m in span, 31 m in height): two-bundled conductors $\times 2$ lines, ACSR1160 mm² conductor or less

Lower arm (300 m in span, 25 m in height): single conductor $\times 5$ lines*, ACSR810 mm² conductor or less

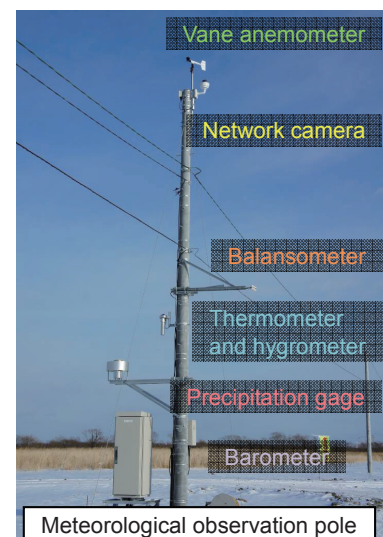
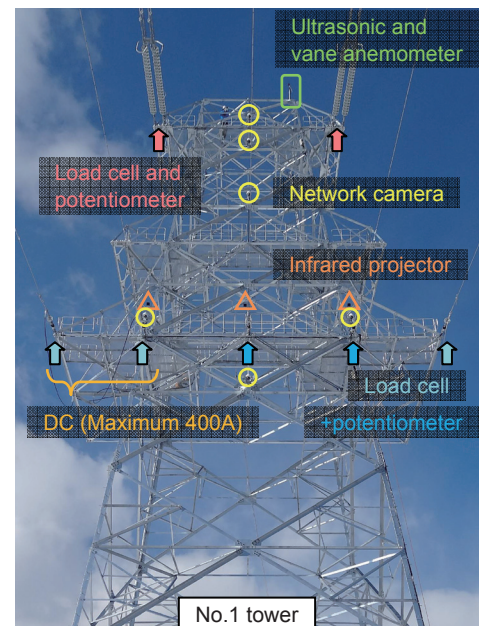
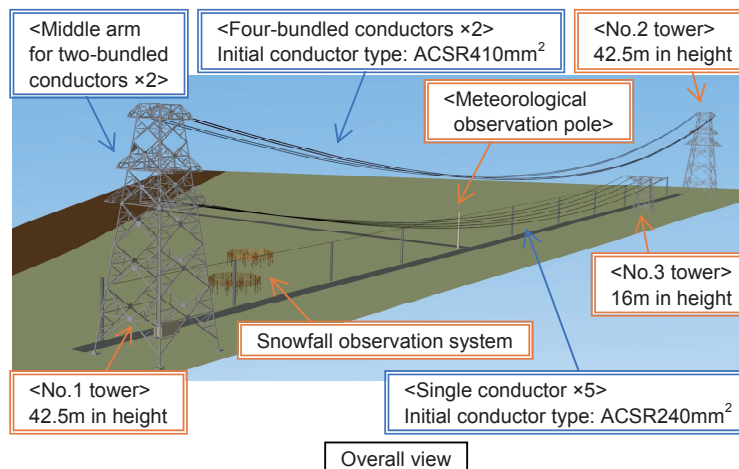
*Difference in support level is 9 m. A DC voltage is applied to provide current up to 400 A for the two lines.

[Observation items]

Wind direction and speed (vane type and ultrasonic type), temperature, humidity, atmospheric pressure, amount of snowfall (tipping bucket type and weighing bucket type with double fence), radiation balance (long and short, upward and downward), drop size distribution and velocity of falling snow, conductor tension, support angle of conductor (horizontal and vertical direction), image (network camera and spacer camera), displacement of conductor at the target, surface temperature of conductor

[Location and date of installation]

Otanosike area in Kushiro city / March, 2014



Full-scale test facilities for snow-storm damage to overhead transmission lines

Advanced Combustion Test Facility for Diversification of Available Fuel Types

Background

From the view point of fuel security and fuel cost, diversification of available fuel types including low grade coals is important in Japanese coal-fired power stations. Furthermore, in order to reduce CO₂ emission, biomass co-firing with coal is proceeding. This facility consists of two furnaces, namely combustion test furnaces with a single burner and a small combustor (TCMF; Turbulent Combustion Modeling Furnace). The combustion test furnace

with a single burner is able to evaluate grinding and combustion characteristics of solid fuels since the combustion conditions are almost the same as that of actual power stations. In TCMF, combustion phenomena of various fuels are investigated. The results improve a numerical analysis model for combustion, which is effective in the advancement of combustion technologies.

Outline

- Combustion test furnace with a single burner
Combustion conditions in the test furnace simulate those of actual power stations. It is possible to evaluate the grinding characteristics of solid fuel using a roller mill, combustion characteristics such as ignitability and combustion efficiency, as well as the emission characteristics of a pollutant. Advanced combustion technologies such as oxygen enriched combustion are also developed for various types of fuel.

- Turbulent Combustion Modeling Furnace (TCMF)
Precise laser measurements of gas velocity, temperature, particle diameter and gas components in the simple combustion field are utilized to improve a numerical analysis model for combustion. Estimated combustion characteristics using this model are utilized to reasonably decide combustion conditions and investigate scale-up effects.

Specifications

- Combustion test furnace with single burner
Pulverizer: Roller mill (Coal grinding rate; approx. 300 kg/h)
Furnace: Water cooled and horizontal cylindrical type with single burner (Φin 850 mm × Length 8,000 mm)
Thermal input; 760 kW
Function: Coal feeding rate; approx. 100 kg/h, Liquid fuel injecting rate; approx. 30 L/h
Oxy-fuel combustion (Flue gas recirculation and oxygen injection (max. 200 m³/h))
- Turbulent Combustion Modeling Furnace (TCMF)
Furnace: Vertical cylindrical type (I.D. of 250 mm × height of 2,000 mm)
Thermal input: 10 to 80 kW
Function: Coal feeding rate: 1 to 10 kg/h
Measurement equipment: LDV (Laser Doppler Velocimeter), PIA (Particle Image Analyzer), TDLAS (Tunable Diode Laser Absorption Spectrometry) and so on.

[Location and date of installation]

Yokosuka area / January, 2014

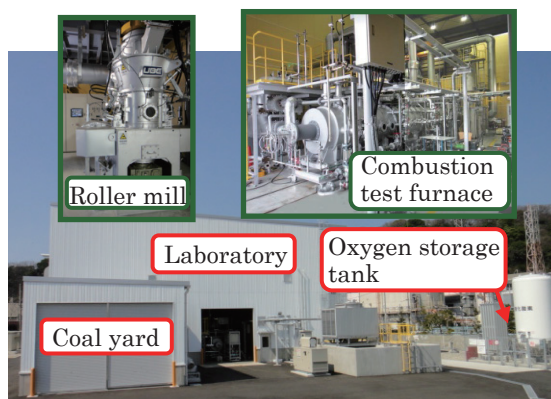


Photo 1: Coal combustion test facilities in the laboratory
Roller mill and combustion test furnace with single burner

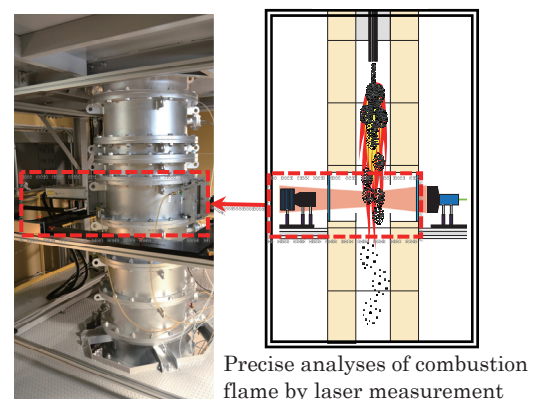


Photo 2: Turbulent Combustion Modeling Furnace (TCMF)
Measuring point in the furnace center

Test Facility for the Carbonization of Biomass

Background

The electric power industry is promoting the use of biomass co-firing in coal-fired power plants, and assumes that approximately 400,000 tons of woody biomass is consumed per year. However, the co-firing rate remains at a few percent due to the grindability of woody biomass being substantially lower than that of coal. If biomass grindability is improved and co-fired at a high mixing rate, there will be a considerable reduction in power plant CO₂ emission. Biomass carbonization is one of the technologies which enable biomass co-firing at a high mixing rate in coal-fired power plants. By carbonizing the woody biomass, some advantageous effects such as improvement of grindability, increased

heat value and water repellency are expected. On the other hand, there are some issues to resolve such as the reduction of heat loss in the biomass carbonization process, the suppression of spontaneous ignition and the control of pulverization during transportation and storage of carbonized biomass. The aim of this test facility is optimization of carbonization conditions such as temperature, the residence time in the carbonization process and the moisture/size of raw biomass from the viewpoint of selection of raw biomass, advantage of carbonization, reduction of energy consumption and ensuring safety of carbonized biomass.

Outline

The facility is capable of carbonizing high moisture biomass in addition to low moisture biomass by installing a hot-air dryer and two types of conveyance systems for biomass moisture. In order to analyze the heat balance of the carbonization process and to understand carbonization performance, process information (over 170 points

of measurements such as temperature, pressure and flow rate) can be stored in the data acquisition system. The analysis of pyrolysis gas components is also possible. In terms of achieving commercial scale, an indirect heating type rotary kiln was adopted as a carbonizer.

Specifications

- High-temperature rotary kiln for carbonizing machine
 - Feed rate of raw biomass : Max. 200 kg/h (moisture 30%)
 - Carbonization temperature : 200 to 600 degC
 - Residence time of biomass : 20 to 60 min
- Hot-air dryer
 - Feed rate of raw biomass : Max. 500 kg/h (moisture 80%)
 - Moisture of dried biomass : 10 to 30%
- Analyzing device
 - Micro GC, GS, HPLC, UV-Vis-NIR

[Location and date of installation]

Yokosuka area / July, 2013

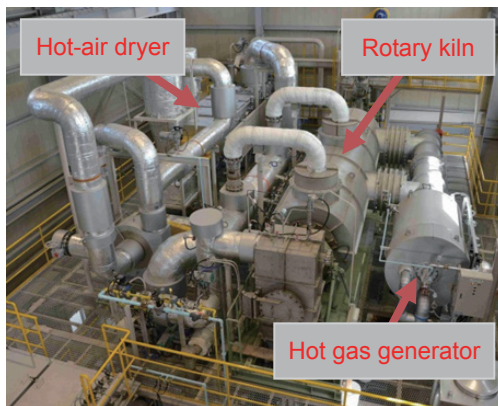


Photo 1: External view of the test

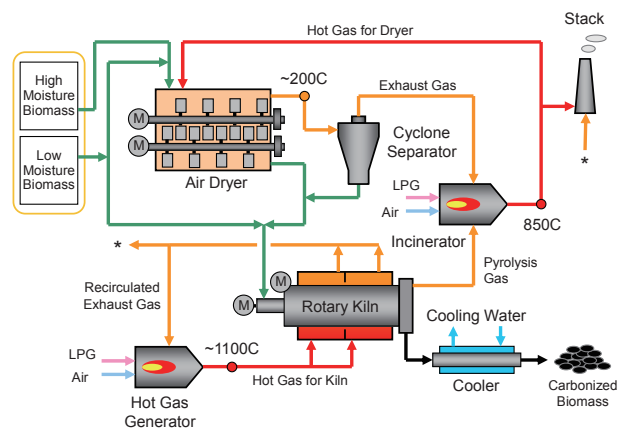


Fig. 1: Schematic diagram of the test facility

Test Facility for Development and Evaluation of Heat Pumps in Industrial and Commercial Use

Background

Heat pumps are attracting attention both in and outside Japan as an effective technology to promote energy conservation and reduce CO₂ emissions. Much research and development is carried out to improve efficiency, to use low-GWP (global warming potential) refrigerants,

and to expand applications to a wide variety of thermal demand.

With this facility, we aim to develop and evaluate highly efficient, compact, and low-priced heat pumps using low-GWP refrigerants in industrial and commercial use.

Outline

The facility is able to evaluate heat pumps such as industrial steam generating heat pumps, industrial hot air generating heat pumps, turbo chillers, etc. under various operating

conditions with parameters of heat source/sink, air temperature & humidity, heat source water temperature, steam temperature and so on.

Specifications

- [1] Specification of Tested Heat Pumps
 - (1) Industrial Hot Water Generating Heat Pump
Heating Capacity: Max. 600 kW, Output Water Temperature: Max. 90°C
 - (2) Industrial Steam Generating Heat Pump
Heating Capacity: Max. 600 kW, Output Steam Temperature: Max. 200°C
 - (3) Industrial Hot Air Generating Heat Pump
Heating Capacity: Max. 200 kW, Output Air Temperature: Max. 200°C
 - (4) Turbo Chiller
Cooling Capacity: Max. 2,100 kW
 - (5) Air Source Chiller
Cooling/Heating Capacity: Max. 350 kW
- [2] Conditions of Temperature and Humidity
 - Heat Source/Sink Air Temperature & Humidity: -20 to 50°C, 30 to 90%
 - Heat Source/Chilled Water Temperature, Heated/Cooling Water Temperature: 10 to 90°C
- [3] Inner Size of Air Temperature and Humidity Control Room
W8m × D14m × H5m

[Location and date of installation]

Yokosuka area / June, 2013

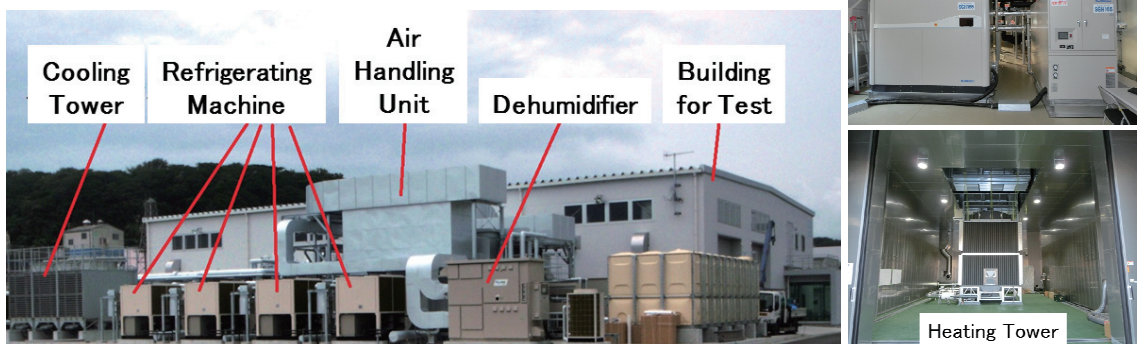


Photo 1: External view of the test facility and tested machines

Left: Test Facility, Upper Right: Steam Generating Heat Pump (SGH165), Lower Right: Heating Tower

4. Activities

4. Activities

The activities of the CRIEPI in FY 2013 are outlined below.

1 Human Resources

The CRIEPI employs 820 people as of 31st March, 2014. 722 people are employed in research fields while 98 people are involved in clerical work. Fig. 1 shows the breakdown of researchers working in diverse fields. 409 people working at the CRIEPI have a Ph.D. Of these, 73% and 10% have an engineering and science background respectively.

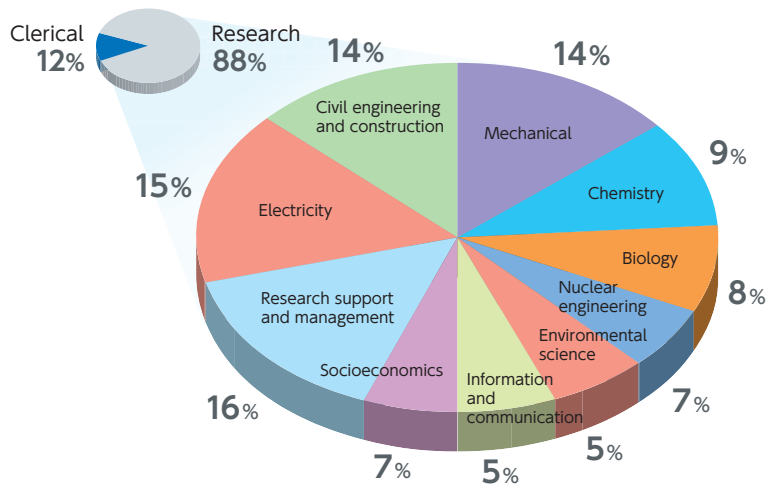


Fig. 1: Staff breakdown

2 Research Reports

A total of 436 CRIEPI research reports were produced in FY 2013. Of these, 270 were research reports and 166 were reports on funded research by electric power companies, the central government and others. Fig. 2 shows the breakdown of reports by subject field. The titles of the research reports, etc. which are publicly accessible are listed in Appendix (1). The body text of these research reports and corresponding leaflets*1 can be downloaded from the CRIEPI's website.

*1The timing of leaflet publication may differ from the publication timing of the corresponding report.

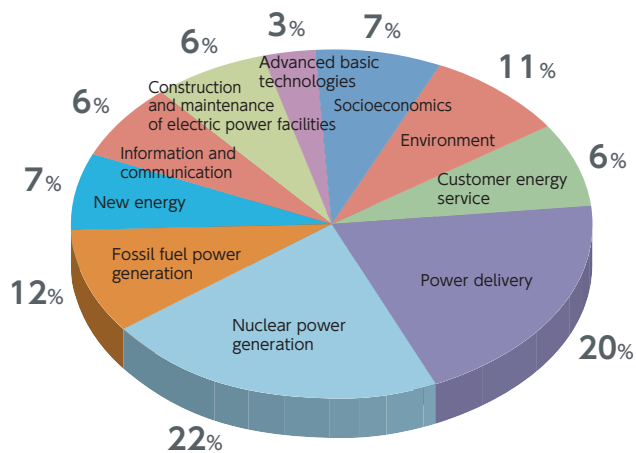


Fig. 2: Breakdown of reports by subject field

3 Presentation of Research Papers

A total of 1,409 research papers were presented in bulletins of academic societies and academic journals and at academic conferences. Of these, 360 papers were peer reviewed. Fig. 3 shows the breakdown of research papers by subject field. The titles of these papers are contained in the research paper database under "Research Results/Reports, etc." on the CRIEPI's website.

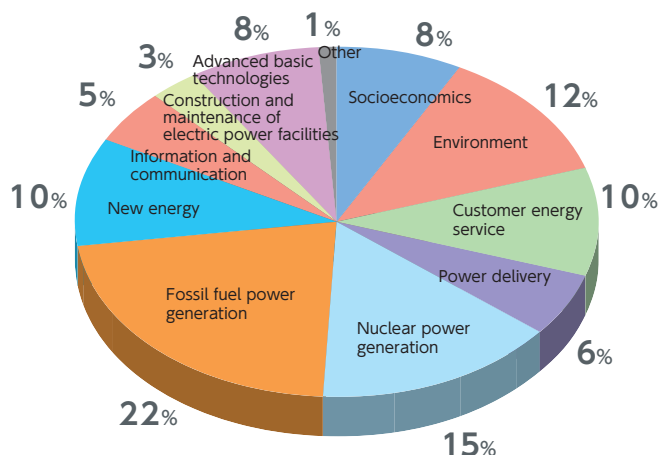


Fig. 3: Breakdown of research papers by subject field

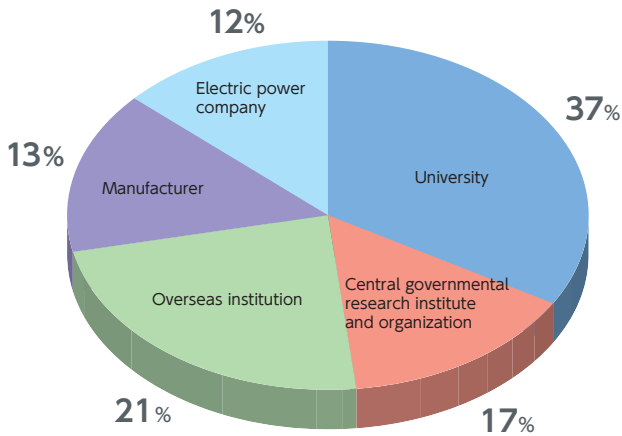


Fig. 4: Classification of research partners

4 Research Cooperation / Interchanges

4-1 Joint Research

A total of 187 joint research projects were conducted in FY 2013. As shown in Fig. 4, universities and central governmental research institutes, etc. accounted for 37% and 17% of the research partners respectively.

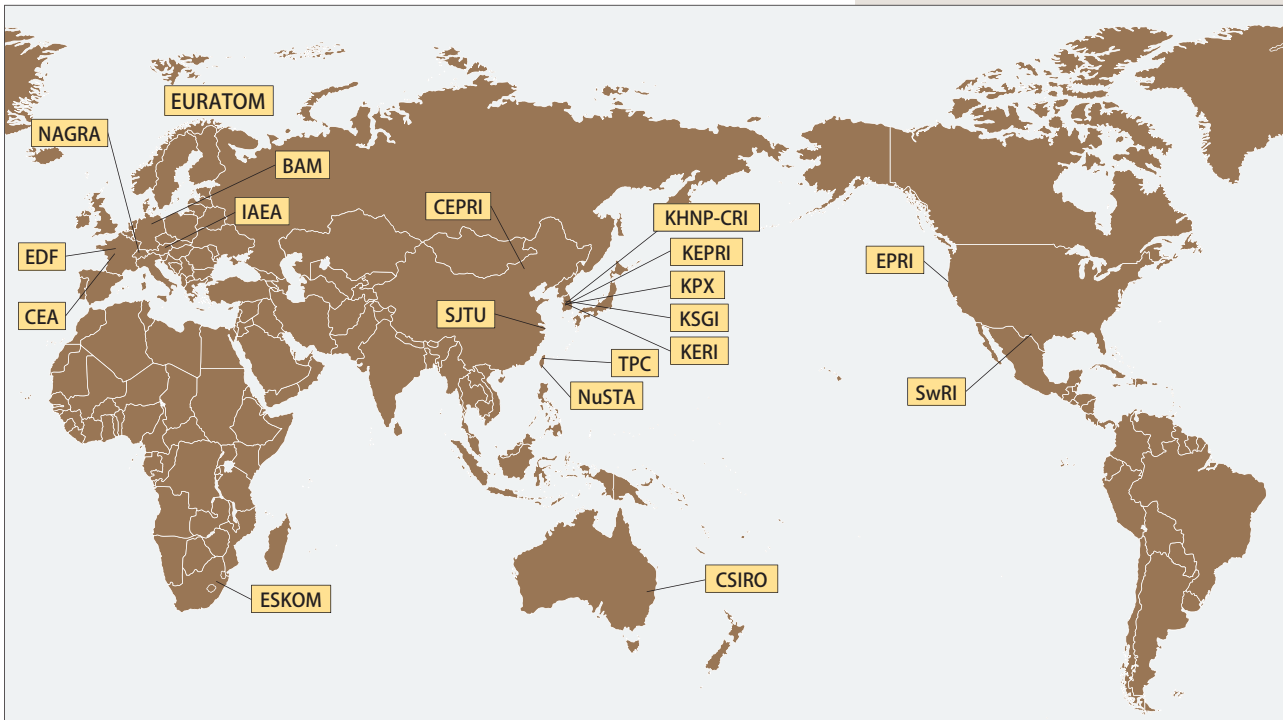


Fig. 5: Main partners for research cooperation

The European Atomic Energy Community (EURATOM) is based in Europe.

4-2 Main International Cooperation/ Interchange Schemes

The CRIEPI has been moving ahead with joint research, information exchange and human interaction with a number of research institutes overseas. Fig. 5 shows the main overseas institutes with which the CRIEPI has concluded an international agreement for cooperation. Table 1 (p.96) lists the main partners of the CRIEPI for international cooperation / interchange.

4. Record of Activities The following is a summary

Table 1 Main international cooperation/interchange partners

Main Partners for Research Cooperation Agreement	
Asia	
Korea Electric Power Research Institute (KEPRI)	China Electric Power Research Institute (CEPRI)
Korea Electrotechnology Research Institute (KERI)	State Grid Electric Power Research Institute (SGEPRI), China
Korea Power Exchange (KPX)	Shanghai Jiao Tong University (SJTU), China
Korea Smart Grid Institute (KSGI)	Taiwan Power Company (TPC)
Korea Hydro and Nuclear Power Company Central Research Institute (KHNP-CRI)	Nuclear Science and Technology Association of Taiwan (NuSTA)
USA	
Electric Power Research Institute (EPRI)	Southwest Research Institute (SwRI)
Europe	
European Atomic Energy Community (EURATOM), EU	Électricité de France (EDF)
National Cooperative for the Disposal of Radioactive Waste (NAGRA), Switzerland	Federal Institute for Materials Research and Testing (BAM), Germany
French Atomic Energy Commission (CEA)	International Atomic Energy Agency (IAEA)
Oceania	
Commonwealth Scientific and Industrial Research Organisation (CSIRO), Australia	
Africa	
ESKOM, South Africa	
Main Partners for Joint Research in Progress	
Asia	
Taiwan Power Research Institute (TPRI)	Korea Institute of Nuclear Security (KINS)
Korea Atomic Energy Research Institute (KAERI)	Korea University
North America	
Electric Power Research Institute (EPRI)	United States Nuclear Regulatory Commission (USNRC)
Idaho National Laboratory (INL)	National Institute of Standards and Technology (NIST)
National Center for Atmospheric Research (NCAR)	Nuclear Waste Management Organization (NWMO), Canada
United States Department of Energy (DOE)	Atomic Energy of Canada Limited (AECL)
Europe	
French Atomic Energy Commission (CEA)	European Atomic Energy Community (EAEC/EURATOM), EU
Électricité de France (EDF)	Institute for Transuranium Elements (ITU), Germany
National Agency for Radioactive Waste Management (ANDRA), France	Gesellschaft für Nuklear-Service mbH (GNS), Germany
Institute de Radioprotection et de Sûreté Nucléaire (IRSN), France	Federal Ministry of Economics and Technology (BMWi), Germany
Swedish Nuclear Fuel and Waste Management Company (SKB)	Friedrich Schiller University Jena, Germany
Studsvik Nuclear AB, Sweden	Leibniz Institute for Solid state and Materials Research (IFW), Dresden, Germany
Studiecentrum voor Kernenergie - Centre d'étude de l'Energie Nucléaire (SCK · CEN)	Gesellschaft für Anlagen – und Reaktorsicherheit mbH (GRS), Germany
National Cooperative for the Disposal of Radioactive Waste (NAGRA), Switzerland	Helmholtz-Zentrum Dresden-Rossendorf (HZDR), Germany
VTT Technical Research Centre of Finland	Jacobs University Bremen, Germany
POSIVA, Finland	Karlsruhe Institute of Technology (KIT), Germany
Radioactive Waste Repository Authority (RAWRA), the Czech Republic	Polytechnic University of Turin, Italy
Comenius University in Bratislava, Slovakia	National Research Council, Italy
Organization for Economic Co-operation and Development/Nuclear Energy Agency (OECD/NEA)	University of Twente, Netherlands
Institute for Energy Technology (IFE), Norway	Nuclear Research and Consultancy Group (NRG), Netherlands
Oceania	
Curtin University, Australia	
Other (involvement of institutes from multiple countries)	
Mont Terri Consortium	Halden Reactor Project
Participation in International Organizations	
Union of the Electricity Industry (EURELECTRIC)	International Electric Research Exchange (IERE)
Association of Electricity Supply Industry of East Asia and the Western Pacific (AESIEAP)	Electromagnetic Transients Program-Development Coordination Group (EMTP-DCG) Committee
World Nuclear Association (WNA)	International Atomic Energy Agency (IAEA), Austria

of the activities that the CRIEPI was engaged in FY 2013.

5 Forums, Seminars and Other Events

The following forums, seminar and open laboratory were organized in FY2013.

- Research Results Debriefing Session 2013
"Securing Reliability for Thermal Power Generation and Distribution Facilities which Support Stable Power Supply"
May 23th, 2013, IINO Hall, Tokyo
- Open Laboratory
May 26th, 2013, Akagi Testing Center
October 5th, 2013, Abiko Area
October 19th, 2013, Yokosuka Area
October 27th, 2013, Komae Area

6 Industrial Property Rights

140 patents were registered and 81 patent applications were made in FY 2013. 19 patents or know-how*2 were newly licensed in FY 2013.

7 Software

The CRIEPI has its own software registration system for the management of copyright. A registered software may be licensed to electric companies, other profit-making enterprises and

universities in response to their request. The number of new software registrations and the number of new licenses awarded were 74 and 312 (1127 copies) respectively.

8 Other

The CRIEPI or its executives and regular employees wrote or edited 7 major books in FY 2013 while executives and regular employees received external awards on 52 occasions (total of 67 persons). The "CRIEPI's World Wide Information Service" (<http://criepi.denken.or.jp/>) is a free and publicly accessible service that has been running since FY 1995. Although the above sites are offered in Japanese, the CRIEPI also offers an English language site with wealth of information. (<http://criepi.denken.or.jp/en/index.html>)

They provide access to the summaries of a number of non-confidential research documents and annual research reports, as well as publications such as the "CRIEPI News" (<http://criepi.denken.or.jp/research/news>) which is a series of leaflets that uses plain language, photographs, and illustrations to introduce the research findings of the CRIEPI in a way that is easy for the general public to understand.

*2 This figure is based on the number of actually licensed intellectual property rights and know-how.

Locations

- Otemachi Area**
 - Head Office 1-6-1 Otemachi, Chiyoda-ku, Tokyo 100-8126
 - Socio-economic Research Center Phone: +81-3-3201-6601
Tokyo Metro Otemachi Station, Exit C7
- Komae Area**
 - Center for Intellectual Property & Technology Licensing 2-11-1 Iwadokita, Komae-shi, Tokyo 201-8511
 - System Engineering Research Laboratory Phone: +81-3-3480-2111
 - Nuclear Technology Research Laboratory 7 minutes walk from Kitami Station [Odakyu line]
 - └ Radiation Safety Research Center
 - └ Human Factors Research Center
 - Komae Operation & Service Center
 - Administrative Support Center
- Abiko Area**
 - Civil Engineering Research Laboratory 1646 Abiko, Abiko-shi, Chiba 270-1194
 - └ Nuclear Fuel Cycle Backend Research Center Phone: +81-4-7182-1181
 - Environmental Science Research Laboratory 20 minutes walk from Abiko Station [JR Joban line] (shuttle bus available)
 - Abiko Operation & Service Center
- Yokosuka Area**
 - Electric Power Engineering Research Laboratory 2-6-1 Nagasaka, Yokosuka-shi, Kanagawa 240-0196
 - └ High Power Testing Laboratory Phone: +81-46-856-2121
 - Energy Engineering Research Laboratory Approx. 35 minutes by bus from Zushi Station [JR Yokosuka line]
 - Materials Science Research Laboratory
 - └ PD Center
 - Yokosuka Operation & Service Center
- Akagi Testing Center**
 - 2567 Naegashima-machi, Maebashi-shi, Gunma 371-0241
 - Phone: +81-27-283-2721
 - Approx. 40 minutes by taxi from Maebashi Station [JR Ryomo Line]
- Shiobara Testing Yard**
 - 1033 Sekiya, Nasushiobara-shi, Tochigi 329-2801
 - Phone: +81-287-35-2048
 - Approx. 30 minutes by taxi from Nasushiobara Station [Tohoku Shinkansen]





Central Research Institute of Electric Power Industry

Annual Research Report Fiscal Year **2013**

Published in September 2014

Central Research Institute of Electric Power Industry (Planning Group)

1-6-1 Otemachi, Chiyoda-ku, Tokyo 100-8126 JAPAN

Tel.+81-3-3201-6601 Fax.+81-3-3212-0080 E-mail▶www-rdd-ml@criepi.denken.or.jp URL▶<http://criepi.denken.or.jp/>

ISBN978-4-7983-1282-8